Role of matrix metalloproteinase-2 in sarcoplasmic reticulum dysfunction during myocardial ischemia-reperfusion injury

by

Andrej Roczkowsky

A thesis submitted in partial fulfillment of the requirements for the degree of

Master of Science

Department of Pharmacology
University of Alberta

Abstract

Matrix metalloproteinase-2 (MMP-2) is an intra- and extra-cellular protease which is activated during myocardial ischemia-reperfusion (IR) injury by reactive oxygen and nitrogen species, namely peroxynitrite. Upon its activation, MMP-2 impairs cardiac contractility by cleaving sarcomeric and other intracellular proteins. MMP-2 has been localized to several subcellular sites inside cardiac myocytes, including the sarcoplasmic reticulum (SR); however, its precise role in this organelle is unknown. I investigated two critical SR proteins, which are known to be proteolyzed during IR injury, as putative targets of MMP-2: the Ca^{2+} ATPase SERCA2a, which pumps cytosolic Ca^{2+} into the SR to facilitate muscle relaxation, and the structural protein junctophilin-2 (JPH-2), which maintains T-tubule structure. I hypothesized that MMP-2 is activated near the SR during cardiac IR injury, resulting in the proteolysis of SERCA2a, to impair its activity, and JPH-2, to impair cardiac contractile function.

Isolated rat hearts were perfused in working mode aerobically or subjected to IR injury in the presence and absence of the MMP inhibitor ARP-100. Inhibition of MMP activity significantly improved the recovery of contractile function of hearts following IR injury. I found a putative 70 kDa degradation product of SERCA2a increased two-fold in IR hearts, which was prevented with ARP-100. SERCA activity assessed in SR enriched microsomes prepared from rat hearts was decreased by IR injury; however, this was not prevented with ARP-100. Incubation of purified proteoliposomes containing SERCA2a with MMP-2 in vitro resulted in its proteolysis. Similarly, incubation of SR enriched microsomes isolated from control rat hearts with MMP-2 caused proteolysis of SERCA2a to ~70 kDa products. The presence of MMP-2 in SR enriched microsomes was confirmed by gelatin zymography. JPH-2 was identified as a target of MMP-2 using in silico software. A potential JPH-2 degradation product was increased by IR in an MMP-

dependent manner. MMP-2 cleaves JPH-2 in vitro. This is the first study to identify two novel substrates of MMP-2 in the SR, as well as identify MMP-2 activity in SR enriched microsomes. Understanding the diverse repertoire of MMP-2 substrates may aid in the development of selective MMP inhibitors for use in ischemic heart disease to mitigate IR injury.

Preface

Experiments involving animals were approved by the University of Alberta Institutional Animal Care and Use Committee and were performed according to the Guide to Care and Use of Experimental Animals published by the Canadian Council of Animal Care (AUP 329).

Dedicated to my Parents who supported me throughout my studies. I would not have been able to accomplish this without them.

Acknowledgements

I express my deepest gratitude to my supervisor and friend, *Dr. Richard Schulz*, for his guidance, his wisdom and his patience in me during my graduate studies. Through his mentorship, I gained much confidence in both myself and my research. He was always there to talk to about issues in both life and science, and this made it a great pleasure to work in his lab for both my undergraduate and graduate studies.

I would like to thank my fellow members of the Schulz lab *Brandon Chan* and *Mathieu Poirier* for their friendship as well as their aid in my project. *Mathieu Poirier* helped me learn the technique of isolated rat heart perfusions. *Brandon Chan* aided in my project in both performing experiments and problem solving.

I would also like to thank all the additional members of the Schulz lab who have aided me: *Dr. Javier Garcia, Nils Moser, Tim Lee, and Dr. Ramses Ilarraza*. I would like to thank *Javier Garcia* for his help with both scientific and life issues. I look up to him as a scientist and as a good guy. He was my go to for problem solving issues. I would also like to thank *Tim Lee* for his help with the junctophilin-2 experiments.

I would like to thank my supervisory committee members *Dr. Howard Young* and Dr. *Harley Kurata. Dr. Howard Young* aided greatly in this project as a collaborator.

I have the deepest love for my parents *Ann Boyda* and *Jerry Roczkowsky* who supported my graduate studies with both love and advice. I would not have been able to get through the difficult times in my graduate studies without them.

I also thank my girlfriend *Shabnum Teja* who supported me emotionally during the past year. I love you deeply.

Table of contents

List of Tables

Page

List of Figures

List of Abbreviations

ADAM	a disintegrin and metalloproteinase
ANOVA	analysis of variance
BCA	bicinchoninic acid
DWORF	dwarf open reading frame
ECM	extracellular matrix
HAX-1	Heat shock-associated protein X-1
IC_{50}	Concentration of antagonist or enzyme inhibitor which inhibits 50% of measured response
JPH	junctophilin
IR	ischemia-reperfusion
MAM	mitochondria-associated membrane
miR	micro ribonucleic acid
MMP	matrix metalloproteinase
MT-MMP	membrane-type matrix metalloproteinase
NO	nitric oxide
$O_2^{\cdot -}$	superoxide anion
$ONOO^-$	peroxynitrite
RONS	reactive oxygen and nitrogen species

SDS-PAGE	sodium dodecyl sulfate polyacrylamide gel electrophoresis
SERCA	sarco/endoplasmic reticulum calcium ATPase
siRNA	small interfering ribonucleic acid
SR	sarcoplasmic reticulum
TIMP	tissue inhibitor of metalloproteinases

Chapter 1: Introduction

1.1.1 History of matrix metalloproteinases

Matrix metalloproteinases (MMPs) are a family of Zn^{2+}-dependent endopeptidases. The first member of the MMP family was discovered in 1962 by Gross and Lapiere who reported a collagen degrading activity secreted from tadpoles undergoing metamorphosis.[1] The second member of the MMP family (MMP-2, also known as type IV collagenase and Gelatinase A) was identified almost two decades later by Liotta et al. (1978) who found an enzyme released from a murine tumour capable of degrading basement membrane type IV collagen.[2] These authors likely described the activity of both MMP-2 and MMP-9, which were later realised to be separate enzymes, termed 72 kDa type IV collagenase and 92 kDa type IV collagenase, respectively.[3] Since these seminal discoveries, 25 members of the MMP family have been discovered, although only 23 are found in humans.[4, 5] Most MMPs were initially named and subsequently categorized after their first discovered extracellular matrix (ECM) protein targets: collagenases (MMP-1, MMP-8, MMP-13, and MMP-18), type IV collagenases (gelatinases, MMP-2 and MMP-9), stromelysins (MMP-3, MMP-10 and MMP-11), matrilysins (MMP-7 and MMP-26), and membrane-type MMPs (MMP-14, MMP-15, MMP16, MMP-17, MMP-24 and MMP-25).[5] This nomenclature was highly arbitrary, however, as only a few extracellular proteins were tested for each enzyme.[4] In the 1980s, the current nomenclature for MMPs was introduced.[6] It is now known that MMPs target proteins beyond ECM proteins both outside and inside cells.[7] Accordingly, MMPs are involved in numerous physiological and pathophysiological processes, including angiogenesis, embryogenesis, inflammation, metastasis, and ischemic heart disease among many others.[8]

1.1.2 Matrix metalloproteinase-2

MMP-2 is ubiquitously expressed in all organs of the human body, including the heart, where it is expressed in vascular smooth muscle cells, endothelial cells, fibroblasts and cardiomyocytes.[7, 9] It is one of the most researched MMPs due, in part, to its ease of measurement using gelatin zymography and its abundance in a variety of cell types.[4] As a consequence, MMP-2 is implicated in numerous physiological and pathophysiological processes, including development of the heart and several cardiovascular diseases.[7, 9, 10] Increased MMP-2 activity is associated with acute coronary syndrome, heart failure and ischemia-reperfusion injury.[9] Although much research in the past focused on the role of MMP-2 in ECM remodeling during cardiac pathologies,[11] it is now known that MMP-2 has a number of non-ECM targets both outside and inside of cardiac myocytes.[5, 8] The first identified intracellular MMP-2 substrate was troponin I, which is cleaved by MMP-2 during myocardial ischemia-reperfusion injury.[12] Since then, numerous intracellular substrates of MMP-2 have been identified, particularly in cardiomyocytes, including titin,[13] α-actinin,[14] and glycogen synthase kinase-3β[15] among others.

1.1.3 Structure of matrix metalloproteinases

The general structure of MMPs includes an endoplasmic reticulum targeting signal sequence (aa 1-29 in MMP-2) which targets MMPs for secretion, an autoinhibitory pro-domain (aa 30-109 in MMP-2), a catalytic Zn^{2+}-containing domain (aa 110-435 in MMP-2), a linker region, and a hemopexin domain which confers substrate specificity (aa 460-660 in MMP-2).[16] The domain structures of MMP-2 isoforms is depicted in Figure 1.1. All MMPs contain a conserved Zn^{2+}-binding motif (HEXXHXXGXXH) in their catalytic domain, which coordinates a catalytic Zn^{2+} between three histidine residues.[17] MMPs contain at least two Ca^{2+} binding sites and

an additional non-catalytic Zn^{2+} binding site which aids in the folding and structure of the enzyme.[17] Membrane type MMPs (MMP-14, 15, 16, 17, 24, 25) contain either a C-terminal transmembrane domain or a glycosylphosphatidylinositol anchor. MMP-2 and MMP-9 are unique amongst MMPs as they contain three fibronectin type II repeats in the catalytic domain which aid in gelatin binding.[16] Two additional isoforms of MMP-2 have been identified which lack the signal sequence and part of the pro domain.[18, 19]. These novel isoforms are discussed more in the following sections.

1.1.4 Synthesis of MMP-2 isoforms

The human MMP-2 gene is located on chromosome 16 in the q12.2 region. It contains 17 exons and spans 27.9 kilobases. Although it was once believed that MMP-2 is constitutively expressed, it now recognized that MMP-2 gene expression is dynamic and tightly regulated.[9] Its expression is modulated by several factors, including endothelin-1[20], interleukin 1,[21] angiotensin II[20], tumor necrosis factor-α,[21] estrogen,[22] progesterone,[22] hypoxia,[20] and mechanical stress.[23] Full length MMP-2 mRNA translates into a protein containing a signal peptide which targets MMP-2 mRNA/ribosome complex to the ER to complete translation and ultimately be secreted.[8] However, the signal sequence of MMP-2 is inefficient at targeting MMP-2 to the ER, resulting in approximately half of synthesized MMP-2 remaining inside of the cell.[19] As mentioned above, two exclusively intracellular isoforms of MMP-2 have been identified which lack the signal peptide.[18, 19] These N-terminally truncated isoforms of MMP-2 lack either 50 or 76 amino acids and are thus termed MMP-$2_{NTT-50,}$[19] and MMP-$2_{NTT-76,}$[18] respectively (Figure 1.1). MMP-2_{NTT-50} is produced via alternative splicing,[19] whereas MMP-2_{NTT-76} is thought to be produced via an alternative start site within the first intron under conditions of oxidative stress.[18] From here on I will use MMP-2 to

denote the full length form of MMP-2. However, due to the recent discovery of these isoforms, the majority of the literature on MMP-2 does not distinguish between isoforms. Their existence probably went undetected due to their abundance, similar molecular weights to 72 kDa and 64 kDa MMP-2, and their resolution and activity in gelatin zymography.

1.1.5 MMP-2 activation pathways

MMP-2 mRNA is translated into a 72 kDa zymogen.[24] The sulfhydryl group of a critical cysteine residue (C^{102}) in the prodomain forms a coordination bond with the catalytic Zn^{2+} ion, rendering MMP-2 inactive.[25] Disruption of this bond to the catalytic Zn^{2+} results in the activation of MMP-2 (and other MMPs in a similar fashion). This was coined the "cysteine switch" mechanism of inhibition and activation.[25] Activation of MMP-2 can occur either through post-translational modification of the prodomain or its proteolytic removal.[7] The latter occurs in the extracellular environment and involves binding of secreted MMP-2 to tissue inhibitor of metalloproteinase-2, followed by tethering of this complex to the plasma membrane through binding to MT1-MMP.[26] MT1-MMP hydrolyzes the peptide backbone of the MMP-2 prodomain between N^{56} and L^{57}.[27] This results in a partially active MMP-2 intermediate which is further processed by other MMPs to its active 64 kDa isoform, lacking the full propeptide domain up to N^{109}.

72 kDa MMP-2 zymogen can also be activated by post-translational modification of its prodomain under conditions of oxidative stress, such as occurs during cardiac ischemia-reperfusion injury.[28] Peroxynitrite ($ONOO^-$), a highly reactive oxygen and nitrogen species formed from nitric oxide (NO) and superoxide anion ($O_2^{\cdot -}$),[29] can react with glutathione to form an intermediate (S-nitroglutathione).[30] This intermediate can then react with the sulfhydryl group of

the critical inhibitory cysteine residue on MMP-2 (C^{102}).[28] The resultant S-glutathiolated MMP-2 is active as the modification by glutathione disrupts the binding of the critical cysteine to the catalytic Zn^{2+}. The same activation mechanism has been identified in MMP-1, 8 and 9 as well.[30] S-glutathiolation of MMP-2 has been shown to be increased in the aorta of lipopolysaccharide treated rats (a model of septic shock) compared with control, and this was associated with the degradation of a calponin-1 and vascular smooth muscle dysfunction.[31]

1.1.6 Post-translational regulation of MMP-2 activity

Endogenous inhibitors of MMPs, known as the tissue inhibitors of metaloproteinases (TIMPs), tightly regulate the activity of MMPs by non-covalently binding to the catalytic Zn^{2+} ion in a 1:1 stoichiometric ratio.[16] There are four known TIMP isoforms (TIMP1-4) which have different affinities for MMPs. Although it was once hypothesized that TIMPs show some specificity towards particular MMPs, it is now understood that each TIMP can bind any MMP with differing selectivity.[4, 32] Out of the four TIMPs, the most selective for MMP-2 is TIMP-2.[10] TIMP-4 is the most abundant TIMP in the heart and is localized within cardiomyocytes along the Z-disc of sarcomeres.[33] In the setting of myocardial ischemia-reperfusion injury, TIMP-4 is secreted from cardiomyocytes and this loss contributes to increased intracellular MMP-2 activity.[33] TIMP-3, which has the broadest inhibitory profile, binds tightly to the extracellular matrix and is abundant in the heart. A reduction in TIMP-3 levels in the myocardium is associated with the transition from compensated to end-stage congestive heart failure in humans.[34] Knockout of TIMP-3 in mice causes spontaneous dilated cardiomyopathy,[35] illustrating its importance in maintaining MMP homeostasis in the heart, among other roles.

MMP-2 is also regulated through phosphorylation as incubation of MMP-2 with alkaline phosphatase increases its activity in vitro.[36] There are five confirmed phosphorylation sites on human MMP-2: S^{32}, S^{160}, T^{250}, Y^{271}, and S^{365}. Both protein kinase C and protein kinase CK2 decrease MMP-2 activity in vitro,[36, 37] however, it is unknown which kinases and phosphatases are responsible for MMP-2 regulation in vivo. MMP-2 is also regulated through dimerization which is formed between C^{102} on neighbouring MMP-2 molecules.[38] Homodimerization of pro-MMP-2 was shown to increase its basal activity without removal of the prodomain as well as increase the activation of pro-MMP-2 by thrombin.

1.1.7 Intracellular localization and substrates of MMP-2

Gelatinolytic activity (MMP-2 and MMP-9) was initially found to be associated with sarcomeric structures in ventricles of patients with dilated cardiomyopathy using in situ zymography.[39] MMP-2 was subsequently localized inside isolated human adult cardiomyocytes by Coker et al. in 1999,[40] who found a sarcomeric staining pattern when using an anti MMP-2 antibody and immunofluorescent microscopy. However, the significance of the finding was overlooked by the authors of this study. Wang et al. (2002) continued on this research, and they showed that MMP-2 was localized to the thin filament and that it could cleave troponin I during IR injury in isolated rat hearts.[12] Since then, MMP-2 has been localized to numerous subcellular compartments, including the mitochondria,[41] nucleus,[42] cytoskeleton,[14] caveolae,[43] and a specialized region of the sarcoplasmic reticulum known as the mitochondria-associated matrix (MAM).[41] At the sarcomere, MMP-2 is localized along the Z disc where it cleaves myosin light chain 1 and titin in addition to troponin I during cardiac IR injury [13, 44]. Cytoskeletal targets of

MMP-2 include α-actinin and dystrophin,[14, 45] critical proteins for maintaining the integrity of the sarcomere and cardiomyocyte as a whole.

Using both immunogold electron microscopy and subcellular fractionation techniques, MMP-2 was found both within the mitochondria and surrounding the mitochondria in the MAM.[41] The MAM is a highly specialized region of the SR which is important site of cross-talk between the mitochondria and the SR.[46] The relative enrichment of MMP-2 between the mitochondria and the MAM indicates there is more MMP-2 localized at the MAM.[41] Inside of the mitochondria, putative substrates of MMP-2 have been identified using siRNA and 2D SDS-PAGE techniques in healthy adult rat cardiomyocytes, including ATPase synthase β subunit and electron transfer flavoprotein subunit β.[47] In this same study, inhibition of MMP-2 was shown to increase ATPase synthase activity. Targets of MMP-2 in the MAM have yet to be explored, but may include calriticulin, which is a substrate of MMP-2 in vitro.[41]

1.1.8 Small molecule MMP inhibitors

The first identified pathological roles for MMPs were in cancer and inflammation.[4] Accordingly, the initial MMP inhibitors were primarily designed as anti-cancer or anti-inflammatory drugs.[48] The first generation MMP inhibitors were designed as Zn^{2+} chelators and were non-specific as it was not known which MMP(s) were the most important to target. Of the 50 plus MMP inhibitors tested in clinical trials for anti-cancer efficacy, none made it to the market. This was primarily due to the unexpected and unwanted side effect of musculoskeletal pain which lead to patient drop-out and/or drastic dose reduction in many studies. Hypotheses put forward to explain the musculoskeletal syndrome include inhibition of MMP-1, targeting the “a disintigrin and metalloproteinase family of proteases”(ADAMs), and off-target metal ion chelation.[49, 50] One

of many reasons that these early MMP inhibitors failed was due to a lack in understanding by the scientific community of the diversity of MMP actions. It is now known that many MMPs have specific roles in diseases and targeting all MMPs is unwanted in certain scenarios. Recently, new MMP inhibitors have been designed to be selective for certain MMPs over others, such as ARP-100.[51] ARP-100 is more selective for MMP-2 and MMP-9 over other MMPs, having an IC_{50} of 12nM, 200nM and 4500nM for MMP-2, MMP-9 and MMP-3, respectively.[51] ARP-100 does not appreciably inhibit MMP-1 or MMP-7 (both have a IC_{50} >50 μM)

Some tetracyclines were found to be inhibitors of MMPs, including minocycline and doxycycline.[52] This is due to a distinct part of the tetracycline molecule, separate from its site of antimicrobial activity, which chelates the Zn^{2+} in MMPs. Doxycycline is somewhat selective for MMP-8 and 13 over MMP-1.[53] Modification of the tetracycline molecule has led to the discovery of several compounds known as chemically modified tetracyclines, which retain MMP inhibitory properties but lack antimicrobial activity.[54] If the MMP-1 hypothesis for musculoskeletal syndrome stands true, doxycycline may be a desirable drug for MMP inhibition. Furthermore, doxycycline is a MMP inhibitor at sub-antimicrobial doses.[52] Currently, a sub-antimicrobial dose formulation of doxycycline (20 mg twice a day) is the only Health Canada approved MMP inhibitor on the market. It is prescribed for the treatment of periodontitis[55] and rosacea.[56] In a recent clinical trial, doxycycline was shown to have efficacy in reducing adverse cardiac remodeling when given for only seven days immediately following percutaneous coronary intervention in patients with myocardial infarction.[57]

1.2.1 Cardiac ischemia-reperfusion injury

Ischemic heart disease, which is caused by a reduction in blood supply to the heart, is one of the leading causes of mortality and morbidity worldwide.[58] Acute coronary syndrome is a form of ischemic heart disease which is a medical emergency requiring immediate intervention.[59] Acute coronary syndrome is comprised of several pathologies which share a common underlying pathophysiology: unstable angina, non-ST segment elevation myocardial infarction and ST segment elevation myocardial infarction.[59] The pathophysiology of acute coronary syndrome involves the accumulation of atherosclerotic plaque in the coronary circulation.[60] Numerous factors can lead to plaque instability, which can cause thrombus formation in the plaque, primarily through plaque rupture or plaque erosion. If a thrombus forms in a coronary artery such that it significantly reduces or halts blood flow to a part of the heart, then this can result in significant tissue damage and cell death downstream of the clot. Timely restoration of blood flow to the heart is critical for limiting the damage due to ischemia, however, reperfusion itself can cause additional damage to the heart beyond the ischemic insult.[58] Outcomes of cardiac ischemia-reperfusion (IR) injury range from reversible injury, called myocardial stunning, to irreversible infarct and scarring depending on the duration of ischemia.[61] The mechanism of IR injury is multifactorial and not fully understood, however, two well established mechanisms are increased production of reactive oxygen and nitrogen species (RONS),[62] and intracellular Ca^{2+} overload.[58]

During reperfusion there is a burst of RONS as oxygen is returned to the ischemic myocardium.[58, 62] Superoxide anion ($O_2^{\cdot -}$) is generated from many sources in the heart, including damaged electron transport chain proteins, xanthine oxidoreductases, NAD(P)H oxidoreductases, and infiltrating neutrophils.[62-64] $O_2^{\cdot -}$ rapidly reacts with NO, which is produced in vascular endothelium and cardiac myocytes, among other sources, to produce $ONOO^-$ (rate constant of

formation: $k=6.7x10^9$).[62, 65] Under normal conditions, the vast majority of $O_2^{\cdot -}$ is scavenged by superoxide dismutase (rate constant of formation: $k=2.0x10^9$). However, when there is abundant production of NO, such as during IR injury, the reaction to form $ONOO^-$ predominates. $ONOO^-$ is protonated at pH less than 8 to form the unstable intermediate peroxynitrous acid (ONOOH). It rapidly decomposes to form highly reactive species, including the hydroxyl radical ($OH^{\cdot}$) and nitrating species such as the nitronium ion (NO_2^+). This can result in lipid peroxidation, MMP and poly ADP ribose polymerase activation,[28, 30, 66, 67] and damage to critical proteins [62]. The rapid biosynthesis of $ONOO^-$ in the first minutes of reperfusion in IR hearts leads to contractile dysfunction as occurs in stunning,[68] and ultimately necrosis and apoptosis.[68, 69]

Intracellular Ca^{2+} overload also occurs during ischemia and during reperfusion.[58] During ischemia, both the intracellular and extracellular milieu in the heart become acidic due to increased lactate production.[70] Upon reperfusion, the extracellular space rapidly returns to physiological pH. This results in an influx of Na^+ into the myocyte through the Na^+-H^+ exchanger. Na^+ cannot be extruded through the Na^+-K^+ ATPase due to a lack of ATP in the cell, and is thus extruded through the Na^+-Ca^{2+} exchanger, thereby resulting in Ca^{2+} uptake by the cell. Ca^{2+} overload can cause activation of Ca^{2+}-dependent proteases, namely calpains, and activation of the mitochondrial permeability transition pore.[71, 72]

1.2.2 MMPs in the heart

Collagenases (most probably MMP-1) were first described in healthy rat heart tissue in the mid-1970s.[73] The observation of collagen fiber disruption in the myocardium from patients with dilated cardiomyopathy led to the hypothesis that collagenase activity may contribute to thinning and dilation of the heart wall.[74] Throughout the 1980s and early 1990s, it became apparent that

ECM degradation and remodeling through secreted proteases played a major role in heart failure and myocardial infarction.[10] The normal adult heart expresses several MMPs, including MMP-1, 2, 3, 7, 8, 9, 13, and 14.[10] Under conditions of cardiovascular stress and injury, the activity and levels of several MMPs (including MMP-2 and -9) are known to increase significantly in the heart contributing to contractile dysfunction, infarct and scar formation.[10, 39]

As mentioned in section 1.1.7, Rouet-Benzineb et al. (1995) first identified gelatinolytic activity (MMP-2 and MMP-9) inside cardiac myocytes and hypothesized that it was associated with myofibrilysis in ventricles from patients with dilated cardiomyopathy.[39] MMP-2 and 9 were subsequently found inside of cardiac myocytes by immunoblot by Coker et al. (1999), with MMP-2 showing a distinct sarcomeric staining pattern by immunofluorescent microscopy.[40] The observed MMP-9 signal by these investigators, however, did not show up at a molecular weight near the MMP-9 standard (at ~90 kDa). The signal detected was instead around 200 kDa, which may be dimers of MMP-9.[75] Both MMP-2 and MMP-9 activity have also been found in nuclear extracts from human hearts by gelatin zymography.[42] The role of intracellular MMP-2 in IR injury is discussed in the next paragraph in greater detail. Using confocal microscopy, MMP-9 was found to colocalize with mitochondria in adult ventricular myocytes.[76] MMP-7 has also been found inside cardiac muscle cells.[5, 77] Connexin 73 has been identified as a possible target of intracellular MMP-7 and there is evidence using MMP-7 knockout mice that MMP-7 mediated connexion 73 cleavage during myocardial infarction disrupts normal electric conduction in the heart.[78]

1.2.3 Role of MMP-2 in cardiac IR injury

Cheung et al. (2000) were the first to demonstrate that inhibition of MMP activity (using either doxycycline or ortho-phenanthroline) was protective against IR (stunning) injury in isolated

rat hearts perfused according to the Langendorff method.[79] The authors noticed the release of MMP-2 into the perfusate during the first minutes of reperfusion which became greater as the duration of ischemia increased.[79] Infusion of semi-purified MMP-2 into the perfusate exacerbated stunning injury whereas infusion of a neutralizing MMP-2 antibody improved contractile recovery during reperfusion in a concentration-dependent manner. Subsequent to this study, the first bona fide intracellular substrate was identified, troponin I.[12] Troponin I is degraded during ischemia and reperfusion and thereby contributes to stunning injury.[12, 80, 81] It is also secreted into the blood following cardiac stress and is used as a clinical biomarker for myocardial infarction.[82] In the seminal study by Wang et al. (2002), troponin I proteolysis in myocardial IR injury was prevented with doxycycline or ortho-phenanthroline.[12] They also showed that MMP-2 was bound to the thin myofilament fraction and colocalized with troponin I. Since then numerous intracellular targets of MMP-2 have been identified, including glycogen synthase kinase-3β[15] and alpha-actinin.[14] More recently, MMP-2 has been shown to co-localize with titin resulting in its degradation during IR injury.[13] Titin is the largest mammalian protein and is the molecular spring of the sarcomere, determining both passive and active stiffness of heart muscle to a great extent.[83] MMP-2 null mice demonstrated reduced titin degradation following in vivo IR injury compared to wildtype.[13]

Direct evidence for increased intracellular MMP-2 activity following IR injury in isolated rat hearts was shown using in situ zymography.[33] This technique allows for direct measurement of gelatinolytic activity in intact tissue slices without separating MMP-2 and 9 from their endogenous inhibitors. Increased gelatinolytic activity in ventricular homogenates was also observed following IR using a spectrophotometric technique with a fluorescent MMP2/9 substrate.[84] It should be noted that both these studies were performed using rat hearts, and although MMP-9 has been reported in rat hearts before, it is absent in rat hearts perfused completely free of blood.[79, 85]

1.3.1 Excitation-contraction coupling in the heart and the role of calcium

The level of free $[Ca^{2+}]_i$ in cardiac myocytes couples myocyte depolarization to myofilament contraction.[86] At rest, free $[Ca^{2+}]_i$ in myocytes is ~ 100 nM. This increases tenfold upon membrane depolarization due to entry of extracellular Ca^{2+} and mobilization of intracellular Ca^{2+} stores from the SR causing sarcomere contraction. Relaxation is initiated by the removal of Ca^{2+} from the cytosol through Ca^{2+} pumps and exchangers residing in the SR and plasma membrane as will be discussed in greater detail below. A general depiction of Ca^{2+} cycling in cardiac myocytes is provided in Figure 1.2.

A depolarizing potential in an adult cardiac myocyte is initiated by movement of positively charged ions from an adjacent cardiac myocyte through gap junctions, resulting in unidirectional activation of voltage gated sodium channels on the plasma membrane.[86] This depolarizing event runs down invaginations in the plasma membrane called T-tubules. Voltage gated Ca^{2+} channels (mostly L-type calcium channels) in the T-tubule become activated, resulting in an influx of Ca^{2+}. This can increase the local $[Ca^{2+}]_i$ in the junctional cleft to 10-20 μM.[87] Influx of Ca^{2+} through voltage gated calcium channels activates closely positioned ryanodine receptors on the SR membrane inducing Ca^{2+} mobilization from the SR. The structure of the T-tubule and its close relationship with junctional SR is maintained by the anchoring protein junctophilin-2 (JPH-2), which appears to be critical for both cardiomyocyte development and maintenance of normal excitation-contraction coupling.[88] The local rise in $[Ca^{2+}]_i$ can peak up to 400 μM at the junctional cleft following release from ryanodine receptors, which then diffuses throughout the rest of the cell, causing myofilament contraction.[87]

The basic unit of striated muscle contraction is the sarcomere, which is bound by Z-discs at either end.[89] Muscle contraction occurs when the sarcomere is shortened due to ATPase-

dependent motor activity in the thick filament myosin which binds to and pulls thin filament actin. The signal for cardiac contraction is a rise in $[Ca^{2+}]_i$. Under resting Ca^{2+} concentration the troponin-tropomyosin complex blocks thick filament myosin from binding to actin, thus preventing cross-bridge cycling and sarcomeric shortening. When $[Ca^{2+}]_i$ is increased in the region of the sarcomere, Ca^{2+} binds to troponin C in the troponin complex, which removes the troponin-tropomyosin complex from myosin binding sites on actin, allowing ATPase generated muscle contraction to occur.

Relaxation is initiated by clearance of Ca^{2+} from the cytosol through several Ca^{2+} channels and pumps, including the plasma membrane Ca^{2+} ATPase, the sarco/endoplasmic reticulum ATPase (SERCA), sarcolemmal Na^+/Ca^{2+} exchanger, mitochondrial Ca^{2+} uniporter and the secretory pathway Ca^{2+}/Mg^{2+} ATPase.[86, 90] In cardiac myocytes, the majority of cytosolic Ca^{2+} is translocated into the SR lumen via the Ca^{2+} ATPase SERCA2a. SERCA2a is responsible for approximately 70% of cytosolic Ca^{2+} clearance in rats and 90% in humans.[86] The majority of the remaining cytosolic Ca^{2+} is cleared through the Na^+/Ca^{2+} exchanger. Very little cytosolic Ca^{2+} (~2%) is cleared through the mitochondrial Ca^{2+} uniporter and plasma membrane Ca^{2+} ATPase.[86] In SR microsomes obtained from rat hearts, uptake of radioactive Ca^{45} was inhibited 97% by the specific SERCA inhibitor thapsigargin, suggesting that the secretory pathway Ca^{2+}/Mg^{2+} ATPase contributes minimally to cytosolic Ca^{2+} clearance.[90] However, this is likely dependent on the method of SR microsomal preparation.

Some investigators have suggested that under normal physiological conditions, Ca^{2+} independent processes within the sarcomere largely govern the rate of relaxation.[91] Evidence for this theory comes from computational models suggesting that Ca^{2+} dissociates from the troponin complex during the ejection phase of the heart prior to muscle relaxation.[91, 92] However, this

hypothesis has not been directly tested, and alterations in Ca^{2+} affinity of troponin C during contraction may explain the lag between Ca^{2+} clearance and muscle relaxation.[87] Nonetheless, SERCA2a mediated Ca^{2+} clearance is a major driving force of cardiac lusitropy in both healthy and diseased myocardium.[87, 91]

1.4.1 Sarco/Endoplasmic Reticulum Calcium ATPase 2a

Sarco/endoplasmic reticulum calcium ATPase (SERCA) is a member of the P-type ATPase family of membrane transporters responsible for translocating cytosolic Ca^{2+} into the SR lumen.[93] SERCA can maintain a 1000 fold higher Ca^{2+} concentration in the SR compared with the cytosol.[94] Three SERCA genes encode for thirteen currently known isoforms of this protein (SERCA1a-b, SERCA2a-d, and SERCA3a-f). SERCA2a is the predominant isoform expressed in the heart in both rodents and humans (97.5% of total cardiac SERCA in murine hearts), and is also expressed in smooth muscle cells and slow-twitch skeletal muscle cells.[93, 95] It should be noted that cardiomyocytes also express SERCA2b, SERCA2c and SERCA3b.[96]

Human SERCA2a is a 997 aa protein (110 kDa) which contains ten trans-membrane helices with both the N- and C-terminus exposed to the cytosol [93]. SERCA2a translocates two Ca^{2+} into the SR lumen for every ATP hydrolyzed. Binding of Ca^{2+} to the first site allows a conformational change forming Ca^{2+} binding site 2. Hydrolysis of ATP fuels a conformational change allowing the Ca^{2+} to exit into the SR lumen. As discussed above, the proper function of SERCA2a is essential for cardiac muscle relaxation and maintaining intracellular Ca^{2+} at ~100 nM during diastole.

1.4.2 Binding partners of SERCA2a

The most studied binding partners of SERCA2a are phospholamban and sarcolipin.[95] The main regulator of SERCA2a function in ventricular muscle is phospholamban. Phospholamban is a 52 aa (6 kDa) SR membrane protein which reversibly regulates SERCA function.[97] Binding of phospholamban to SERCA decreases SERCA affinity for Ca^{2+}, and this inhibition is relieved upon phosphorylation of SERCA2a at two critical sites, S^{16} and T^{17}.[93, 97] Protein kinase A-dependent phosphorylation of S^{16} occurs during beta adrenergic stimulation and is responsible for increased SERCA activity and greater SR calcium reserve.[97] T^{17} is phosphorylated by Ca^{2+}/calmodulin-dependent kinase II.[93] Phosphorylation of S^{16} seems to be the most important mode of regulation, whereas T^{17} phosphorylation may be responsible for fine tuning.[93, 98] Phosphorylation of these sites is not mutually exclusive and may occur simultaneously.[97] Phosphorylation of phospholamban is thought to promote its pentamerization, which may act as a reserve of phospholamban.[97] Sarcolipin is a small 31 aa transmembrane protein which decreases both Ca^{2+} affinity and maximal activity of SERCA.[93] Sarcolipin is the main regulator of SERCA in atrial and skeletal muscle.

Recently, small open reading frames which encode for small SERCA binding partners have been identified in regions of the genome that were previous thought to encode long noncoding RNA.[93] The first of these to be identified was sarcolamban, which was first discovered in hearts from drosophila, but is conserved in many species including humans.[99] Using a bioinformatics approach, Nelson et al. (2016) discovered a micropeptide in a small open reading frame which encodes for dwarf open reading frame (DWORF).[100] DWORF is unique among the small peptide binding partners of SERCA2a as it is the only known endogenous peptide to positively regulate SERCA2a activity. Overexpression of DWORF in the murine cardiomyocytes resulted in

increased peak Ca^{2+} transients, as well as increased SR Ca^{2+} load. It is thought that DWORF exerts its positive effect on SERCA by displacing inhibitory peptides, such as phospholamban.

A binding partner of phospholamban has also been identified, named heat shock-associated protein X-1 (HAX-1). HAX-1 is a 279 aa protein which was first shown to interact with phospholamban in vitro.[101] Subsequent authors found that HAX-1 negatively regulates SERCA2a function by promoting phospholamban monomerization.[102] Interestingly, the hearts of a tamoxifen-inducible, cardiac-specific knockout of HAX-1, in 8 week old mice, had impaired contractile recovery following ex vivo IR injury compared with control.[103] This was attributed to an antioxidant property of HAX-1.

1.4.3 Post-translational modifications of SERCA2a

Several post translational modifications of SERCA2a effect its turnover or function, including S-glutathiolation,[104] SUMOylation,[105] glycosylation,[106] O-glnNAcylation,[107] and sulfonylation among others.[104, 108] Glycosylation of SERCA2a was found to be associated with decreased SERCA2a protein levels in hearts from diabetic rats.[106] O-glcNAcylation was also found to be associated with decreased protein levels in cardiac myocytes from diabetic mice.[107] SUMO-1 dependent SUMOylation of SERCA2a increases its function, and this SUMOylation of SERCA2 is decreased in patients with heart failure.[105] Peroxynitrite-dependent glutathionylation of SERCA2a at C^{674} increases SERCA2a Ca^{2+} uptake into SR vesicles.[104] Sulfonylation of SERCA2a at C^{674} may decrease its activity by preventing S-glutathiolation.[104] Increased sulfonylation of SERCA2a is associated with its degradation to a 70 kDa fragment, and it is hypothesized that sulfonylation of C^{674} increases the susceptibility of SERCA2a to degradation.[109]

1.4.4 SERCA2a dysfunction in cardiac pathologies

Decreased SR Ca^{2+} uptake into SR vesicles isolated from the hearts of infarcted animals was noted as early as the 1970s.[110] It was, therefore, hypothesized that SR dysfunction contributes significantly to cardiac IR injury. Seminal studies from Naranjan S Dhalla's group demonstrated impaired SR Ca^{2+} transport in isolated perfused rat hearts subjected to IR injury compared with aerobically perfused hearts.[111, 112] This was associated with decreased protein and mRNA levels of key SR proteins, such as SERCA2a, ryanodine receptor 2 and phospholamban. It was later shown that SR dysfunction and decreased protein levels were prevented with calpain inhibitors (ALLN and MDL-28170).[113, 114] It has been recently demonstrated, however, that these calpain inhibitors are also effective MMP-2 inhibitors at concentrations employed for calpain inhibition.[115] Further evidence for the role of SR dysfunction in IR injury comes from studies using hearts from heterozygous SERCA2a knockout mice, which showed increased stunning injury when subjected to ex vivo IR injury, and showed increased infarct size following in vivo IR injury as compared with wildtype.[116, 117] Decreased levels of SERCA2a also result in infarction occurring at durations of ischemia which do not cause infarct in wild type mice.[117] Although heterozygous SERCA knockout mice do not show any cardiac dysfunction under baseline conditions, they are more sensitive to pressure overload than wild type mice.[118] Decreased levels of SERCA2a have been observed in both humans and animal models following myocardial infarction and other heart diseases (heart failure), and although it may not be the initial cause of heart injury, it is a contributing factor to diminished cardiac function following injury.[119]

1.5.1 JPH-2

Human JPH-2 is a 696 aa protein (apparent molecular weight of 97 kDa by gel electrophoresis) which tethers the junctional SR membrane to the T-tubules in cardiac myocytes.[88] In adult cardiomyocytes, the junctional SR membrane forms a complex with the T-tubules along the Z lines of the sarcomere, allowing for proper calcium-induced calcium release and excitation-contraction coupling (Figure 1.2). This T-tubule/SR interaction, called a dyad junction, is maintained at a gap size of ~12 nm by JPH-2.[120] The C-terminus of JPH-2 contains a single trans-membrane segment which embeds in the SR.[88] The N-terminus of JPH-2 contains eight membrane occupation and recognition nexus domains which interact with phospholipids, particularly sphingomyelin and phosphatidylcholine in the plasma membrane.[88, 120]

Invaginations in the cardiomyocyte plasma membrane occurs after birth (10 days in mice) and eventually forms T-tubules through a process known as tubulogenesis.[121] In the embryonic heart, JPH-2 is present and anchors the SR to the plasma membrane surface.[121] The initial formation of invaginations is thought to be facilitated by caveolin-3 and bridging integrator-1, whereas JPH-2 is critical for forming mature T-tubules.[88] Embryonic cardiomyocytes from JPH-2 knockout mice still have peripheral coupling between the SR and plasma membrane in the absence of T-tubule formation.[120] shRNA mediated knockdown of JPH-2 in mice results in the inability to form mature T-tubules.[122] This results in development of a heart failure phenotype by postnatal day 10 followed by premature death.

1.5.2 JPH-2 in heart disease

Disruption of T-tubule structure and uncoupling between the T-tubules and SR have both been observed in human patients with heart failure. [123, 124] T-tubule disruption was associated with

decreased expression of JPH-2 and increased miR-24, which supresses JPH-2 expression.[123] Conditional knockdown of JPH-2 in mice using RNA interference results in development of systolic heart failure and mortality.[125] In a reversible model of heart failure caused by inducible $G_{\alpha q}$ activation in mice, the calpain/MMP-2 inhibitor MDL-28170 prevented JPH-2 proteolysis and T-tubule disruption.[126] JPH-2 proteolysis has also been implicated in both in vivo and ex vivo models of IR injury.[127, 128] In isolated rat hearts subjected to IR injury, the calpain inhibitor MDL-28170 prevented JPH-2 degradation.[127] As MDL-28170 is also an inhibitor of MMP-2,[115] it is possible that MMP-2 may be responsible for JPH-2 proteolysis during IR injury in the heart.

1.6 Hypothesis

I hypothesize that MMP-2 is activated during IR injury inside cardiomyocytes at or near the SR. Upon its activation, MMP-2 cleaves numerous intracellular substrates within the cardiac myocyte contributing to impaired contractile function. Among many other substrates, SERCA2a and JPH-2 are cleaved by MMP-2 during IR injury contributing to impaired SERCA2a activity and cardiac contractile dysfunction.

1.7 Study Objectives

1. Determine if SERCA2a and JPH-2 are substrates of MMP-2 during IR injury using isolated working rat hearts subjected to ischemia and reperfusion in the presence or absence of the MMP inhibitor ARP-100.
2. Analyze potential MMP-2 cleavage sites on SERCA2a and JPH-2 using in silico cleavage prediction software
3. Determine if SERCA2a and JPH-2 are substrates of MMP-2 in vitro.
4. Test if inhibition of MMPs with ARP-100 prevents SERCA2a dysfunction by measuring SERCA2a activity in SR enriched microsomes prepared from fresh isolated working rat hearts.
5. Measure MMP-2 activity in ventricular extracts and SR enriched microsomes by gelatin zymography.

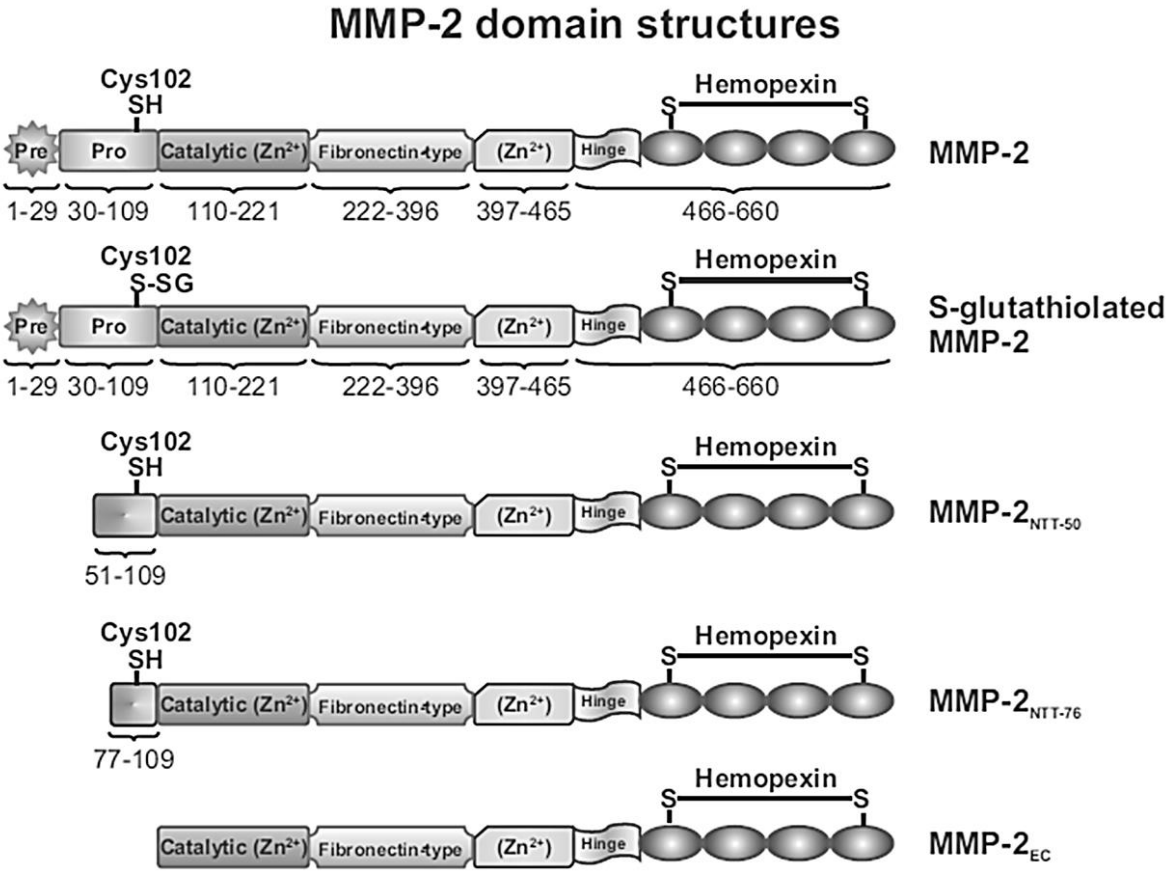

Figure 1.1: Domain structures of different MMP-2 isoforms modified from Chan et al.[8] MMP-2 is synthesized as a 660 aa protein (including the signal peptide). MMP-2 is activated by peroxynitrite and glutathione to form S-glutathiolated MMP-2. MMP-2 can also be activated in the extracellular space by proteolytic cleavage (MMP-2_{EC}). Two intracellular N-terminally truncated isoforms of MMP-2 have been recently identified, which lack either 50 amino acids (MMP-2_{NTT-50}) or 76 amino acids (MMP-2_{NTT-76}) from the N-terminus.

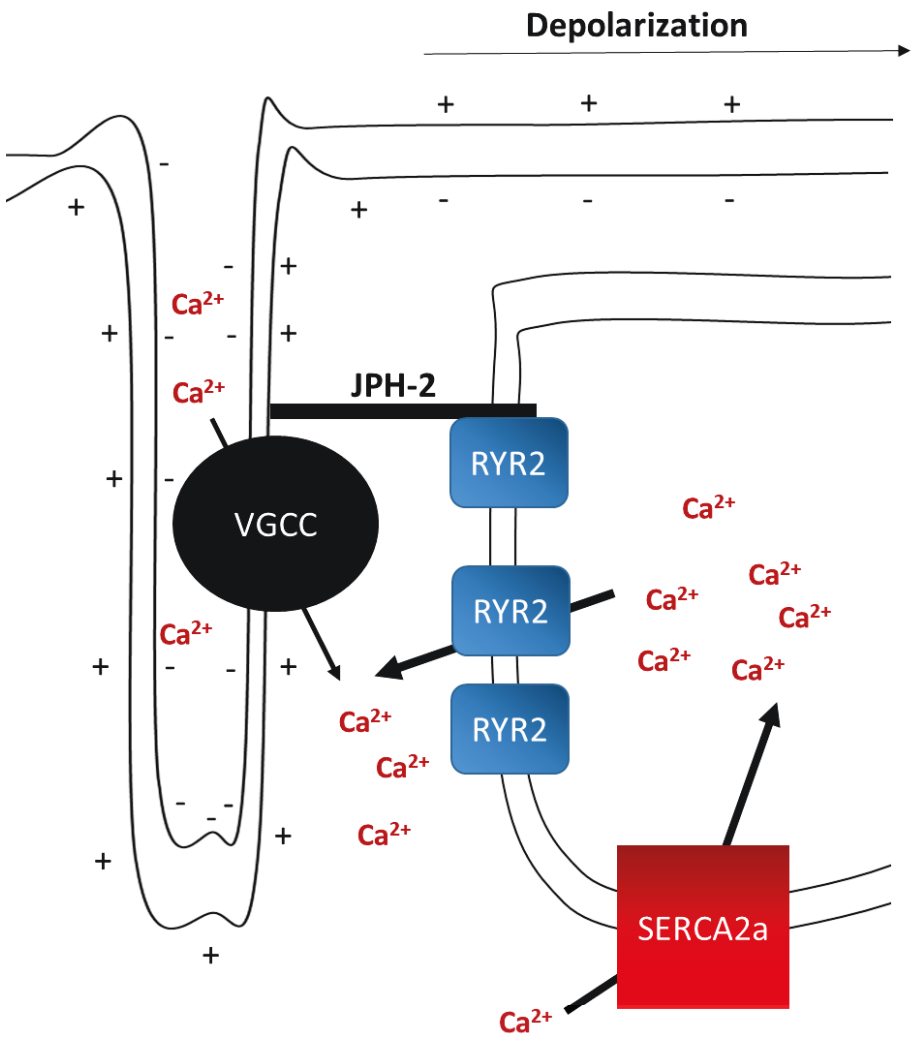

Figure 1.2: Excitation-contraction coupling and the role SERCA2a. 1) Unidirectional membrane depolarization in an adult cardiomyocyte travels down t-tubules, 2) resulting in the activation of voltage gated calcium channels (VGCC). 3) Ca^{2+} enters the VGCC which stimulates the ryanodine receptor-2 (RYR2) to release Ca^{2+} from the sarcoplasmic reticulum. 4) The rise in intracellular Ca^{2+} levels initiates muscle contraction. Muscle relaxation is largely determined by 5) SERCA2a activity, which translocates cytosolic Ca^{2+} back into the SR for subsequent heart beats.

Chapter 2- Methods

2.1.1 Reagents

Salts and other reagents used for this study were purchased from Sigma-Aldrich (Oakville, Ontario) unless otherwise stated. HEPES, $CaCl_2$-$2H_2O$, NaCl, and NaN_3 were purchased from Fisher Scientific (Ottawa, Ontario). The MMP inhibitor ARP-100 was purchased from Cayman Chemicals (13321, Ann Arbor, Michigan). The calpain inhibitor MDL-29170 was purchased from Cayman Chemicals (14283, Ann Arbor, Michigan). Insulin (Humulin R) was purchased from Lilly (Indianapolis, Indiana). Bovine serum albumin (BSA) was purchased from Equitech-Bio Inc (Kerrville, Texas).

2.1.2 Antibodies

Two antibodies were used to probe for SERCA2a: 1) a monoclonal antibody produced in rabbit using a synthetic peptide encoding human SERCA2a (within aa 1000-1100, exact sequence proprietary) as the antigen (EPR9393 epitope, ab137020, Abcam, Cambridge, UK), or 2) a monoclonal antibody produced in mice using purified canine sarcoplasmic reticulum vesicles as the antigen, followed by hybridoma generation with a single clone (2A7-A1 epitope, MA3-919, Invitrogen, Carlsbad, California). The latter antibody was never mapped and its binding region is unknown. The antibody used to detect PLN was monoclonal and produced in mice using a synthetic peptide encoding canine PLN aa 2-25 (ab2865, Abcam, Cambridge, UK). In order to detect PLN phosphorylated at residue S^{16}, a polyclonal antibody developed in rabbits, using as an antigen a synthetic peptide of human PLN (aa 14-25) with S^{16} phosphorylated (ab15000, Abcam, Cambridge, UK), was used.

A custom antibody purchased from Bethyl Laboratories (uncatalogued, Montgomery, Texas) was used to detect a sulfonic acid modification of SERCA2a at C^{674}. The antibody was produced in rabbits using a chemically synthesized peptide of human SERCA2a aa 669-678 with C^{674} sulfonylated [109].

To assess the purity of SR enriched microsomes prepared from fresh rat ventricles, antibodies were used to detect possible contamination from mitochondria (VDAC1), cytosol (GAPDH), and the plasma membrane (Na^+/K^+ ATPase). To assess SR enrichment, SERCA2a levels were assessed by immunoblot using ab137020 from Abcam as described above. The monoclonal VDAC1 antibody was produced in mice against a recombinant full length human VDAC1 protein (ab14734, Abcam, Cambridge, UK). The antibody used to detect GAPDH was a monoclonal antibody produced in rabbits to a synthetic human peptide (14C10, Cell Signaling Technology, Beverly, MA). The antibody used to detect Na^{2+}/K^+ ATPase was a monoclonal antibody developed in rabbits against synthetic peptide of human Na^{2+}/K^+ ATPase (aa 1-100).

In order to detect JPH-2 by immunoblot, a rabbit polyclonal antibody detecting the c-terminal region of mouse JPH-2 was used (40-5300, Invitrogen, Carlsbad, California). Rabbit anti-GAPDH (14C10, Cell Signalling Technology, Beverly, MA) was used as a loading control.

The polyclonal secondary antibody against rabbit IgG was made in goats and is conjugated with horseradish peroxidase (CLCC42007, Cedarlane, Burlington, Ontario). The polyclonal secondary antibody against mouse IgG was also produced in goats followed by purification by column chromatography and conjugation to horseradish peroxidase (CLCC30007, Cedarlane, Burlington, Ontario).

2.1.3 Markers and standards

Porcine SERCA2a embedded in proteoliposomes, purified according to Reddy et al. (1996), was used in the in vitro degradation assay with MMP-2.[129] This was a gift from Dr. Howard Young (Department of Biochemistry). The primary amino acid sequences of rat, human and porcine SERCA2a are highly similar (98.6% sequence homology).

Blueye prestained protein ladder (FroggaBio, Toronto, Ontario) was used as the molecular weight marker in immunoblot, gelatin zymography and in vitro degradation experiments.

Serum free conditioned media from phorbol ester treated human fibrosarcoma cells (HT1080 cell line, American Type Culture Collection, Manassas, Virginia) was used as a standard for MMP-2 and MMP-9 in gelatin zymography.

2.2 Animal protocol

Experiments involving animals were approved by the University of Alberta Institutional Animal Care and Use Committee and were performed according to the Guide to Care and Use of Experimental Animals published by the Canadian Council of Animal Care (AUP protocol number 329).

2.3 Calpain inhibition assay

In order to test the calpain inhibitory properties of the MMP inhibitor ARP-100, purified rat calpain-2 (2 ng, a gift from Dr. Peter Davies, Queens University, Department of Biochemistry) was added to tubes containing calpain incubation buffer (150 mM NaCl, 50 mM Tris-HCl, 5 mM

$CaCl_2$, 10 μM dithiothreitol, pH 7.6) in the presence or absence of DMSO vehicle (0.1% v/v), the calpain inhibitor MDL-28170 (30 μM) or ARP-100 (30 μM). Calpain was preincubated with inhibitors or DMSO vehicle for 10 min at room temperature. 1 μg of a known calpain substrate (recombinant human troponin I aa 1-77, a gift from Dr. Peter Hwang, Department of Biochemistry, University of Alberta) was added to each tube and the reaction was incubated at 37ºC for 1 hr. The samples were then loaded onto a Tris-tricine 16% polyacrylamide gel and electrophoresed at 80 V until the dye front crossed the stacking and spacer layer. The voltage was then increased to 140 V and the gel was run until the dye front reached the bottom of the gel. The gel was stained with Coomassie blue and destained with destaining solution (*appendix*). Gels were scanned with a GS-800 densitometer (Bio-Rad, Hercules, California) using Quantity One (Bio-Rad, Hercules, California) image processing software.

2.4 Preparation of ARP-100 for working heart:

ARP-100 (Cayman Chemical, Ann Arbor, Michigan) was purchased at exact weight (10 mg at a time) and dissolved in DMSO (Fisher Scientific, Ottawa, Ontario) to a concentration of 20 mM in DMSO, aliquoted, and stored at -80ºC until use.

2.5 Isolated working rat heart perfusions:

Male Sprague-Dawley rats (300-400 g) were anesthetized with sodium pentobarbital (240 mg/kg, i.p.). Hearts were rapidly excised and briefly rinsed in ice cold (4°C) Krebs-Henseleit solution (118 mM NaCl, 25 mM $NaHCO_3$, 4.7 mM KCl, 1.2 mM $MgSO_4$, 1.2 mM KH_2PO_4, 11 mM glucose, 0.5 mM EDTA, and 3 mM $CaCl_2$, pH 7.4). The hearts were mounted onto a cannula

by the aorta and perfused in Langendorff mode for 10 min at a constant pressure of 60 mmHg with Krebs-Henseleit solution at 37°C oxygenated with 5% CO_2 in 95% O_2. During this time, non-cardiac tissue was removed from the heart and the left atria was cannulated. Hearts were then switched to working mode and perfused with recirculating Krebs-Henseleit solution (100 mL volume) with the addition of 100 μU insulin (Humulin R, Lilly, Indianapolis, Indiana), 0.1% bovine serum albumin (BSA, Equitech-Bio Inc, Kerrville, Texas) and 5 mM pyruvate. Purfusate entered the heart via the left atria with a preload pressure of 15 mmHg and is ejected by the left ventricle against an afterload pressure of 75 mmHg. Cardiac output and aortic flow were measured with calibrated ultrasonic flow probes (Transonic Systems Inc, Ithaca, New York). Heart rate and peak systolic pressure were measured with a pressure transducer (Harvard Apparatus, Holliston, Massachusetts) in the aortic outflow line. The main parameter of cardiac mechanical function was measured as cardiac work (the product of peak systolic pressure and cardiac output). Hearts were kept at 37°C for the duration of the experiment via a water-jacketed glass heart chamber. All spontaneously beating hearts were equilibrated for 10 min in working heart mode before any parameters were recorded.

The heart perfusion protocols are depicted in figure 2.1. The aerobic control hearts were perfused aerobically for 70 minutes. Ischemic-reperfused hearts were perfused aerobically for 20 min followed by 20 min global, no-flow ischemia and 30 min aerobic reperfusion. Either vehicle (0.05% DMSO) or the MMP inhibitor ARP-100 (50 μl of 20 mM stock to a final concentration of 10 μM, Cayman Chemical, Ann Arbor, Michigan) were added into the recirculating modified Krebs-Henseleit solution 10 min prior to the onset of ischemia, forming the IR and IR+ARP-100 groups, respectively. At the end of perfusion protocol the ventricles were flash frozen with Wollenberger clamps cooled to liquid nitrogen temperature and stored at -80°C for later processing.

Additional sets of hearts were perfused as above and, instead of freezing, fresh ventricular tissues were used for preparation of SR enriched microsomes (n=4-5/group).

2.6 Preparation of ventricular extract

Frozen ventricles were pulverized using a mortar and pestle cooled to the temperature of liquid nitrogen. Liquid nitrogen was added to the crushed heart powder in the mortar and allowed to boil off. The frozen heart powder was then carefully added to liquid nitrogen cooled 5 mL cryovials and stored at -80ºC.

A portion of the frozen heart powder (~100 mg) was placed in ice-cold radioimmunoprecipitation assay (RIPA) buffer (150 mM NaCl, 1.0% IGEPAL CA-630, 0.5% sodium deoxycholate, 0.1% SDS and 50mM Tris, pH 8.0) at 1:10 (w/v) and homogenized using a PRO200 tissue homogenizer (Bio-Gen, Cambridge, Massachusetts) for 2 minutes (15 seconds on, 15 seconds off) at a setting of 2. Protease inhibitor cocktail (1:1000 v/v, Sigma-Aldrich, St. Louis, Missouri) was added to RIPA buffer immediately before use. The homogenate was then centrifuged for 10 min at 10,000 g (4°C). The supernatant (ventricular extract) was collected, aliquoted, and stored at -80°C.

2.7 SR enriched microsomal preparation from fresh ventricle

The protocol was based on the method of Vasanji et al. (2006)[130] with several modifications as follows. Immediately at the end of the perfusion protocol, the ventricles were cut from the cannula and placed in a plastic weigh boat on ice. Ventricles were weighed on ice and immediately minced into approximately 1 mm pieces using a scalpel and small scissors in ice cold SR

homogenization buffer (250 mM sucrose, 5 mM HEPES, 0.2% sodium azide w/v, pH 7.5). Protease inhibitor cocktail (1:1000 v/v, P8340, Sigma-Aldrich, St. Louis, Missouri) was added to the SR homogenization buffer right before use. Minced ventricles were transferred to a 15 mL glass test tube containing SR homogenization buffer (1:10 w/v) and were homogenized on ice using a PRO200 tissue homogenizer at a setting of 2 (Bio-Gen, Cambridge, Massachusetts) for 2 min (repeated cycles of 15 seconds on then 15 seconds off). The resultant homogenate was transferred to a Duall glass homogenizer (Kontes Glass Co, Vineland, New Jersey) and was further homogenized by hand with five strokes on ice. All following centrifugation steps were performed at 4°C using a S100-AT rotor (ThermoFisher, Waltham, Massachusetts) in a mTX 150 micro-ultracentrifuge (ThermoFisher, Waltham, Massachusetts). Homogenates were briefly vortexed, and divided in half. Each sample was added to two 4 mL polycarbonate tubes (ThermoFisher, Waltham, Massachusetts). Samples were placed into a pre-cooled rotor and centrifuged for 10 min at 4,000 g to remove tissue debris. The supernatant was collected and centrifuged for 18 min at 10,000 g to pellet mitochondria. The supernatant was collected and centrifuged again for 18 min at 10,000 g. The supernatant was then centrifuged at for 60 min at 50,000 g to pellet the membrane fraction. The resultant pellet was resuspended in 3 mL of SR homogenization buffer containing 600 mM KCl and equilibrated on ice for 30 min. This solution was centrifuged for 10 min at 7,000 g. The supernatant was then spun for 60 min at 50,000 g. In order to make the final suspension of SR enriched microsomes compatible with the SERCA activity assay, the pellet was gently resuspended in SR homogenization buffer which was adjusted to pH 7.0 using 8-10 strokes with a small Duall glass homogenizer (Kontes Glass Co, Vineland, New Jersey), aliquoted, and stored at -80°C.

2.8 Protein assay

Protein concentrations for all samples were assessed by bicinchoninic acid assay (Sigma-Aldrich, St. Louis, Missouri). Bovine serum albumin (ThermoFisher, Waltham, Massechusetts) was used to produce a standard curve ranging between 31.25-1000 µg/mL. Ventricular homogenate or SR enriched microsomes were diluted in H_2O to a ratio of 1:10 or 1:2, respectively. 10 µL of standard or sample was loaded per well in a clear 96 well plate in duplicates. Copper (II) sulfate solution was added to bicinchoninic acid at a ratio of 1:50 and mixed in a plastic basin. 200 µL of this solution was added to the wells of the 96 well plate using a multi channel pipette. The plate was incubated at 37ºC for 30 minutes and the absorbance in the wells was assessed using a UVmax Kinetic microplate reader (Molecular Devices, San Jose, California). SoftMax Pro (v 5.2 C) was used to acquire and analyze date from the plate reader.

2.9 SERCA activity assay

ATPase activity in SR enriched microsomes was measured by an coupled-enzyme spectrophotometric assay.[131] SERCA activity reagents were purchased from Sigma-Aldrich and were of the highest purity available. Ten mL of activity assay buffer (50 mM imidazole pH 7.0, 100 mM KCl, 5 mM $MgCl_2$, 0.5 mM EGTA, 0.5 mM phosphoenolpyruvate, 2.4 mM ATP, 0.18 mM NADH, 9.6 units/mL pyruvate kinase, 9.6 units/mL of lactate dehydrogenase) was prepared fresh on ice for each experiment. Three concentrations of Ca^{2+} (0, 0.25 or 1 µM) were prepared in activity assay buffer and then loaded into individual plastic basins.

At the same time as the activity assay buffer was made, SR enriched microsome samples were prepared in 10% sucrose to a concentration of 0.1 mg protein/ml followed by addition of 5 µM calcium ionophore A23187 (T9033, Sigma-Aldrich). Samples were then added to a black

Nuclon coated 96 well plate (5 µL/well) in duplicates for each Ca^{2+} concentration. Each reaction was run in the presence or absence of the SERCA inhibitor thapsigargin (5 µM, C7522, Sigma-Aldrich). The reaction was initiated by adding 150 µL of activity assay buffer containing Ca^{2+} from the individual plastic basins prepared above to the microsomal samples in the 96 well plate. The plate was placed in a Synergy H1 plate reader (BioTek, Winooski, Vermont) within 5 min of starting the reaction. The decrease in absorbance of NADH (340 nm) was monitored. The difference in ATPase specific activity (µmol ATP hydrolyzed • mg SR enriched microsomes^{-1} • min^{-1}) between SR enriched microsomes without thapsigargin and those with thapsigargin was used as a measure of SERCA ATPase activity.

2.10 Western blot analysis

Tris-tricine and Tris-glycine sodium dodecyl sulfate polyacrylamide gels were prepared according to the Appendix. For detection of SERCA2a, VDAC1, Na^+/K^+ ATPase, and GAPDH, ventricular homogenates or SR enriched microsomes (20-30 µg total protein) was diluted in RIPA buffer and loaded into tubes containing 1x SDS-PAGE loading buffer (from a 6x stock). Samples were denatured by heating at 95ºC for 5 min. Samples were loaded into a Tris-glycine 10% polyacrylamide gel under reducing conditions and electrophoresed for 120 V until the dye front ran off the gel. For detection of JPH-2, 5 µg of ventricular extract protein was prepared and denatured as described above. The samples were loaded on a Tris-glycine 10% polyacrylamide gel under reducing conditions and electrophoresed in the same manner as above.

For detection of PLN and S^{16} phosphorylated PLN, 5 µg of ventricular extract protein was prepared as above and loaded on a Tris-tricine 16%-polyacrylamide gel under reducing conditions and electrophoresed at 80 V until the dye front passed the stacking and spacing layers. After which,

the voltage was increased to 140 V and the gel was run until the dye front reached the end of the gel but did not run off. Every gel was electrophoresed having a lane containing BLUeye prestained protein ladder (FroggaBio, Toronto, Ontario) as a molecular weight marker. Proteins were wet transferred to a polyvinylidene difluoride membrane (0.2 μm pore size, Bio-Rad, Hercules, California) for 60 min at 100 V. Membranes were then placed in clean plastic trays and blocked in 5% (w/v) skim milk (Carnation, Markham, Ontario) prepared in Tris-buffered saline with Tween 20 (TBS-T) buffer for 2 hr at room temperature. Membranes were then added to 50 mL conical tubes containing primary antibody diluted to the appropriate concentration in 5 % (w/v) skim milk prepared in TBS-T buffer. Primary antibodies for SERCA2a (ab137020), GAPDH, and VDAC1 were diluted at a ratio of 1:10,000. Primary antibodies for SERCA2a (MA3-919), PLN and JPH-2 were diluted at a ratio of 1:2000. Tubes containing membranes were then rotated with primary antibody at 4ºC overnight.

The next day, membranes were washed in TBS-T 7 times (5 min each). Either horseradish peroxidase conjugated goat anti-mouse (Cedarlane, CLCC30007) or horseradish peroxidase conjugated goat anti-rabbit IgG (Cedarlane, CLCC42007) secondary antibodies were used where appropriate. Secondary antibodies were diluted in 5% (w/v) skim milk in TBS-T and then incubated with the membrane for 1 hr at room temperature under gentle shaking. Excess secondary was washed from the membranes with 7 washes with TBS-T (5 min each). Bands on the membrane were detected using Clarity^{TM} ECL western substrate (Bio-Rad, Hercules, California) and exposed to blue x-ray film (Fujifilm, Minato, Tokyo, Japan). Films were developed with an OPTIMAX X-Ray film processor (PROTEC GmbH & Co, Dorfwiesen, Oberstenfeld, Germany) and scanned with a GS-800 densitometer (Bio-Rad, Hercules, California). Bands were quantified using Quantity One (Bio-Rad, Hercules, California) and ImageJ (NIH, v 1.48). Membranes were stained

with Coomassie blue (15 min of staining and 15 min of destaining using destaining solution) and a band was quantified as a loading control.

2.11 Gelatin zymography

Either 20 µg of ventricular extract protein or 30 µg of SR enriched microsomal protein were prepared with RIPA buffer and 1x zymography buffer. Samples were loaded into a Tris-tricine 8% polyacrylamide gel co-polymerized with 2 mg/mL of porcine gelatin (G8150, Sigma-Aldrich, St. Louis, Missouri). 5 µL of Blueye prestained protein ladder (FroggaBio, Toronto, Ontario) and 2 µL of HT1080 cell conditioned media were run on every gel. Samples were electrophoresed at 100 V for 80 min. Gels were then washed at room temperature three times (20 min each) in 2.5% (v/v) Triton X-100 (Fisher Scientific, Ottawa, Ontario) in H_2O with gentle agitation to remove sodium dodecyl sulphate and allow proper refolding of gelatinases.

Gels were incubated for 40-48 hours in zymography incubation buffer at 37 ºC. Following incubation, gels were stained with Coomassie blue for 3 hr at room temperature. Gels were destained using 2% methanol and 4% acetic acid (v/v) in H_2O under gentle agitation for at least 24 hr before scanning.

Gels were scanned with a GS-800 densitometer and activity bands (clear against a dark blue background) were quantified using QunatityOne (v 4.6.6, Bio-Rad, Hercules, California) and ImageJ (v 1.48, NIH).

2.12 In vitro proteolysis assay

2.12.1 4-aminophenylmercuric acetate activation of MMP-2

4-aminophenylmurcuric acetate (APMA) activates the zymogen form of MMP-2 by disrupting the sulfhydryl bond between C^{102} and the catalytic zinc ion.[132] Human full length MMP-2 purified from TIMP-2 knockout human fibrosarcoma cells (HT1080 cell line) prepared in our lab (0.2 mg/mL)[85] was added to activity buffer (150 mM NaCl, 50 mM Tris-HCl, 5 mM $CaCl_2$, pH 7.6) containing 1 mM APMA to a final volume of 200 µL. The reaction was incubated at 37 ºC for 2 hr. After, a small portion of the APMA activated MMP-2 was diluted to 1 ng/mL in order to confirm its activity by gelatin zymography. APMA activated MMP-2 was then aliquoted and stored at -80°C.

2.12.2 SERCA2a proteolysis in SR enriched microsomes

SR enriched microsomes (2 µg) prepared from the ventricles of the perfused hearts (aerobic group) were incubated with increasing concentrations of APMA activated MMP-2 (1, 10 and 100 ng of MMP-2) for 2 hr at 37°C in activity buffer (150 mM NaCl, 50 mM Tris-HCl, 5 mM $CaCl_2$, pH 7.6). ARP-100 (100 µM) was added to an additional reaction. One sample of SR enriched microsomes was kept for 2 hr at 4°C to rule out non-specific degradation of SERCA2a. Samples were prepared with SDS-PAGE loading buffer and electrophoresed on a Tris-glycine 10% polyacrylamide gel under reducing at 120 V for 80 min. Proteins on the gel were transferred to a polyvinylidene difluoride membrane (0.2 µm pore size, Bio-Rad, Hercules, California) for immunoblot analysis using mouse anti-SERCA2a (Invitrogen MA3-919, 1:2000) as described above. Membranes were scanned with a GS-800 densitometer and bands were quantified using QunatityOne (v 4.6.6, Bio-Rad, Hercules, California) and ImageJ (v 1.48, NIH).

2.12.3 Purified porcine SERCA2a proteolysis

SERCA2a purified from porcine cardiac muscle was reconstituted in proteoliposomes as described previously described.[129] APMA activated MMP-2 was incubated with 7 μg of purified porcine SERCA2a in proteoliposomes (1:500-1:10 molar ratio MMP-2:SERCA2a) for 2 hr at 37°C in activity buffer. An additional reaction (1:10 MMP-2:SERCA2 molar ratio) was performed in the presence of ARP-100 (30 μM). After the reaction was complete, samples were electrophoresed under reducing conditions using a Tris-glycine 10% polyacrylamide gel for 80 min at 120V. Proteins in the gel were stained with Coomassie blue. Gels were scanned with a GS-800 densitometer and bands were quantified using QuantityOne (v 4.6.6, Bio-Rad, Hercules, California) and ImageJ (v 1.48, NIH).

2.12.4 In vitro proteolysis of JPH-2

5 μg of ventricular extract protein from an aerobic rat heart was added to a tube containing MMP-2 (1-100 ng) in MMP-2 incubation buffer to a final volume of 20 μL. ARP-100 (30 μM) was added to one tube to inhibit MMP-2 activity. The samples were incubated at 37°C for 2 hr. After, samples were prepared with SDS-PAGE loading buffer and electrophoresed on a Tris-glycine 10% polyacrylamide gel under reducing at 120 V for 80 min. Proteins on the gel were transferred to a polyvinylidene difluoride membrane (0.2 μm pore size, Bio-Rad, Hercules, California) for immunoblot analysis using mouse anti-SERCA2a (Invitrogen MA3-919, 1:2000) as described above. Membranes were scanned with a GS-800 densitometer and bands were quantified using QuantityOne (v 4.6.6, Bio-Rad, Hercules, California) and ImageJ (v 1.48, NIH).

In order to assess the time course of JPH-2 degradation and to better detect degradation products, 20 µg of ventricular extract protein (from the same aerobic sample above) was incubated with and without MMP-2 (molar ratio 1:50) for 15, 30, 45, and 60 minutes at 37ºC. Products were prepared, electrophoresed and visualized by the same method above.

In a similar experiment, 20 µg of ventricular extract protein (from the same aerobic sample above) was incubated with and without MMP-2 (molar ratio 1:50) for 30, 60 and 90 minutes at 37ºC. Products were prepared, electrophoresed and visualized by the same method above.

2.13 In silico cleavage site analysis of SERCA2a by MMP-2

The primary amino acid sequences for rat SERCA2a was on Uniprot (https://uniprot.org) and entered into CleavPredict (http://cleavpredict.sanfordburnham.org/) in order to predict cleavage sites of MMP-2. CleavPredict is a free online server which predicts the cleavage sites and resulting fragment sizes for proteolysis by 11 different human MMPs. High probability cleavage sites were mapped on a 3D structure of rat SERCA2a using PyMOL (v 2.1.1). This stricture was created by homology modeling of SERCA2a (UNIPROT: P115087) using SWISS-MODEL[133] with the template of rabbit SERCA2a (PDB ID: 5MPM) from Protein Data Bank (www.rcsb.org).[134] Three dimensional structure of rat SERCA2a from the homology modeling was refined using KoBaMIN.[135] Structural Analysis and Verification Server (SAVES) was implemented for evaluating the quality and validation of the refined 3-D structure model.[136] Finally, PyMOL was used to analyze and visualization of the refined structure.

2.14 Statistical analysis

Data are expressed as mean ± SEM for *n* independent experiments. Either two-way or one-way ANOVA was performed where appropriate. Either Tukey's multiple comparison test or Dunnett's test was used for post-hoc comparisons for all experiments.

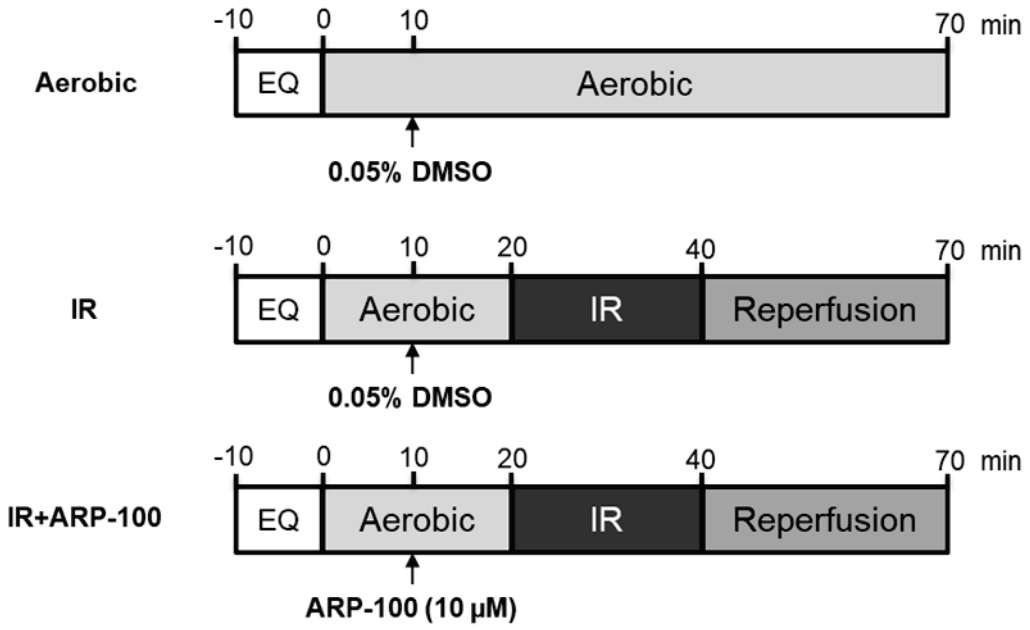

Figure 2.1: Schematic diagram of perfusion protocol for the three groups of isolated rat hearts: aerobic hearts (n=6), IR hearts (n=7), and IR + ARP-100 hearts (n=6). IR hearts were subjected to 20 min of global, no-flow ischemia, followed by 30 min of aerobic reperfusion. ARP-100 (10 µM) or DMSO vehicle (0.05%) was added to the recirculating buffer 10 min into perfusion.

Chapter 3: Results

3.1 Determining possible inhibitory effect of MMP inhibitor ARP-100 on calpain activity

Troponin I is a known substrate of calpain in vitro.[137] In order to determine if ARP-100 inhibits calpain activity, calpain-2 was incubated (1 hr at 37°C) with a troponin I fragment (aa 1-77) in the presence or absence of DMSO vehicle, ARP-100 or MDL-28170 (30 μM each). Incubation of calpain with troponin I aa 1-77 at a ratio of 1:500 resulted in limited proteolysis of the main band into several smaller degradation products as shown in lane 2 (Figure 3.1). These degradation products were prevented by pre-incubating calpain with MDL-28170 but not with ARP-100. This suggests that ARP-100 does not inhibit calpain activity up to a concentration of 30 μM.

3.2 Effect of ARP-100 on cardiac performance of rat hearts subjected to IR injury

Prior to the start of the isolated working rat heart experiments, the solubility of ARP-100 was confirmed in the recirculating modified Krebs-Henseleit buffer system for 2 hr at 37°C. The effect of ARP-100 (10 μM) on parameters of aerobic heart function was also assessed, and it was determined that ARP-100 had no effect on measured parameters (peak systolic pressure, heart rate, aortic flow and cardiac output) over 90 min on an aerobic control heart (n=2, data not shown).

Three groups of isolated rat hearts were perfused in working mode for a total of 70 min: Aerobic (n=6), IR (n=7), and IR+ARP-100 (n=6). Either ARP-100 or DMSO vehicle were added into the recirculating buffer system at 10 min into the perfusion. Initial 20 min of aeobic perfusion were followed by 20 min ischemia and 30 min reperfusion in the IR and IR+ARP-100 groups. The main parameter measured to assess contractile function was cardiac work, which is the product of

peak systolic pressure and cardiac output. Other measured and derived parameters include aortic flow, coronary flow, and heart rate (Table 3.1). There was no difference between the three groups in any of these parameters prior to ischemia (20 min into the perfusion) as shown in Table 3.1. The cardiac contractile function of the aerobic group was stable for the full 70 min perfusion as measured by cardiac work (Figure 3.2a). IR hearts showed a significant impairment in the recovery of cardiac work during reperfusion as compared with aerobic hearts (Figure 3.2a). The MMP inhibitor ARP-100 significantly improved the recovery of cardiac work during reperfusion as compared to the IR hearts at 70 min ($p<0.05$, Figure 3.2a). This was reflected by a significant improvement in cardiac output ($p<0.05$, Figure 3.2b), but not peak systolic pressure, between IR+ARP-100 and IR groups (Figure 3.2c). Heart rate was significantly depressed in the IR group at the end of perfusion compared with aerobic, but not the IR+ARP-100 group compared with aerobic ($p<0.05$, Table 3.1). ARP-100 also improved coronary flow at the end of reperfusion versus IR hearts ($p<0.05$, Table 3.1). This is the first study to show a cardioprotective effect of ARP-100 against myocardial stunning.

3.3 SERCA2a levels in hearts following perfusion

The level of SERCA2a in ventricular extracts was not different between the three experimental groups, as measured using two different antibodies (Figure 3.3a, b). A longer exposure of the membrane probed with mouse anti-SERCA2a (2A7-A1) revealed several lower molecular weight bands which may be proteolytic products of SERCA2a between 48 and 75 kDa (Figure 3.4a). Of interest, 3 prominent bands were observed of ~70, 65 and 50 kDa. The 70 kDa product was increased two-fold in IR hearts compared to aerobic hearts ($n=6$-7, $p<0.05$, Figure 3.4b). This increase was absent in the IR+ARP-100 group hearts. In contrast, the 65 kDa product

was increased in both IR and IR+ARP-100 groups compared to vehicle, suggesting this product is formed in an MMP-independent manner (n=4, $p<0.05$, Figure 3.3c). The 50 kDa band was unchanged across all heart groups (n=4, Figure 3.3d). Due to the low density for the 50 and 65 kDa bands, only n = 4/group could be quantified. The density of the 70 kDa band mentioned above correlated negatively with cardiac work at the end of perfusion (r^2=0.33, Figure 3.3e).

3.4 Sulfonic acid modification of SERCA2a in hearts following perfusion

SERCA2A degradation to products at 60 and 70 kDa was associated with increased cysteine sulfhydryl oxidation to sulfonic acid of SERCA2a residue C^{674} in aorta from hyperlipidemic pigs compared to control aorta.[109] We therefore wanted to see if the increased 70 kDa SERCA2a product found using the MA3-919 anti-SERCA2a antibody in the IR group was associated with an increase in C^{674} sulfonylation of SERCA2a. A representative membrane is shown in Figure 3.5a. This antibody detected numerous bands between 65 kDa and 235kDa. No clearly identifiable band was detected at 110 kDa. Prominent bands were found above 135 kDa and at ~70 kDa. The 70 kDa band was approximately the same molecular weight as the prominent degradation band found with the 2A7-A1 SERCA2a antibody. Quantification of this band showed no changes between the three groups of isolated rat hearts (Figure 3.5b). Due to the poor signal to noise ratio for the bands detected using this antibody, only an n = 4-5 hearts per group could be quantified.

3.5 Phospholamban levels in hearts following perfusion

Phospholamban is a key negative regulator of SERCA2a function in cardiac ventricular tissue. [108] Phosphorylation of phospholamban relieves this inhibition. We therefore looked at levels of phospholamban and phosphorylated phospholamban. The levels of phospholamban in ventricular extracts were the same in all groups (Figure 3.6a). When phosphorylated, phospholamban tends to form pentamers.[97] Because of this, the 25 kDa product of S^{16} phosphorylated phospholamban is thought to be a more accurate reflection of total S^{16} phosphorylated phospholamban. Levels of S^{16} phosphorylated phospholamban pentamer were unchanged between groups (Figure 3.6b). A longer exposure revealed additional bands which when quantified together which showed no change (data not shown). An increase in the ratio of S^{16} phosphorylated phospholamban pentamer : phospholamban was observed in the IR+ARP-100 group compared with the aerobic group ($p<0.05$, Figure 3.6c). Levels of total S^{16} phosphorylated phospholamban pentamer : phospholamban were also increased in the IR+ARP100 group compared with the aerobic group (data not shown).

3.6 Verification of purity and activity in response to calcium of SR enriched microsomes

Ventricular tissue was isolated freshly (without freezing) from perfused rat hearts (aerobic, IR and IR+ARP-100 groups). It was then immediately used to isolate the cytosolic fraction and SR enriched microsomes. The purity of the SR enriched microsomes was assessed against the starting homogenate and cytosolic fraction by immunoblot using antibodies against organelle specific markers (Figure 3.7a). The SR marker used was SERCA2a, the plasmalemmal marker was Na^+/K^+ ATPase, the mitochondrial marker was VDAC1 and the cytosolic marker was GAPDH. SERCA2a was highly enriched in SR enriched microsomes compared with the

homogenate. SR enriched microsomes also contained contaminants from the mitochondria and plasma membrane as shown by some signal for VDAC1 and Na^+/K^+ ATPase. SR enriched microsomes are free from cytosolic contamination as only the starting homogenate and cytosolic fraction showed the presence of GAPDH.

A Ca^{2+} titration curve was performed on SR enriched microsomes from an aerobic heart (Figure 3.7b). We found maximal thapsigargin dependent ATPase activity, attributable to SERCA activity, at a Ca^{2+} concentration of 1 μM and a midpoint SERCA activity at a Ca^{2+} concentration of 0.25 μM. This is an expected Ca^{2+} response in relation to the change in $[Ca^{2+}]_i$ in cardiac myocytes during systole and diastole.[86] These calcium concentrations were then used to assess SERCA2a activity at so denoted intermediate (0.25 μM) and high (1 μM) calcium concentrations in SR enriched microsomes from the three groups.

3.7 SERCA2a activity in SR enriched microsomes

One of the main objectives of this study was to determine if MMPs, activated in the myocardium as a result of IR injury, impair SERCA2a function following IR injury. SERCA2a activity was assessed by thapsigargin dependent ATPase activity in SR enriched microsomes obtained from the three groups, and expressed as μmol ATP hydrolyzed • min^{-1} • mg $protein^{-1}$. SERCA2a activity was not statistically different between the groups at 1 μM Ca^{2+} (Figure 3.8a). In contrast, at 0.25 μM Ca^{2+}, SERCA2a activity was decreased in both the IR and IR+ARP-100 groups ($p<0.05$, Figure 3.8b).

3.8 MMP-2 activity in SR enriched microsomes and ventricular extracts by gelatin zymography

Activity of gelatinases (MMP-2 and MMP-9) was assessed by gelatin zymography in SR enriched microsomes and ventricular extracts from the three groups of isolated working rat hearts. HT1080 cell conditioned media was run with every gel as a standard for MMP-2 and MMP-9 (Figure 3.9). As previously reported, ventricular extracts showed a major band of 72 kDa MMP-2 activity and a faint band of 64 kDa. We report here for the first time that SR enriched microsomes contain 72 kDa, and to a lesser extent 64 kDa, MMP-2 activity. SR enriched microsomes should not encompass the MAM as it pellets with the mitochondria, therefore here we show that MMP-2 is also localized to regions of the SR outside of the MAM. Neither the ventricular extracts nor SR enriched microsomes showed MMP-9 signal. In the ventricular extracts, IR+ARP-100 hearts had less MMP-2 activity than the aerobic hearts ($p<0.05$, Figure 3.9a). There was no difference in MMP-2 signal in SR enriched microsomes from the three groups of hearts (Figure 3.9b).

3.9 In vitro proteolysis of SERCA2a by MMP-2

3.9.1 In vitro proteolysis of SERCA2a in SR enriched microsomes from an aerobic heart by exogenous MMP-2

SR enriched microsomes prepared from aerobic control hearts were incubated with APMA-activated MMP-2 for 2 hr at 37ºC in order to assess the susceptibility of native rat SERCA2a to MMP-2 proteolysis (Fig. 3.10). Products from the in vitro proteolysis experiment were visualized by immunoblot using the SERCA2a (2A7-A1) antibody (Fig. 3.10). Incubation of SERCA2a at 37°C caused the formation of oligomers around 250 kDa. Incubation with increasing amounts of MMP-2 firstly caused a reduction in SERCA2a oligomers which is was accompanied by an

increase in the SERCA2a monomer. The density of the SERCA2a monomer was reduced at a higher concentration of MMP-2 (100 ng). This loss of SERCA2a by MMP-2 was prevented with ARP-100 (Figure 3.10a). A longer exposer of this membrane (Fig. 3.10b) revealed the formation of two ~70 kDa SERCA2a degradation products, which did not appear with ARP-100. This experiment suggests that SERCA2a in its native form is susceptible to proteolysis by exogenously provided MMP-2.

3.9.2 In vitro proteolysis of SERCA2a in purified cardiac SERCA from porcine hearts by exogenous MMP-2

Purified porcine SERCA2a embedded in proteoliposomes was received from Dr. Howard Young as a gift. 7 µg of porcine SERCA2a was incubated with increasing molar ratios of APMA-activated MMP-2 (1:500-1:10) at 37°C for 2 hr (Figure 3.11). One reaction (1:10 MMP-2:SERCA2a) was run in the presence of ARP-100. Purified SERCA2a by itself contained some impurities as shown by several smaller molecular weight bands well below the 100kDa marker. Increasing molar ratios of MMP-2 caused first a degradation of the 110 kDa SERCA band to a slightly lower molecular weight band at around 100 kDa. This was followed by the disappearance of both the main band and the 100 kDa product at a ratio of 1:50. Addition of ARP-100 to the reaction prevented the proteolysis of SERCA2a. Due to the presence of other smaller molecular weight contaminating proteins or already degraded SERCA2a in porcine cardiac SR prep, any smaller MMP-2-dependent degradation products of SERCA2a could not be identified.

3.10 In silico prediction of MMP-2 cleavage sites on SERCA2a

The primary amino acid sequence of rat SERCA2a was obtained on Uniprot (https://uniprot.org). This sequence was then entered into CleavPredict; a free online database for determining potential cleavage sites for several MMPs.[138] CleavPredict predicts secondary structures and disordered regions and takes this into account in its final prediction. Many putative cleavage sites for MMP-2 were found on SERCA2a primary structure. Of interest, three of these sites give potential degradation products of around 70 kDa (Figure 3.12a). These sites were mapped onto a 3-D structure of rat SERCA2a using PyMOL. As only the rabbit crystal structure is available, rat primary sequence was used to create a pseudo 3D rendering using the rabbit crystal structure using SWISS-MODEL. [133] Only two of the three identified cleavage sites are accessible to cleavage in the cytosolic domain, P1 at 609 and 664, and are illustrated in Figure 3.12b

3.11 Levels of JPH-2 in the three groups of isolated working hearts

JPH-2 coordinates the SR in close proximity to the t-tubules, and is essential for proper excitation contraction coupling [88]. Levels of 90 kDa JPH-2 were unchanged between the three groups of rat hearts (Figure 3.13a). When the membranes were overexposed, a smaller band was present around 75 kDa, which may be a JPH-2 degradation product (Figure 3.13b). This band increased in the IR group compared to the aerobic group ($p<0.05$).

3.12 In vitro degradation of JPH-2 by MMP-2 in ventricular extracts

Ventricular extract (4 µg total protein) from an aerobic sample was incubated (1 hr at 37ºC) with increasing amounts of APMA-activated MMP-2 (1-100 ng) followed by immunoblot to detect JPH-2 (Figure 3.14a). MMP-2 proteolyzed JPH-2 in a concentration dependent manner which was prevented with ARP-100.

In order to detect degradation products, 20 µg of ventricular extract was incubated with and without 10 ng MMP-2 at 37 ºC for 15-60 min. Immunoblot was then performed on the products to detect JPH-2 (Figure 3.14b). There was a time-dependent degradation of JPH-2 to ~65 and lower kDa products which was independent of exogenously added MMP-2. In as little as 15 min, a ~65 kDa fragment was observed in the absence of MMP-2. Addition of MMP-2 resulted in increased degradation of the main JPH-2 band at 60 min.

Table 3.1: Parameters of heart performance before ischemia (20 min into perfusion) and at the end of reperfusion (70 min into perfusion) for the three groups of isolated working rat hearts.

*$p<0.05$ vs aerobic using one-way ANOVA followed by Tukey's post hoc test.

‡ $p<0.05$ vs IR using one-way ANOVA followed by Tukey's post hoc test.

Pre-ischemia (t = 20 min)	**Aerobic (n=6)**	**IR (n=7)**	**IR+ARP-100 (10 µM, n=6)**
Cardiac output (mL/min)	62.3±3.5	62.7±4.6	67.3±5.3
Aortic flow (mL/min)	41.5±1.8	43.9±4.6	47.7±4.4
Coronary flow (mL/min)	20.8±2.5	18.9±1.1	19.7±1.4
Heart rate (bpm)	272±6	266±8	262±15
Peak systolic pressure (mmHg)	117±3	112±2	120±2
Cardiac work ($mmHg*mL*min^{-1}*1000^{-1}$)	6.6±0.4	7.0±0.6	7.4±0.8
End of reperfusion (t = 70 min)	**Aerobic (n=6)**	**IR (n=7)**	**IR+ARP-100 (10 µM, n=6)**
Cardiac output (mL/min)	64.8±2.2	23.0±8.1*	45.3±4.4‡
Aortic flow (mL/min)	45.3±1.6	11.1±4.7*	23.0±4.9*
Coronary flow (mL/min)	19.5±0.8	11.9±3.7	22.3±1.8‡
Heart rate (bpm)	277±10	118±45*	194±21
Peak systolic pressure (mmHg)	118±4	79±23	124±6
Cardiac work ($mmHg*mL*min^{-1}*1000^{-1}$)	6.9±0.3	2.6±0.9*	5.1±0.5‡

Table 3.2: Complete list of predicted MMP-2 cleavage sites on rat JPH-2 using CleavPredict. Position weight matrices (PWM, range: 0-12) score rates cleavage sites based on their sequence in relation to the determined consensus sequence of MMP-2. Sec Str pred = predicted secondary structure. E indicates a strand, H indicates a helix, and _indicates no predicted secondary structure. Regions which are predicted to be disordered are designated with an asterisk. Predicted N and C terminal cleavage fragment masses on the right. All predicted sites are in the cytosolic domain of JPH-2.

P1 position	Residues	PWM Score	Sec Str pred	Disorder	N-mass (M_r)	C-mass (M_r)
50	FEVAG-VYTWP	1.12	EEEEEEEE__	··········	5099.11	69131.55
150	SVPYG-MAVVV	0.53	E____EEEEE	··········	16333.29	57897.37
158	VVRSP-LRTSL	1.58	EEE_______	·········**	17172.76	57057.90
165	TSLSS-LRSEH	7.24	__________	.*********	17917.16	56313.50
200	GFALS-LLATA	1.78	_HHHHHHHHH	··········	21378.90	52851.76
201	FALSL-LATAE	3.40	HHHHHHHHHH	··········	21491.98	52738.68
213	RPPGL-FTRGA	4.50	______HHHH	··········	22639.61	51591.05
222	ALLGR-LRRSE	5.91	HHHHHHH___	····******	23611.17	50619.49
241	SRLSF-LKSEL	6.78	HHHHHHHH__	**********	25815.33	48415.33
272	DAAAP-FDADI	2.62	__________	*·········	28628.60	45602.06
288	TYMGE-WKNDK	2.95	EEE_______	··········	30389.32	43841.34
305	ERSSG-LRYEG	0.97	_______HHH	**········	32267.21	41963.45
315	EWLDN-LRHGY	1.29	HHHHH_____	··········	33542.78	40687.88
350	RRVLP-LKSNK	5.07	EEEE______	.*********	37619.98	36610.68
372	QRAAA-IARQK	3.79	HHHHHHHHHH	**********	39977.27	34253.39
382	AEIAA-SRTSH	1.90	HHHHHHH_HH	**********	41028.88	33201.78
399	AEQAA-LAANQ	1.22	HHHHHHHHHH	**********	42736.75	31493.91
411	NIART-LAKEL	2.26	HHHHHHHHHH	**********	44005.39	30225.27
435	RLLQE-ILENS	0.73	HHHHHHHH__	**********	46875.86	27354.80
487	TPPQP-KRPRP	0.88	__________	**********	52457.56	21773.10
494	PRPGS-SKDGL	2.29	__________	**********	53236.00	20994.66
504	LSPGA-WNGEP	1.36	__________	**********	54161.47	20069.19
518	SRPAT-PSDGA	0.61	__________	**********	55557.07	18673.59
547	PPPAP-SREPE	2.82	________HH	**********	58501.52	15729.14
555	PEVAL-YRGYH	4.07	HHHHHHH___	******.····	59382.97	14847.69
594	EPPSP-VSATV	4.94	_______E_E	**********	63720.92	10509.74
607	ESPAP-RSRVP	1.35	__________	**********	65045.53	9185.13
617	AKPAT-LEPKP	2.79	__________	**********	66109.15	8121.51
622	LEPKP-IVPKA	0.62	__________	**********	66673.46	7557.20
640	TEARG-LSKAG	3.96	HHHHHHHHHH	**********	68604.58	5626.08

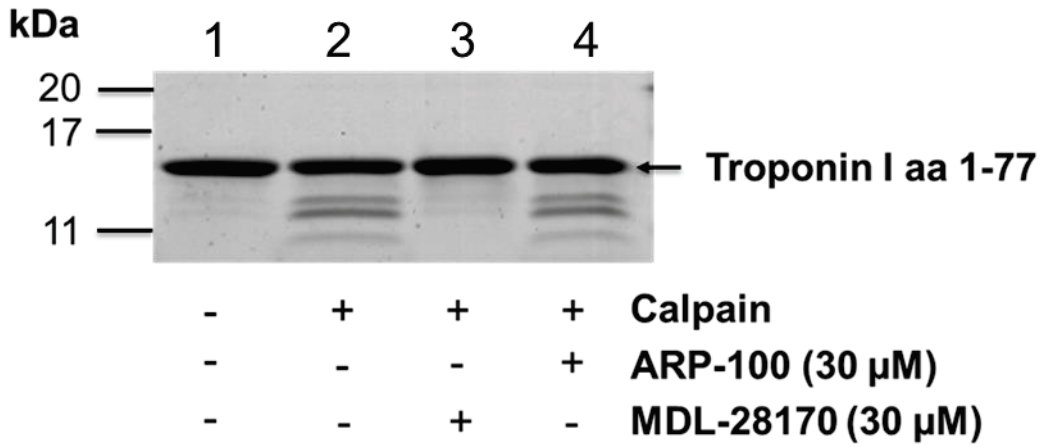

Figure 3.1: Purified calpain-2 (lane 2-4) incubated (1 hr, 37ºC) with troponin I aa 1-77 fragment (lane 1-4) in the presence or absence of vehicle (DMSO, lane 1, 2), 30 µM ARP-100 (lane 3), or 30 µL MDL-28170 (lane 4). ARP-100 had no effect on calpain mediated troponin I aa 1-77 degradation. Position of molecular weight markers is indicated on the left.

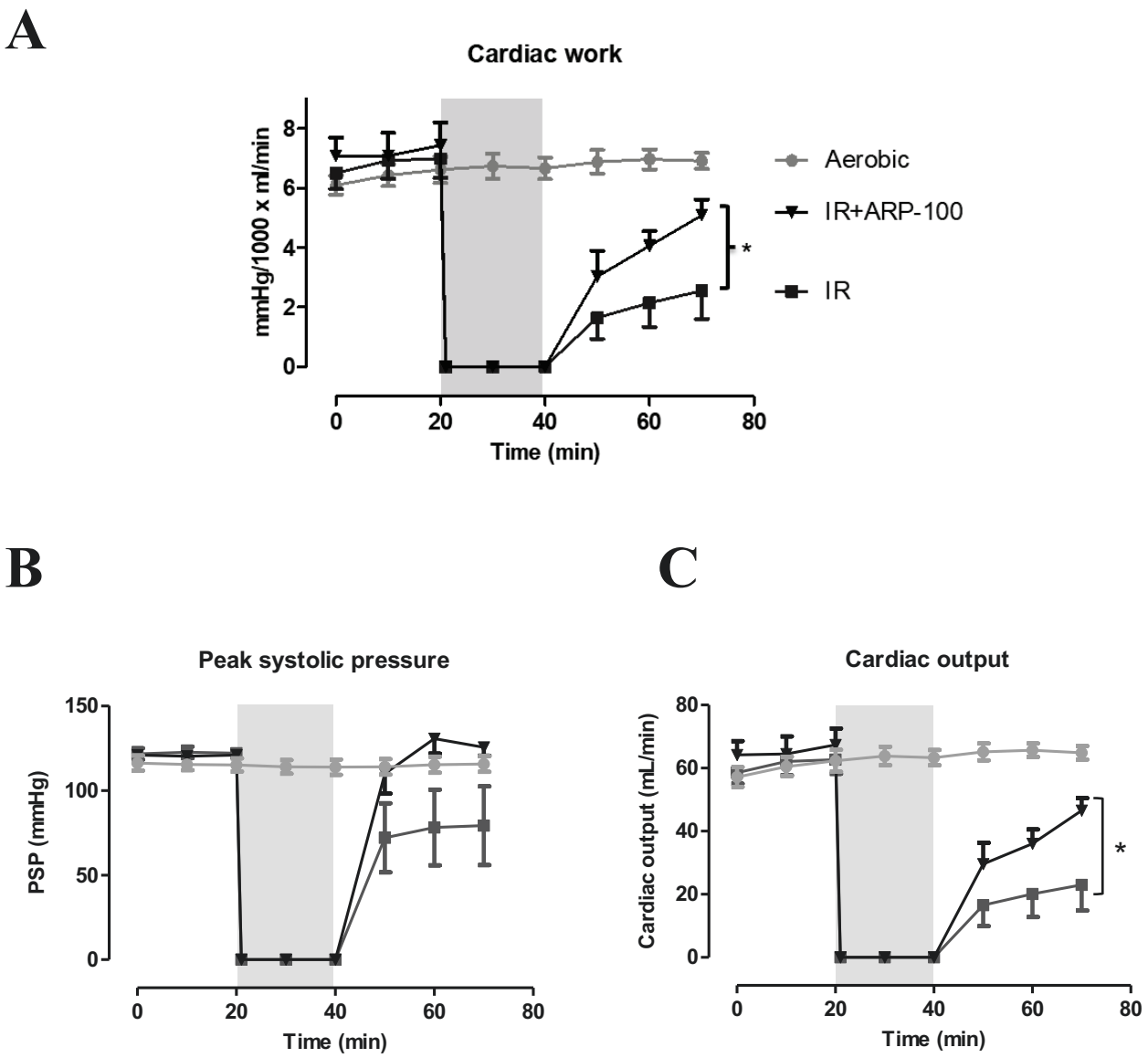

Figure 3.2: Cardiac contractile performance as measured by cardiac work, the product of peak systolic pressure and cardiac output. IR hearts were subjected to 30 min global, no-flow ischemia (indicated by grey box in A-C) followed by 30 min reperfusion in the presence or absence of ARP-100 (10 μM). (A) ARP-100 significantly improved the recovery of cardiac work following IR. (B) Peak systolic pressure during the time course of perfusion. (C) Cardiac output during the time course of perfusion. *$p<0.05$ by two-way ANOVA followed by Tukey's post hoc test.

A

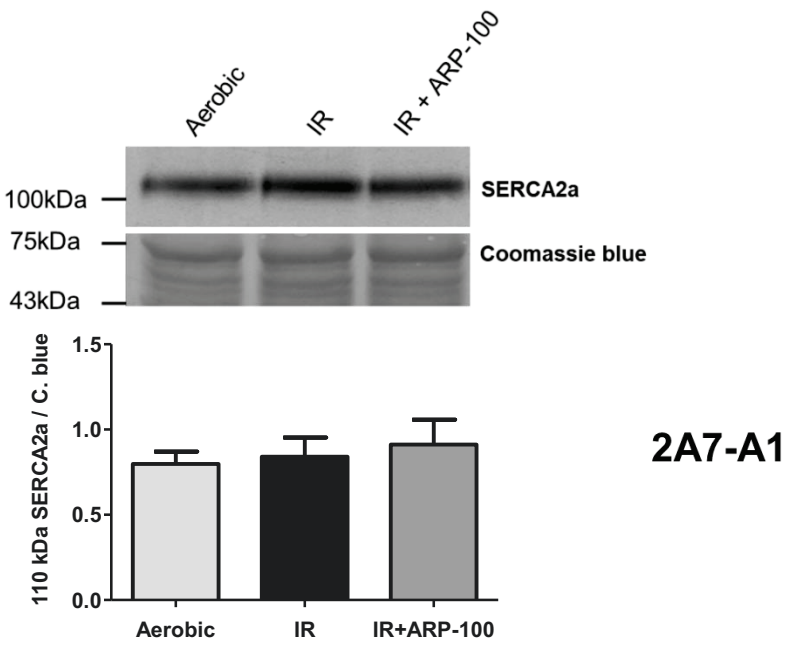

B

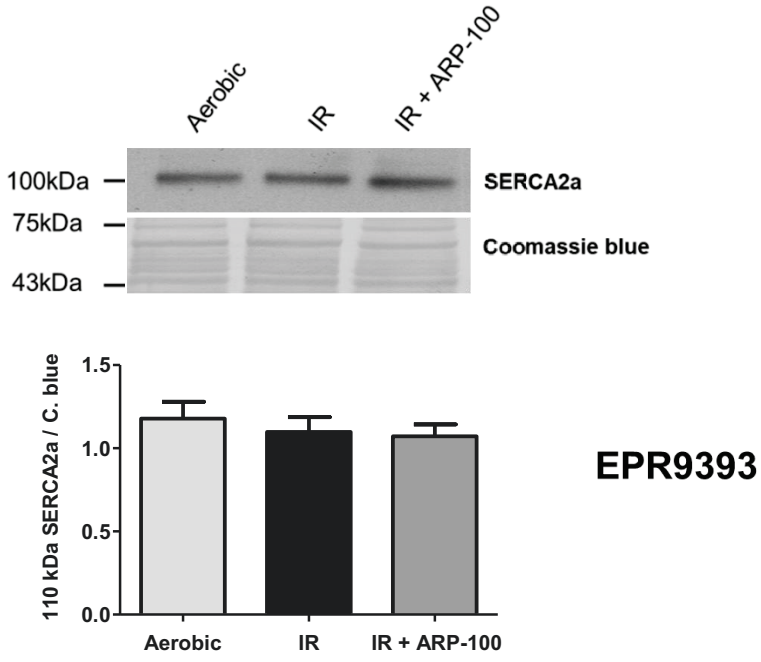

Figure 3.3: SERCA2a protein levels in ventricular extracts from isolated working rat hearts. (A) Representative immunoblot (upper) and quantified results of SERCA2a band density using 2A7-A1 antibody for detection of SERCA2a (n=6-7/group). (B) Representative immunoblot (upper) and quantified results of SERCA2a band density using EPR9393 antibody for detection of SERCA2a (n=6-7/group). Position of molecular weight markers indicated on the left. Test used: one-way ANOVA followed by Tukey's post hoc test.

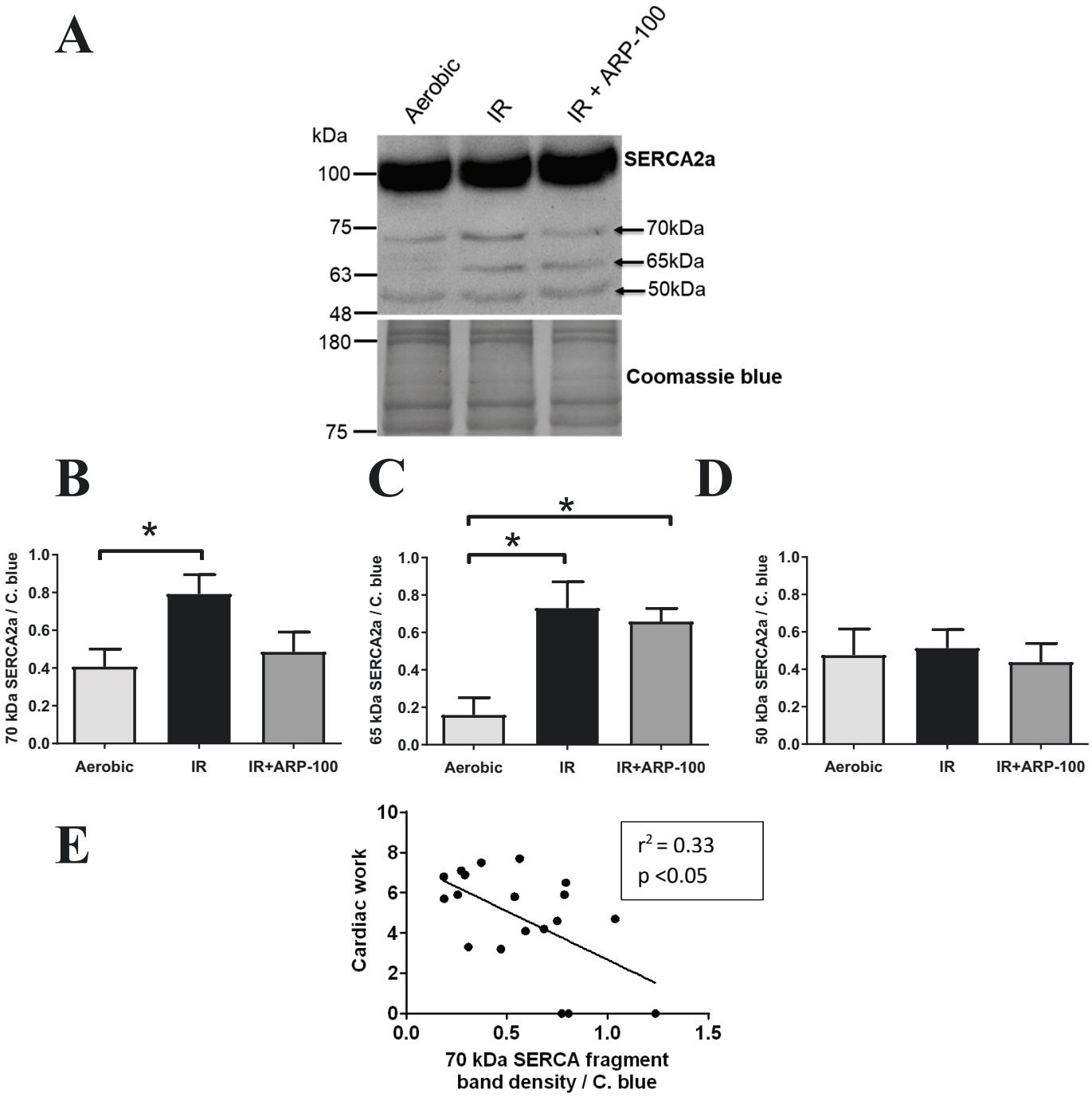

Figure 3.4: Protein levels of SERCA2a and potential degradation products in ventricular extracts from isolated working rat hearts. (A) Detection and quantification of three putative SERCA2a products from the 2A7-A1 epitope antibody at 75 kDa (n=6-7/group), 65 kDa (n=4/group), and 50 kDa (n=4/group). Representative western on top shows position of molecular weight markers on the left and arrows pointing to the three quantified bands on the right. (B) Cardiac work at end of perfusion for all groups plotted against 70 kDa SERCA2a fragment in arbitrary units (n=19). *p<0.05 by one-way ANOVA followed by Tukey's post hoc test.

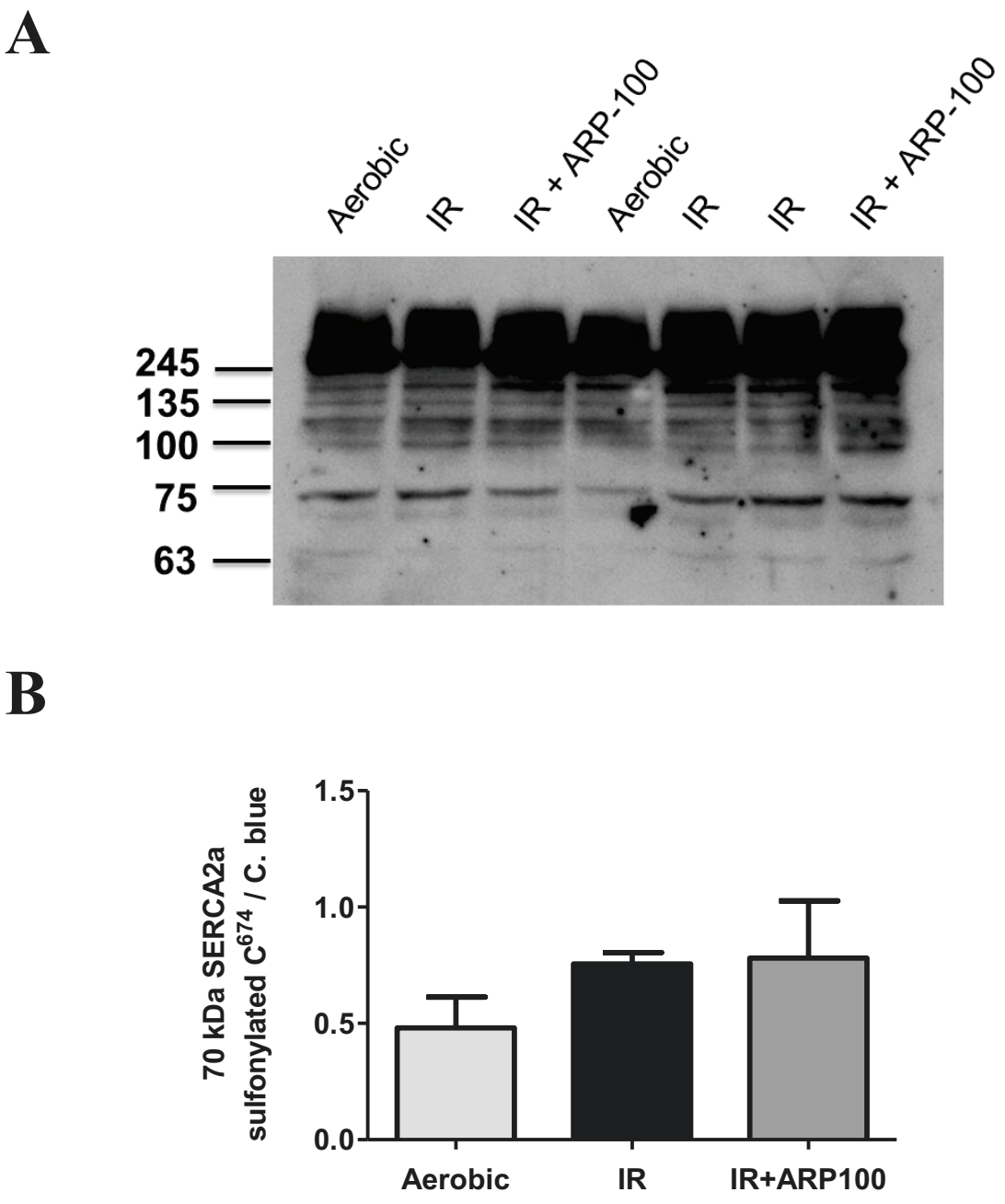

Figure 3.5: Protein levels of C^{674} sulfonylated SERCA2a in ventricular extracts using a custom antibody. (A) A representative western of one membrane showing that the SERCA2a sulfonylated C^{674} antibody detects multiple bands in ventricular extracts including a prominent band at ~ 70 kDa. Positions of molecular weight markers inidicated on the left. (B) Quantification of the 70 kDa C^{674} sulfonylated SERCA2a band normalized to coomassie blue (n=4-5/group). Test used: one-way ANOVA followed by Tukey's post hoc test.

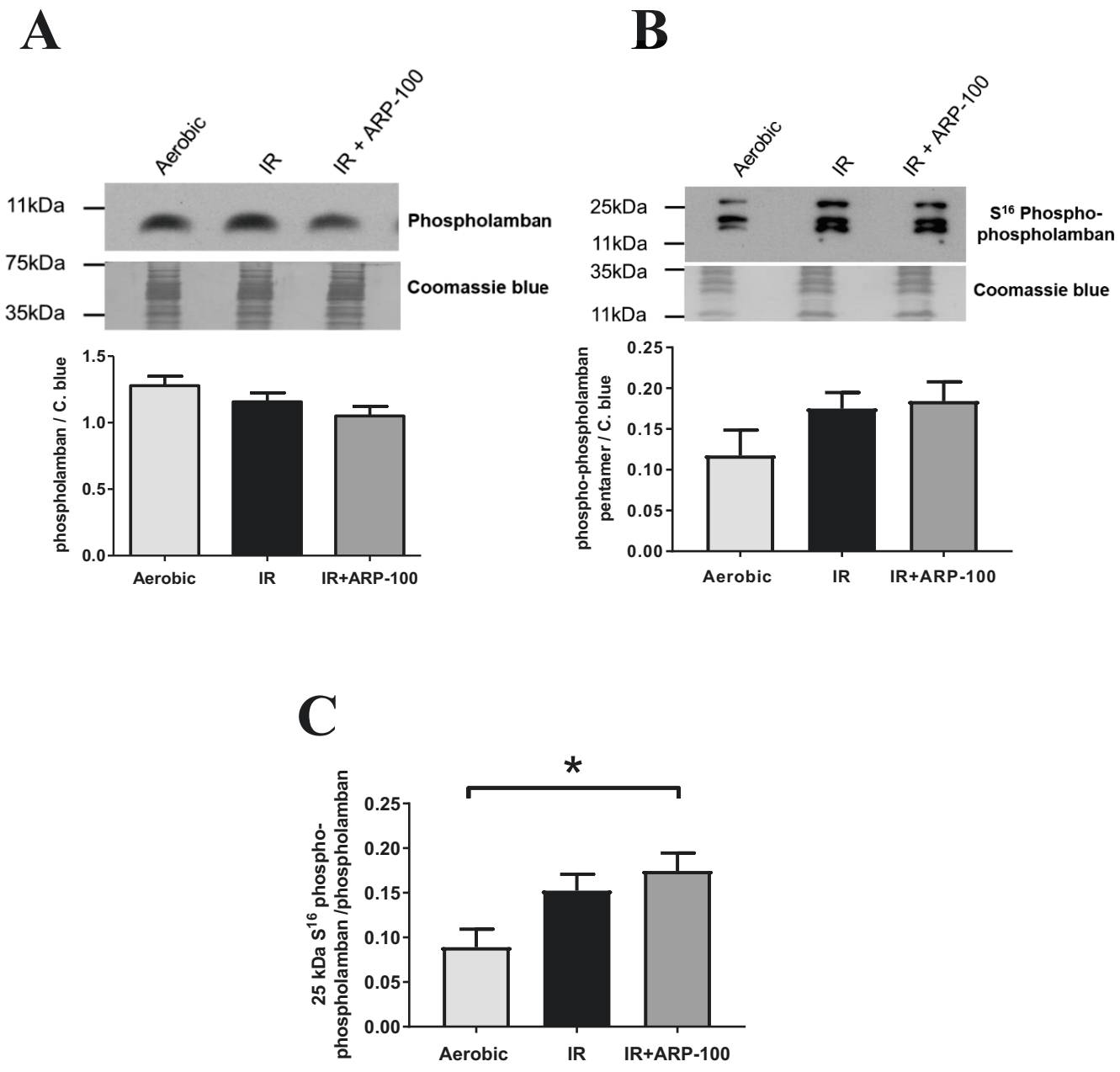

Figure 3.6: Protein levels of phospholamban and S^{16} phosphorylated phospholamban in ventricular extracts from isolated working rat hearts. (A) Levels of phospholamban were unchanged between groups (n=6-7/group). (B) Levels of pentameric (25 kDa) S^{16} phosphorylated phospholamban were unchanged between groups (n=6-7/group). Position of molecular weight markers indicated on the left of representatives. (C) The ratio of S^{16} phosphorylated phospholamban to phospholamban was increased in IR+ARP-100 compared to aerobic group (n=6-7/group). *$p<0.05$ by one-way ANOVA followed by Tukey's post hoc test.

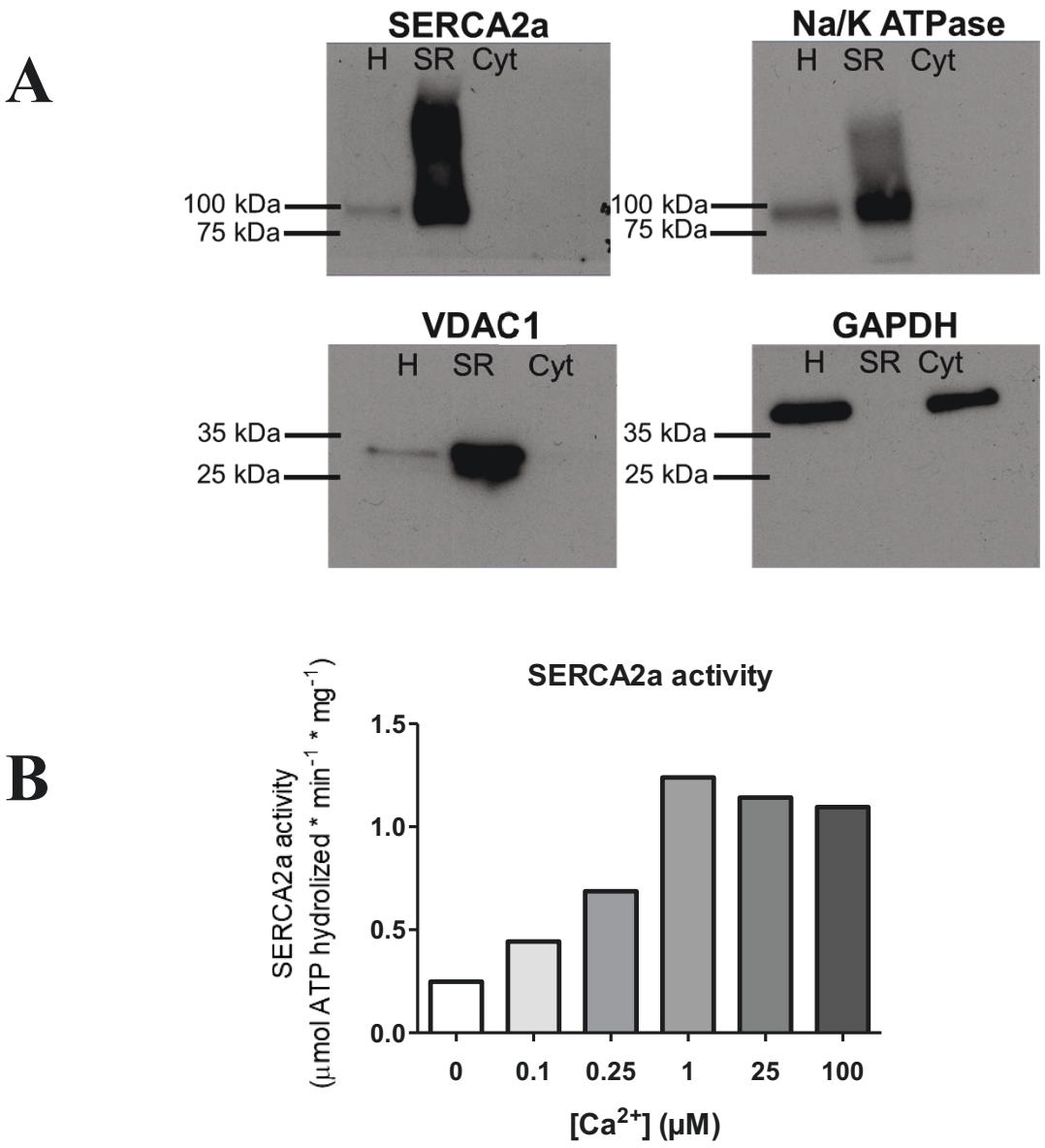

Figure 3.7: Verification of SR enriched mircosome purity and activity in response to Ca^{2+}. (A) Protein levels of organelle marker proteins for 20 µg of starting homogenate after the first 4000 xg spin (H), SR enriched microsomes (SR) and cytosol (Cyt). SERCA2a is a marker of the SR, Na^{2+}/K^{+} ATPase is a marker of the sarcolemma, VDAC is a marker of the mitochondria, and GAPDH is a marker of the cytosol. Position of molecular weight markers is shown on the left. Representative blots from n=2 microsome isolations. (B) SERCA2a activity measured as thapsigargin sensitive activity in one SR enriched microsome from an aerobic heart in response to change in Ca^{2+} concentration (n=1).

A

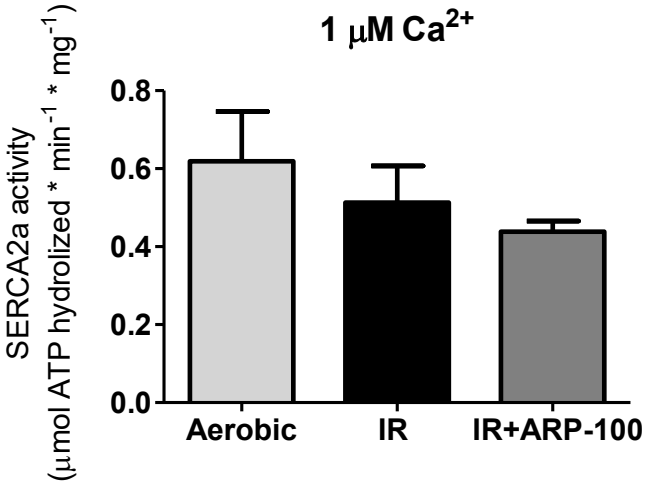

B

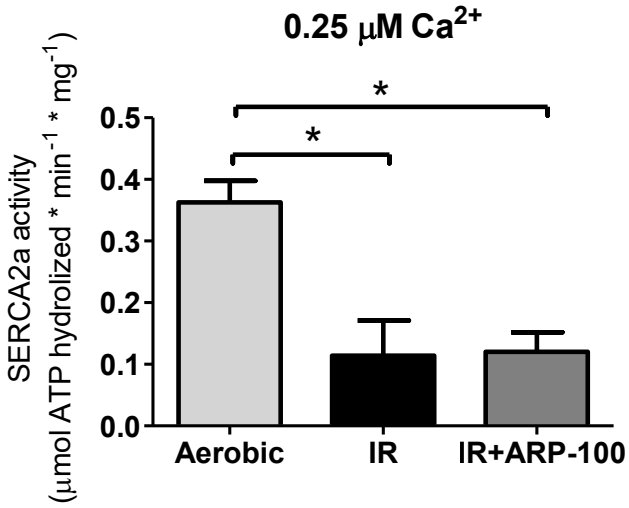

Figure 3.8: SERCA2a activity as measured by thapsigargin sensitive ATPase activity in SR enriched microsomes from the three groups of isolated rat hearts using a coupled-enzyme spectrophotometric assay. (A) SERCA2a activity at Ca^{2+} concentrations of 1 μM (A, n=4-5) and (B) 0.25 μM (B, n=4-5, $p<0.05$). *$p<0.05$ by one-way ANOVA followed by Tukey's post hoc test.

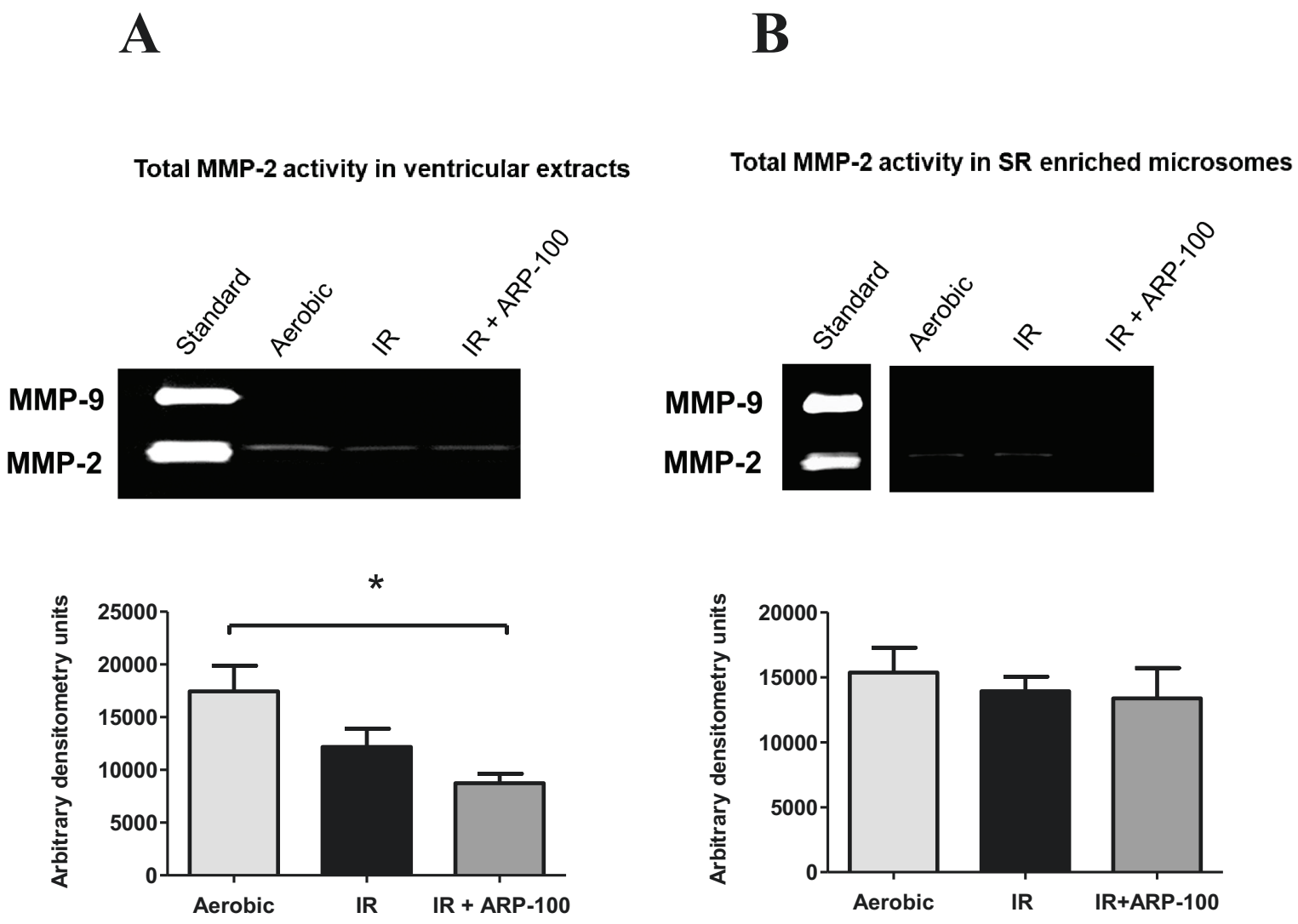

Figure 3.9: Total MMP-2 activity (both 72 and 64 kDa bands) measured by gelatin zymography in ventricular extracts and SR enriched microsomes. (A) Representative zymogram of ventricular extracts from each group is displayed above the quantified results (n=6-7/group). HT-1080 conditioned media was used as a standard for MMP-2 and MMP-9. (B) Representative zymogram of SR enriched microsomes from each group is displayed above the quantified results (n=6-7/group). Standard and samples are cropped from the same gel. *$p<0.05$ by one-way ANOVA followed by Tukey's post hoc test.

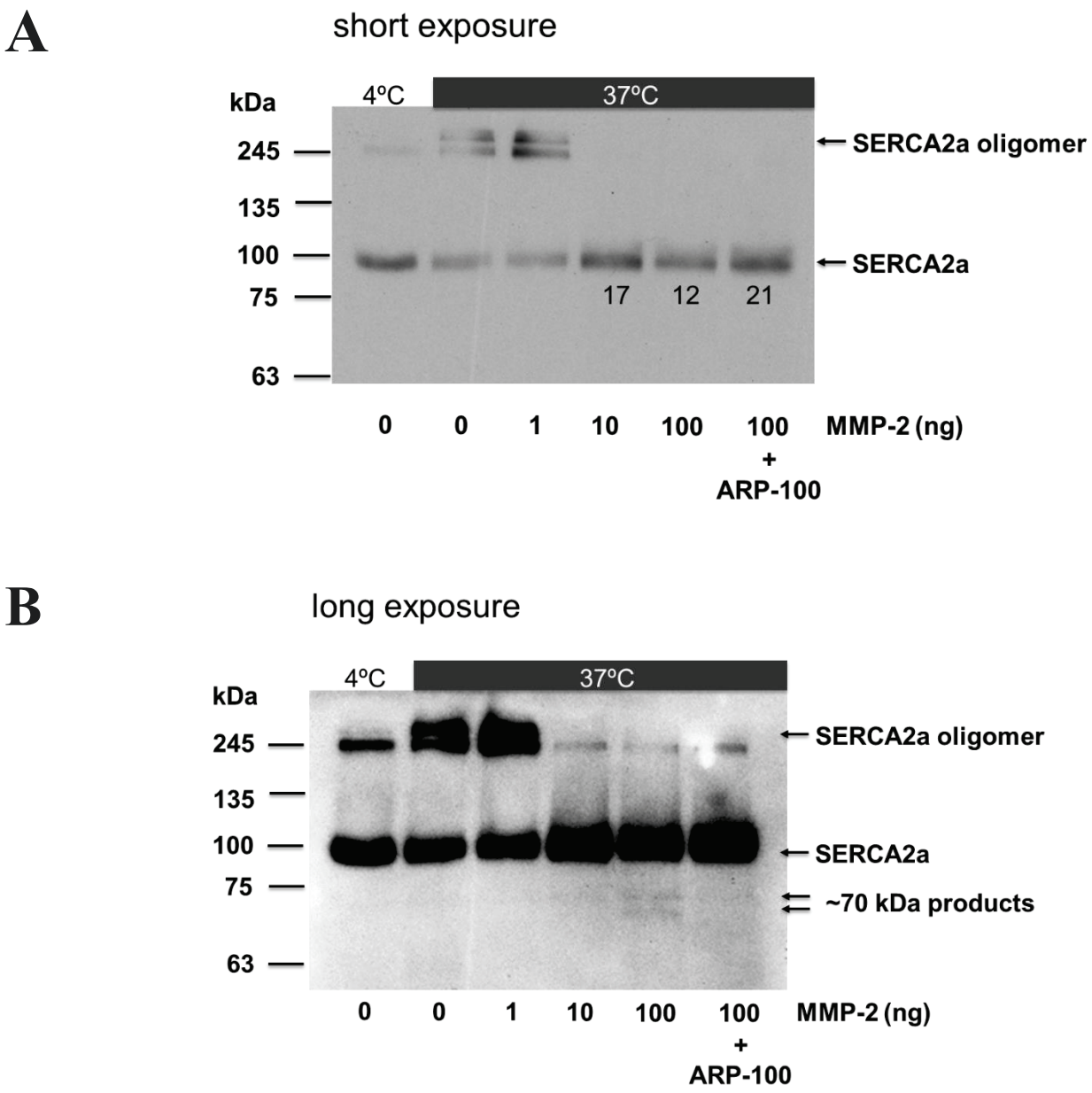

Figure 3.10: Degradation of SERCA2a in SR enriched microsomes by MMP-2. Increasing amounts of MMP-2 incubated with SR enriched microsomes for 2 hr at 37ºC followed by immunoblot of the products for SERCA2a (representative of n=2 experiments). (A) Immunoblot at a short exposure. The first lane was from a sample kept at 4ºC as a control. Molecular weight markers are illustrated on the left. The SERCA2a bands in lane 4-6 were quantified and the raw densitometry is given immediately below the quantified band. (B) Long exposure of the same membrane in panel A to reveal ~70 kDa degradation products.

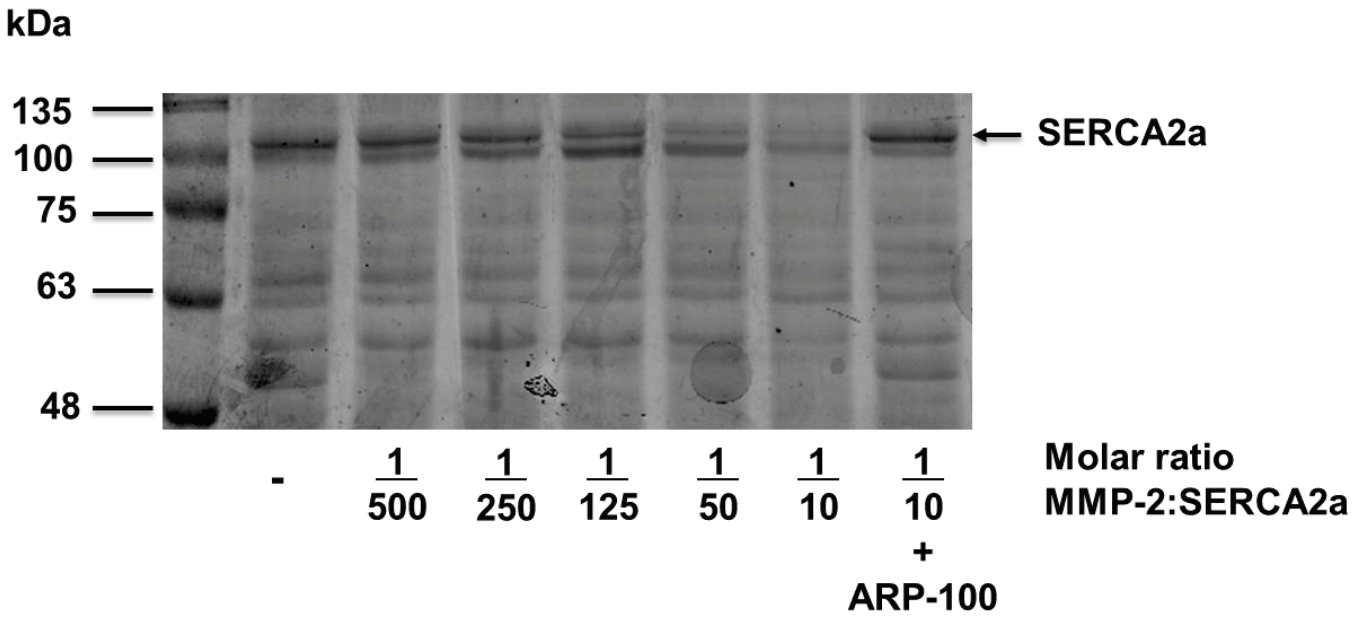

Figure 3.11: Coomassie blue stained gel of in vitro degradation of purified porcine cardiac SERCA embedded in proteoliposomes by APMA activated MMP-2. SERCA was incubated with increasing molar ratios of APMA activated MMP-2:SERCA2a (1/500-1/10) for 2 hr at 37ºC. Increasing amounts of MMP-2 degrade SERCA2a first to a 100 kDa product which is then followed by disappearance of both the main band and 100 kDa product. This was prevented with ARP-100. The first lane contains the molecular weight ladder with their respective molecular weights indicated on the left.

P1 position	Cleavage sequence (P5-P5')	Predicted N-terminal mass	Predicted C-terminal mass
412	DGLVE-LATIC	45.14	69.57
609	EVASS-VKLCR	66.97	47.74
664	LSPSA-QRDAC	72.89	41.82

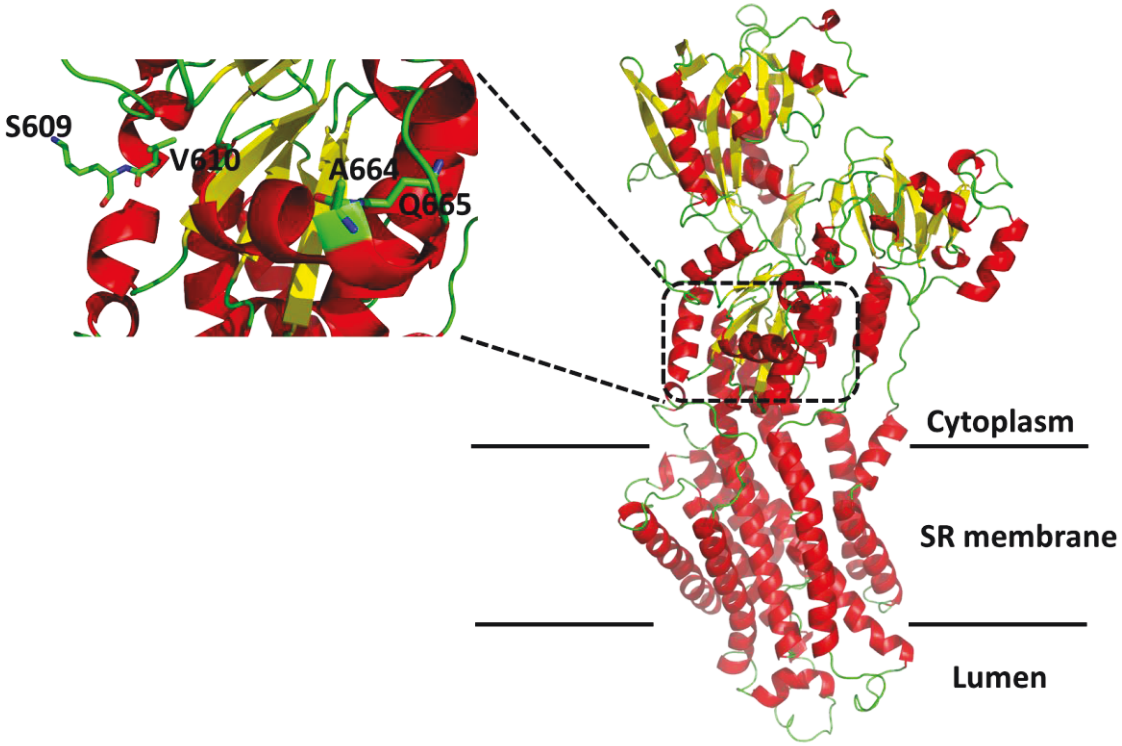

Figure 3.12: Predicted cleavage sites of MMP-2 on rat SERCA2a mapped on SERCA2a structure (rat). (A) Table of predicted cleavage sties giving a product around 70 kDa. (B) Two of the three sites are accessible to proteolytic attack from the outside of the molecular and are sites mapped on a 3D rendering of SERCA2a, S^{609} and A^{664}.

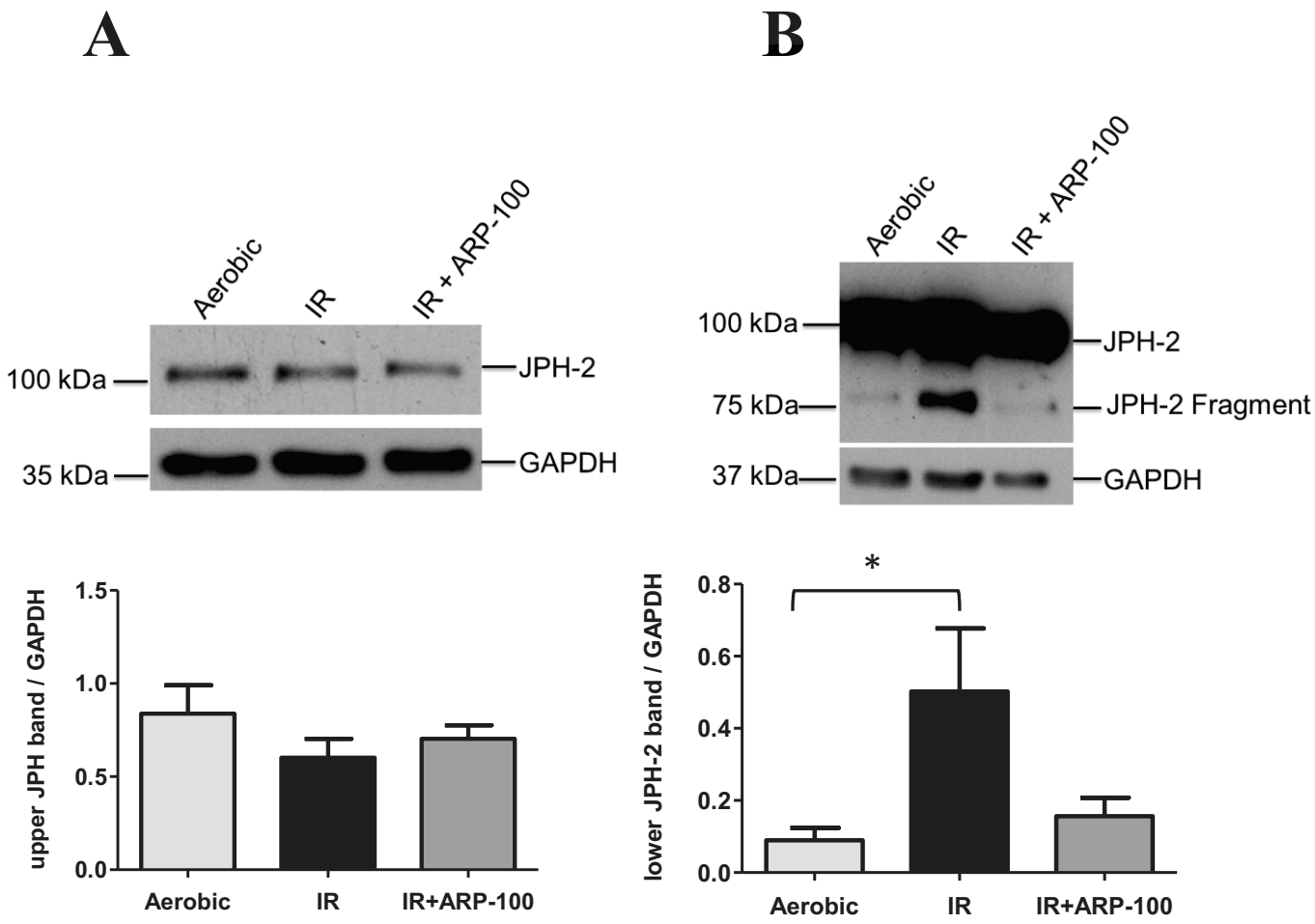

Figure 3.13: JPH-2 levels in ventricular extracts from isolated rat hearts by immunoblot. (A) There was no difference in the JPH-2 upper band (100 kDa) between groups (n=6-7/group). (B) A 75 kDa product trended to increase in IR hearts compared with Aerobic (n=6-7/group, $p<0.05$). *$p<0.05$ by one-way ANOVA followed by Dunnett's post hoc test.

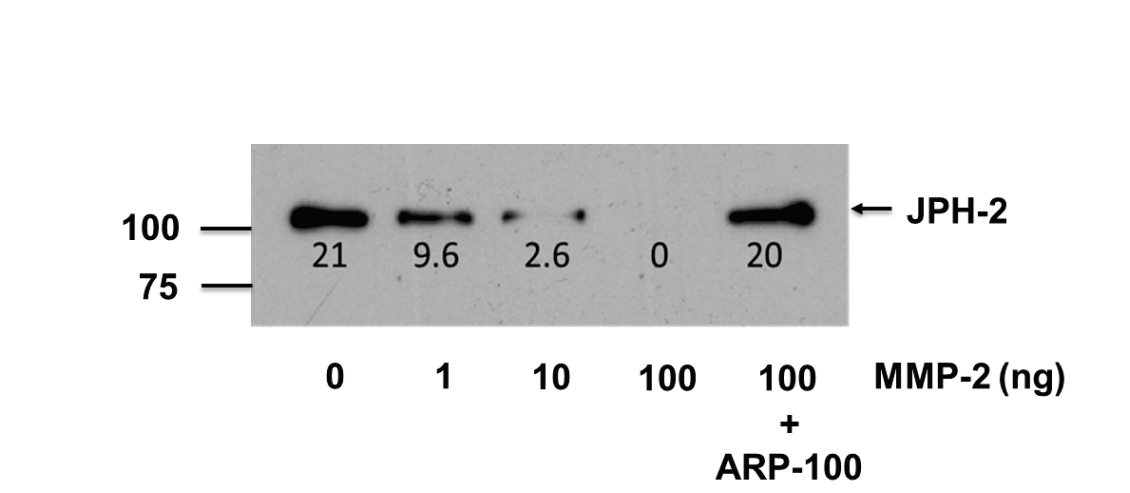

Figure 3.14: Ventricular extracts incubated with MMP-2 followed by immunoblot for JPH-2. (A) 4 µg ventricular extract incubated with increasing amounts of MMP-2 for 1 hr at 37ºC results in the degradation of JPH-2. Densitometry values are shown immediately below bands. (B) 20 µg ventricular extract incubated for 15-60 min at 37ºC in the presence and absence of 10 ng MMP-2.

Chapter 4-Discussion

4.1 Summary of key findings

I found several lines of evidence implicating MMP-2 as an important protease which can cleave SERCA2a during myocardial IR injury. The MMP inhibitor, ARP-100, prevented the formation of a 70 kDa SERCA fragment which was formed during IR injury. Levels of this fragment negatively correlated with cardiac contractile function at the end of perfusion. Exogenously added MMP-2 cleaved native SERCA2a in SR enriched microsomes to form ~70 kDa product(s) similar to the 70 kDa fragment seen in ventricular homogenates. MMP-2 also cleaved purified porcine SERCA2a in a concentration-dependent manner. In silico analysis of MMP-2 cleavage sites on the primary sequence of rat SERCA2a found three potential sites which would give an expected product of approximately 70 kDa. Two of these putative cleavage sites were accessible to proteolysis when mapped on a 3D rendering of rat SERCA2a. I obtained SR enriched microsomes from a separate group of hearts perfused with the same protocol and detected MMP-2, but not MMP-9, activity in the SR enriched microsomes. Activity of SERCA2a in SR enriched microsomes was decreased by IR, however, this was not prevented with ARP-100. This is the first study to identify SERCA2a as a potential novel substrate of MMP-2 in the SR.

I also investigated JPH-2 as a potential target of MMP-2 during IR injury. In silico analysis of JPH-2 revealed many high probability MMP-2 cleavage sites. I found a potential 75 kDa JPH-2 degradation product increased in IR hearts in a MMP-dependent manner. Incubation of ventricular extracts at 37ºC with MMP-2 resulted in the proteolysis of JPH-2, which was prevented with ARP-100. This is the first study to provide evidence of JPH-2 as a putative target of MMP-2.

4.2 MMP-dependent 70 kDa SERCA2a cleavage fragment in IR hearts

Both decreased protein levels and impaired function of SERCA2a have been implicated in IR induced cardiac contractile dysfunction.[112, 139] Homozygous knockout of SERCA2a in mice, but not SERCA2b, resulted in some embryonic lethality due to heart malformations, with most mice surviving until adulthood.[140] These mice demonstrated concentric cardiac hypertrophy. The hearts of heterozygous SERCA2a knockout mice were more susceptible to both in vivo and ex vivo IR injury and showed increased infarct size and impaired contractility.[116, 117] It was proposed that the state of SERCA2a function determines to a large extent if an ischemic insult is reversible or irreversible.[117] The proposed mechanistic role of SERCA2a dysfunction in IR injury is the exacerbation of intracellular calcium overload, leading to activation of Ca^{2+} dependent proteases, increased cell death, and altered intracellular signaling.[114, 116]

Here I report for the first time the presence of degradation products of SERCA2a formed during cardiac IR injury. One of these products at ~70 kDa increased in an MMP-dependent manner, indicating that this cleavage product may be generated by MMP-2. Two other degradation bands were characterized at ~65 and ~55 kDa, but did not exhibit MMP-dependent changes in their levels. Ying et al. (2008)[109] have previously described similar degradation products of SERCA2a (at 70 and 60 kDa) in SR from hyperlipidemic pig aorta compared with control pig aorta. These investigators used the same monoclonal SERCA2a antibody clone (2A7-A1) which I used here. Degradation of SERCA2a to lower molecular weight products as seen by Ying et al. was associated with increased sulfonic acid oxidative modification of C^{674} on SERCA2a. This modification was detected by immunoblot and immunohistochemistry employing a custom antibody to detect this specific modification on SERCA2a. They validated this antibody by peptide blocking assay for use in immunoblot. These authors hypothesized that increased oxidative stress

(as generated during IR) modifies SERCA2a, particularly by oxidizing cysteine sulfhydryl groups to sulfonic acid, increasing its susceptibility to degradation. They, however, did not implicate or identify any proteases. In this study I measured levels of C^{674} sulfonylated SERCA2a in ventricular extracts by immunoblot using the same custom antibody used by Ying et al (2008). The signal to noise ratio of this antibody was poor, making it a challenge to detect clean bands. Immunoblot of ventricular extracts with this antibody produced numerous bands at several different molecular weights, none of which were at 110 kDa, the expected molecular weight of SERCA2a. One band was around 70 kDa, similar to the SERCA2a fragment seen with the anti-SERCA2a 2A7-A1 epitope antibody. However, there was no significant difference in the levels of this band between the groups.

Investigators in the past have found decreased SERCA2a protein levels following IR injury in isolated rat hearts,[111, 112, 114] whereas I did not see any change in total SERCA2a protein levels in the ventricular extracts. One major difference between this study and the previously mentioned studies is that I perfused isolated rat hearts in working mode, whereas the aforementioned studies perfused rat hearts according to Langendorff. In working mode, both the left atria and aorta are cannulated, and the left ventricle of the isolated rat heart is performing external work on the recirculating buffer in order to pump it against a hydrostatic afterload and provide for its own coronary circulation. Hearts perfused according to Langendorff are only cannulated via the aorta and do not perform any external work. Isovolumetric pressure of the left ventricle is instead measured by an inserted balloon catheter. The initial pressure of the balloon catheter (usually around 5 mmHg and termed preload) is set at the beginning of the perfusion. During ischemia and to a larger extent reperfusion, the pressure on the ventricular balloon increases due to ischemic contracture,[141] increasing stress on the left ventricle. This increase in preload does not occur in the working heart as pressure is not measured via balloon catheter but is set by the distance of the

oxygenator to the atrial cannula which is maintained constant during perfusion. Deflation of the balloon catheter during reperfusion, and thus decreasing the preload, prevented troponin I degradation in isolated rat hearts perfused according to Langendorff.[142] As previous studies used the Langendorff technique, increased ventricular wall stress upon reperfusion may be responsible for SERCA2a proteolysis seen in the past. Further discrepancies between this study and previous ones regarding IR induced changes in SERCA2a levels may reflect differences in the age of animals used (not stated in some studies, and unknown in my study), ischemic time, temperature of the hearts during ischemia, and time of total perfusion. These previous studies used a longer ischemic time (30 min) and a longer total perfusion time (120 min).[111, 112] This opens up the possibility of altered SERCA2a mRNA expression effecting SERCA2a levels. In line with this reasoning, decreased SERCA2a levels have been associated with decreased SERCA2a mRNA expression at 120 min perfusion time.[112] Previous authors also used a different monoclonal SERCA2a antibody (IID8),[111, 112, 114, 143] which probably binds to a different epitope.[144] As the exact binding epitope for the IID8 antibody was not mapped, it is possible that it binds to a region of SERCA2a which is post-translationally modified during IR injury. Thus, the antibody epitope may be obscured during IR injury in the absence of altered protein levels. All previously mentioned studies used the IID8 antibody SERCA2a antibody (if stated), whereas I verified my results using two different SERCA2a antibodies with different binding epitopes. I did not test the IID8 antibody here.

I tested if MMP-2 can proteolyze SERCA2a in vitro to support my ex vivo findings. I tested if native SERCA2a in SR enriched microsomes prepared from an aerobic heart was susceptible to proteolysis by MMP-2 and came across several interesting findings. First, I found that SERCA2a in SR enriched microsomes forms oligomers when incubated at physiological temperature. These oligomers were not separated by electrophoresis under reducing conditions. It has been suggested

that SERCA forms homodimers in cells, and interacts with PLN in a 2:1 (SERCA:PLN) stoichiometric ratio.[145] The exact function of SERCA2a dimers and how they regulate its function is unknown. Addition of MMP-2 caused monomerization of oligomers, suggesting that a physical interaction between MMP-2 and SERCA2a may be disrupting its oligomerization. Second, I observed proteolysis of 110 kDa SERCA2a with increasing amounts of MMP-2. This was associated with the appearance of a ~70 kDa degradation products, similar to what was seen in the ventricular extracts. Third, I found that ARP-100 prevented proteolysis of SERCA2a in SR enriched microsomes, but did not restore oligomers of SERCA2a. This suggests that MMP-2 may be binding to SERCA2a at a site distinct from its catalytic site and may still interrupt the oligomerization in the presence of a MMP inhibitor. Lastly, I found that purified porcine SERCA2a is also susceptible to MMP-2 proteolysis, supporting SERCA2a as a target of MMP-2. I detected many bands in the purified porcine SERCA2a prep by Coomassie blue in the absence of MMP-2, which could be already degraded SERCA2a or contaminating proteins. This prevented me from visualizing any smaller molecular weight proteins. Previous investigators have reported that SERCA2a is not a substrate of calpain in vitro.[113, 146]

Knowing that MMP-2 may cleave SERCA2a to ~70kDa products and that a 70 kDa SERCA2a product was formed in a MMP dependent manner as a result of IR injury, I used cleavage prediction software (CleavPredict)[138] to identify potential cleavage sites of MMP-2 on SERCA2a which would result in a 70 kDa fragment. From a long list of predicted sites, I identified only three putative sites which could give a product of around 70 kDa, with P1 at 412, 609 or 664. I will call these putative cleavage sites cleavage site A, B, and C, respectively. These sites were mapped onto a 3D structure of rat SERCA2a in PyMOL, which was produced by homology modeling of rat SERCA2a with rabbit SERCA2a (for which a crystal structure exists). Only cleavage sites B and C were in domains accessible to proteolytic attack. The consensus sequence

of MMP-2 derived from peptide cleavage libraries shows that MMP-2 prefers small amino acids in the positions P2, P1, and P3', particularly alanine.[147, 148] Both cleavage site B and C met this stipulation for positions P2 and P1. Cleavage site C contains a proline in the P3 position, which is a strong preference according to the cleavage consensus sequence of MMP-2.[147] Both cleavage site B and C are positioned within an alpha helix.

The levels of phospholamban in ventricular extracts were also measured, since it is a well-studied cardiac-specific regulator of SERCA2a activity.[149] Binding of phospholamban to SERCA2a decreases SERCA2a activity, and this inhibition is relieved upon phosphorylation of phospholamban at two key sites, S^{16} and T^{17}.[150] Levels of phospholamban were unchanged between groups. I measured the pentameric form of S^{16} phospho-phospholamban as this may be a more accurate measurement of phospholamban phosphorylation than the monomeric form as phosphorylation of phospholamban promotes its pentamerization.[149] I saw no changes in S^{16} phospho-phospholamban between the groups. However, the ratio of phospho-phospholamban to phospholamban was significantly higher in the IR+ARP-100 group compared to Aerobic ($P<0.05$). This suggests less of an inhibitory effect of phospholamban on SERCA2a in the IR+ARP-100 group. ARP-100 may be increasing the phosphorylation of phospholamban through an unidentified cardioprotective mechanism. Previous studies have found reduced PLN levels associated with decreased phospholamban mRNA.[112] It is, therefore, possible that these previous findings were due to decreased phospholamban mRNA expression at longer perfusion times (120 min) as described above.

4.3 SERCA2a activity following IR injury

To investigate if SERCA2a activity is impaired by MMP-2 following injury, I obtained highly purified SR enriched microsomes from fresh (not flash froze) rat heart tissue obtained from an additional series of identically perfused heart groups. Immunoblot using anti-SERCA2a (EPR9393) on SR enriched microsomes from an aerobic heart confirmed enrichment of the SR protein SERCA2a. SR enriched microsomes from the same aerobic heart also contained some contamination from the mitochondria and the plasma membrane, as shown by the presence of VDAC1 and Na^+/K^+ ATPase, respectively, which is expected and observed in other studies.[111, 112] The SR enriched microsomes, however, did not contain any detectible cytosolic contamination as indicated by the absence of GAPDH. As the purpose of isolating the SR enriched microsomes was to measure SERCA2a activity, minor contamination from other membrane organelles is negligible provided that SERCA2a activity could be accurately detected.

I then performed a coupled-enzyme ATPase assay, in the presence and absence of thapsigargin, to determine SERCA2a activity in the SR enriched microsomes. Thapsigargin was used in the assay as an inhibitor of SERCA2a because it is a specific inhibitor of SERCA isoforms.[151] One SR enriched microsome preparation from an aerobic heart was tested at various Ca^{2+} concentrations (0.1-100 μM) in order to determine suitable Ca^{2+} concentrations to be tested in all samples. I found SERCA2a activity in the SR microsomes from the aerobic heart responded to Ca^{2+} in the range of 0.1-1 μM with the maximal SERCA2a activity occurring at 1 μM. Beyond a Ca^{2+} concentration of 1 μM SERCA2a activity decreased. The response to Ca^{2+} we observed in our SR enriched microsomes was in line with other cardiac SR preparations from isolated working rat hearts.[152] It should be noted that there was some SERCA2a activity at zero Ca^{2+} added, suggesting some residual Ca^{2+} contamination in the buffers used for the SR fractionation. I decided

to test all SR microsome samples at both 0.25 μM and 1 μM Ca^{2+} in order to examine SERCA2a activity at its submaximal and maximal ATPase rate.

I found no changes in SERCA2a activity at the high Ca^{2+} concentration (1 μM) between the three groups, showing that IR did not affect SERCA2a maximal activity. This supports our finding that there was no difference in SERCA2a levels between the groups as shown by our immunoblot results on the ventricular extracts. This also suggests that the extent of SERCA2a proteolysis (70 kDa band) I observed in ventricular extracts was not enough to change maximal SERCA2a activity. SERCA2a activity at 0.25 μM Ca^{2+}, however, was decreased in both the IR and IR+ARP-100 group compared with aerobic hearts, showing a decrease in Ca^{2+} sensitivity caused by IR. This phenomenon was MMP-independent as ARP-100 had no effect. These results suggest that either post-translational modification of SERCA2a or alterations in its binding partners may be occurring during IR injury.[108]

4.4 MMP-2 activity in ventricular extracts and SR following IR injury

This is the first study to detect MMP-2 activity in SR enriched microsomes. Intracellular MMP-2 activity has been localized in numerous cell types,[153] including cardiomyocytes, where it plays a central role in numerous injuries involving oxidative stress,[9] including cytokine-induced heart failure[154] and IR injury.[79] MMP-2 was first localized to the sarcomere in the thin myofilament fraction,[12] and has since been localized to the micochondria,[41] nucleus,[42] caveolae,[43] cytoskeleton,[14] and a specialized region of the SR called the mitochondria-associated membrane.[41] The mitochondria-associated membrane is a critical site of cross talk between the SR and the mitochondria, and may therefore play an important role in cell death and survival during IR injury.[155]

Both SR enriched microsomes and ventricular extracts have MMP-2, but not MMP-9, signal by gelatin zymography. The absence of a MMP-9 signal in homogenates from isolated rat hearts perfused free of blood is consistent with previous findings from our lab. MMP-9 was previously detected in isolated adult rat cardiomyocytes using immunoblot.[40] However, in that study, the MMP-9 signal did not line up with the positive control (human epithelial cell conditioned media), bringing into question the identity of the bands detected. Other studies which detect MMP-9 in adult rat hearts may be due to residual blood contamination, as MMP-9 is abundant in platelets[156] and neutrophils.[157] When I was first testing the SR enriched microsome isolation protocol, I used fresh hearts which were only perfused for 10 min in Langendorff mode and they still contained some residual blood as noted by a distinct red tint of the homogenate. SR enriched microsomes from these hearts had MMP-9 signal, suggesting that residual blood components can significantly contribute to MMP-9 signal.

I observed no difference in total MMP-2 activity from SR enriched microsomes between the groups of hearts. The band corresponding 72 kDa MMP-2 was much stronger than that for 64 kDa MMP-2 in both the ventricular extracts and the SR enriched microsomes. Both bands were quantified together as the resolution of electrophoresis was not great enough for them to be quantified separately. In the ventricular extracts, I detected a significant decrease in the total MMP-2 activity between the IR and IR+ARP-100 groups. In the working heart, the drug is always present in the recirculating buffer system and is therefore in the cardiac tissue when it was flash frozen and homogenized. Residual ARP-100 in the ventricular extracts could decrease the apparent activity of MMP-2. In isolated neonatal rat ventricular myocytes, residual ARP-100 in the lysates was enough to significantly reduce MMP-2 activity without affecting its protein levels.[158]

I detected no difference in total MMP-2 activity in the ventricular extracts between the aerobic and IR groups. Previous studies have found a decrease in MMP-2 activity in heart homogenates following IR injury by gelatin zymography, which is associated with an increase release of MMP-2 into the perfusate. These studies were performed in a Langendorff system which has many differences compared with working heart as discussed previously. One study has measured MMP-2 activity by zymography in ventricular homogenates from isolated working rat hearts,[159] however, the authors did not perform the necessary statistical test in order to determine if there was a significant difference in MMP-2 activity between the IR group and control group.

One of the objectives of this project was to determine if inhibition of MMPs with ARP-100 was protective against ischemia-reperfusion injury. I found that ARP-100 is protective against stunning injury, which is in line with over a decade of research from our lab and others demonstrating cardioprotective effects of MMP inhibitors against IR injury.[9, 45, 79, 85] ARP-100 is a competitive MMP inhibitor which is more selective for MMP-2 and MMP-9 over other MMPs.[50, 51] At the dose used, ARP-100 may inhibit MMP-2, MMP-9 and MMP-3. As far as we are aware, MMP-3 has not been localized inside of cardiac myocytes. As discussed above, MMP-9 is absent in rat hearts perfused free of blood. As tested in this study, ARP-100 does not inhibit calpain-2 activity at concentrations up to 30 μM. Thus, the protective effect of ARP-100 in myocardial stunning injury was most likely by inhibiting MMP-2 activity, which is also likely the MMP responsible for SERCA2a proteolysis.

4.5 MMP-dependent JPH-2 degradation fragment formed during IR injury

JPH-2 is a critical structural membrane protein in cardiac myocytes which tethers the SR to the t-tubule allowing for proper calcium-induced calcium release.[88] Recently, JPH-2 was shown

to be proteolyzed during IR injury in isolated rat hearts.[127, 128] Proteolysis of JPH-2 was prevented with the calpain inhibitor MDL-28170,[127] which also inhibits MMP-2. I identified JPH-2 as a putative substrate of MMP-2 using CleavPredict online software.[148] Thirty putative cleavage sites were identified (Table 3.2). The site with the highest probability had a cleavage site with P1 located at S^{165}. This site is in a region with no predicted secondary structure and is in an area of JPH-2 which is predicted to be intrinsically disordered. Intrinsically disordered regions are more likely to be proteolysed due to their inherent flexibility and ease of access for protease catalytic domains.[160]

I measured JPH-2 levels in the ventricular extracts from the three groups of isolated hearts in order to investigate JPH-2 as a target of MMP-2 during IR injury. I found no changes in the levels of JPH-2 between the three groups of isolated working rat hearts. However, I found a lower band at ~75 kDa increased in IR compared with aerobic. This increase was absent in the IR+ARP-100 group. This is the first study to describe a ~75 kDa fragment of JPH-2. Previous authors have characterized a 75 kDa fragment of JPH-1 (the predominant skeletal muscle isoform).[128] It should be noted that there are discrepancies between the theoretical molecular weight of JPH-2 (74 kDa) and observed molecular weight by immunoblot (~90-100 kDa).[127, 161] Analysis of JPH-1 (the main isoform in skeletal muscle) from junctional SR isolated from rabbit fast-twitch muscle identified JPH-1 at a charge to mass ratio of 90,000.[162] This suggests that the JPH proteins may be heavily post translationally modified, however, the exact reason for the discrepancies in theoretical mass and observed mass were not elucidated in that study.

We found that JPH-2 in a ventricular extract from an aerobic heart is susceptible to proteolysis from added MMP-2. Furthermore, 15 min incubation of the ventricular extract at 37°C resulted in the appearance of a 65 kDa JPH-2 degradation fragment which was accompanied by

smaller molecular weight bands at 55 kDa at incubation times 30 min and longer. This strongly suggests JPH-2 is targeted by a protease in the heart. Protease inhibitor cocktail was added to the homogenates and contains inhibitors for both aspartate and cysteine proteases. Therefore, it is not likely that clapain was responsible for this proteolysis as it is a cysteine protease.

4.7 Limitations

In this study I subjected isolated working rat hearts to global, no-flow ischemia followed by reperfusion. This method is useful for studying the effects of interventions, such as drugs, on cardiac contractile performance and substrate utilization. However, despite its several distinct advantages, this method has many limitations. First, excision of the rat heart is invasive and can result in injury and/or stunning to the heart if not performed in a timely manner. This can either cause additional injury to the heart, or be protective against IR injury by causing preconditioning.[111] Second, the isolated working rat heart lacks all external neuronal, hormonal and humoral modulation which occurs in vivo, and which change as a result of ischemic injury to the heart. Krebs-Henseleit solution is used as a nutrient and gas carrying buffer instead of blood. As a direct consequence, the coronary flow is much higher in the isolated heart compared to in vivo because crystalloid buffers have far less oxygen carrying capacity compared with blood. One way to avoid this problem is to perfuse the hearts with blood from a donor animal, or with red blood cell supplemented crystalloid buffers, however, this is highly impractical.[163] Lastly, global, no-flow ischemia is a gross oversimplification of IR injury in the human patient. In patients with acute coronary syndrome, a focal region of ischemia sets up variable extents of injury to the myocardium, resulting in focal points of injury which could be reversibly or irreversibly injured.[60] The latter results in a region of infarcted tissue, a surrounding near infarct zone or border zone

which may be salvageable upon reperfusion, and remote non-ischemic, non-infarcted tissue. We have studied reversible stunning injury which occurs in some form in patients who have acute coronary syndrome and have undergone percutaneous coronary intervention,[164] but is more representative of cardioplegic arrest in patients undergoing coronary artery bypass graft surgery.

The animals used in this study were healthy young male rats. IR injury is lesser in the female rat, which has largely been attributed to the effect of estrogen.[165] Healthy rats are not a good reflection of the human population with acute coronary syndrome. In the INTERHEART study, modifiable risk factors and comorbidities including diabetes, hypertension, obesity, and smoking made up 90% of the population attributable risk across 52 countries.[166] Therefore, acute coronary syndrome is largely preventable.[59] The age of the rats in our study is unknown, however, as they were 300-400g, they were likely around 10-15 weeks old.[167] Increased age is a major risk factor for acute coronary syndrome, and was not addressed in this study.[168]

We only measured MMP-2 activity via one method, gelatin zymography, which has several limitations. Gelatin zymography separates MMP-2 from its endogenous inhibitors, the TIMPs.[169] Furthermore, the latent form of MMP-2 can be chemically activated during gelatin zymography, ostensibly through the removal of C^{102} from the catalytic Zn^{2+}. Therefore, one does not get a true picture of tissue (in situ) MMP-2 activity. MMP-2 stores are also released upon the first few minutes of reperfusion in the heart.[79] Although the levels of MMP-2 may be decreased in IR, this does not mean that the activity is decreased. Measuring true tissue gelatinolytic activity by in situ zymography or detection of S-glutathiolated MMP-2 through co-immunoprecipitation or mass spectrometry would both be better ways to measure MMP-2 activity.

A limitation of this study, and almost any study using an SR enriched microsomal preparation, is the process of differential centrifugation separates subpopulations of SR. This

results in the loss of the mitochondria-associated membrane, which pellets with the mitochondria.[170] As MMP-2 was localized specifically to the mitochondria-associated membrane,[41] it is in this region where I predict SERCA2a degradation is most likely to take place. As the mitochondria-associated membrane is a centre of important cross talk between the SR and the mitochondria,[46] SERCA2a degradation and thus calcium overload in this region of the cell may be critical in determining if the outcome of IR injury is reversible or irreversible, and investigation of IR induced changes to SERCA2a levels and activity in this compartment is warranted.

Specificity of the SERCA2a 2A7-A1 epitope antibody in detection of the ~70 kDa band could not be easily verified by peptide blocking assay as the epitope of this antibody has never been mapped to the secondary structure of SERCA2a. Similarly, the JPH-2 fragment was not verified by peptide binding assay as the JPH-2 antibody used for immunoblot was polyclonal. The identity of these fragments should be verified by additional techniques such as immunoprecipitation followed by mass spectrometry.

4.8 Future directions

This study provides evidence that SERCA2a and JPH-2 are substrates of MMP-2. However, this study does not demonstrate that SERCA2a and JPH-2 interact or are individually colocalized with MMP-2. Future studies looking at the colocalization of MMP-2 activity and levels with SERCA2a and JPH-2 using a combination of in situ zymography and immunofluorescent microscopy (performed by Rizzi et al.[171]) would provide greater evidence of these two proteins as substrates of MMP-2. In addition, co-immunoprecipitation experiments could be performed in order to detect if these two proteins interact.

In this study I found no changes in SERCA2a or JPH-2 protein levels between the groups, possibly because the degree of injury in our model was not great enough. We did, however, characterize several degradation products of SERCA2a and JPH-2 which appear in an MMP-dependent manner. This study, therefore, warrants further investigation of MMP mediated SERCA2a and JPH-2 proteolysis in in vivo studies of IR injury where the degree of injury is greater. In vivo or ex vivo IR injury could be performed in transgenic mice with either cardiac specific overexpression of either catalytically activity MMP-2 or MMP-2_{NTT-76}, both of which show enhanced susceptibility to IR injury. Hearts from MMP-2 knockout mice (used in Ali MAM et al.[13]) could also be used to add further evidence of SERCA2a and JPH-2 as targets of MMP-2.

I found a decrease in SERCA2a activity at a midpoint Ca^{2+} level in IR hearts which was not prevented with ARP-100, however, I was unable to identify the exact cause of SERCA2a dysfunction. As both levels and maximal activity of SERCA2a were unchanged, mass proteolysis can be ruled out for causing SERCA2a dysfunction. Future studies should look at additional binding partners of SERCA2a such as HAX-1. HAX-1 knockout was associated with increased SERCA2a oxidation and dysfunction,[103] and may be a target of MMP-2 mediated proteolysis to measure in the future.

4.7 Conclusions

This is the first study to identify substrates of MMP-2 in the SR, namely SERCA2a and JPH-2. Both of these proteins are critical for excitation-contraction coupling and coordinated calcium cycling. This is also the first study to detect MMP-2 activity in SR enriched microsomes. Pharmacological inhibition of MMPs is able to improve cardiac contractile function following IR injury. This study adds to the repertoire of intracellular MMP-2 substrates and increases our

understanding of the role of MMP-2 in ischemic heart disease. Inhibition of MMPs, particularly MMP-2, during ischemic heart disease may be a viable option for mitigating ischemia–reperfusion injury in patients with ischemic heart disease.

References

1. Gross J, Lapiere CM. Collagenolytic activity in amphibian tissues: A tissue culture assay. *Proc Natl Acad Sci U S A*. 1962;48:1014-1022

2. Liotta LA, Abe S, Robey PG, Martin GR. Preferential digestion of basement membrane collagen by an enzyme derived from a metastatic murine tumor. *Proc Natl Acad Sci U S A*. 1979;76:2268-2272

3. Stetler-Stevenson WG. Type IV collagenases in tumor invasion and metastasis. *Cancer Metastasis Rev*. 1990;9:289-303

4. Iyer RP, Patterson NL, Fields GB, Lindsey ML. The history of matrix metalloproteinases: Milestones, myths, and misperceptions. *Am J Physiol Heart Circ Physiol*. 2012;303:H919-H930

5. Cauwe B, Opdenakker G. Intracellular substrate cleavage: A novel dimension in the biochemistry, biology and pathology of matrix metalloproteinases. *Crit Rev Biochem Mol Biol*. 2010;45:351-423

6. Okada Y, Nagase H, Harris ED, Jr. Matrix metalloproteinases 1, 2, and 3 from rheumatoid synovial cells are sufficient to destroy joints. *J Rheumatol*. 1987:41-42

7. Schulz R. Intracellular targets of matrix metalloproteinase-2 in cardiac disease: Rationale and therapeutic approaches. *Annu Rev Pharmacol Toxicol*. 2007;47:211-242

8. Chan BYH, Roczkowsky A, Ilarraza R, Schulz R. Matrix metalloproteinase-2. In: Choi S, ed. *Encyclopedia of signaling molecules*. Cham: Springer International Publishing; 2018:2996-3005.

9. Hughes BG, Schulz R. Targeting MMP-2 to treat ischemic heart injury. *Basic Res Cardiol*. 2014;109:424

10. Spinale FG. Myocardial matrix remodeling and the matrix metalloproteinases: Influence on cardiac form and function. *Physiol rev*. 2007;87:1285-1342

11. Dollery CM, McEwan JR, Henney AM. Matrix metalloproteinases and cardiovascular disease. *Circ Res*. 1995;77:863-868

12. Wang W, Schulze CJ, Suarez-Pinzon WL, Dyck JR, Sawicki G, Schulz R. Intracellular action of matrix metalloproteinase-2 accounts for acute myocardial ischemia and reperfusion injury. *Circulation*. 2002;106:1543-1549

13. Ali MA, Cho WJ, Hudson B, Kassiri Z, Granzier H, Schulz R. Titin is a target of matrix metalloproteinase-2: Implications in myocardial ischemia/reperfusion injury. *Circulation*. 2010;122:2039-2047

14. Sung MM, Schulz CG, Wang W, Sawicki G, Bautista-Lopez NL, Schulz R. Matrix metalloproteinase-2 degrades the cytoskeletal protein alpha-actinin in peroxynitrite mediated myocardial injury. *J Mol Cell Cardiol*. 2007;43:429-436

15. Kandasamy AD, Schulz R. Glycogen synthase kinase-3β is activated by matrix metalloproteinase-2 mediated proteolysis in cardiomyoblasts. *Cardiovasc Res*. 2009;83:698-706

16. Nagase H, Visse R, Murphy G. Structure and function of matrix metalloproteinases and TIMPs. *Cardiovasc Res*. 2006;69:562-573

17. Tallant C, Marrero A, Gomis-Ruth FX. Matrix metalloproteinases: Fold and function of their catalytic domains. *Biochim Biophys Acta*. 2010;1803:20-28

18. Lovett DH, Mahimkar R, Raffai RL, Cape L, Maklashina E, Cecchini G, Karliner JS. A novel intracellular isoform of matrix metalloproteinase-2 induced by oxidative stress activates innate immunity. *PLoS One*. 2012;7:e34177

19. Ali MA, Chow AK, Kandasamy AD, Fan X, West LJ, Crawford BD, Simmen T, Schulz R. Mechanisms of cytosolic targeting of matrix metalloproteinase-2. *J Cell Physiol*. 2012;227:3397-3404

20. Bergman MR, Cheng S, Honbo N, Piacentini L, Karliner JS, Lovett DH. A functional activating protein 1 (AP-1) site regulates matrix metalloproteinase 2 (MMP-2) transcription by cardiac cells through interactions with Junb-Fra1 and Junb-Fosb heterodimers. *Biochem J*. 2003;369:485-496

21. Galis ZS, Muszynski M, Sukhova GK, Simon-Morrissey E, Libby P. Enhanced expression of vascular matrix metalloproteinases induced in vitro by cytokines and in regions of human atherosclerotic lesions. *Ann N Y Acad Sci*. 1995;748:501-507

22. Grandas OH, Mountain DH, Kirkpatrick SS, Cassada DC, Stevens SL, Freeman MB, Goldman MH. Regulation of vascular smooth muscle cell expression and function of matrix metalloproteinases is mediated by estrogen and progesterone exposure. *J Vasc Surg*. 2009;49:185-191

23. Chesler NC, Ku DN, Galis ZS. Transmural pressure induces matrix-degrading activity in porcine arteries ex vivo. *Am J Physiol*. 1999;277:H2002-2009

24. Okada Y, Morodomi T, Enghild JJ, Suzuki K, Yasui A, Nakanishi I, Salvesen G, Nagase H. Matrix metalloproteinase 2 from human rheumatoid synovial fibroblasts. Purification and activation of the precursor and enzymic properties. *Eur J Biochem*. 1990;194:721-730

25. Van Wart HE, Birkedal-Hansen H. The cysteine switch: A principle of regulation of metalloproteinase activity with potential applicability to the entire matrix metalloproteinase gene family. *Proc Natl Acad Sci U S A*. 1990;87:5578-5582

26. Strongin AY, Collier I, Bannikov G, Marmer BL, Grant GA, Goldberg GI. Mechanism of cell surface activation of 72-kDa type IV collagenase. Isolation of the activated form of the membrane metalloprotease. *J Biol Chem*. 1995;270:5331-5338

27. Nishida Y, Miyamori H, Thompson EW, Takino T, Endo Y, Sato H. Activation of matrix metalloproteinase-2 (MMP-2) by membrane type 1 matrix metalloproteinase through an artificial receptor for proMMP-2 generates active MMP-2. *Cancer Res*. 2008;68:9096

28. Viappiani S, Nicolescu AC, Holt A, Sawicki G, Crawford BD, Leon H, van Mulligen T, Schulz R. Activation and modulation of 72kDa matrix metalloproteinase-2 by peroxynitrite and glutathione. *Biochem Pharmacol*. 2009;77:826-834

29. Crow JP, Beckman JS. Reactions between nitric oxide, superoxide, and peroxynitrite: Footprints of peroxynitrite in vivo. *Adv Pharmacol*. 1995;34:17-43

30. Okamoto T, Akaike T, Sawa T, Miyamoto Y, van der Vliet A, Maeda H. Activation of matrix metalloproteinases by peroxynitrite-induced protein S-glutathiolation via disulfide S-oxide formation. *J Biol Chem*. 2001;276:29596-29602

31. Castro MM, Cena J, Cho WJ, Walsh MP, Schulz R. Matrix metalloproteinase-2 proteolysis of calponin-1 contributes to vascular hypocontractility in endotoxemic rats. *Arterioscler Thromb Vasc Biol*. 2012;32:662-668

32. Baker AH, Edwards DR, Murphy G. Metalloproteinase inhibitors: Biological actions and therapeutic opportunities. *J Cell Sci*. 2002;115:3719-3727

33. Schulze CJ, Wang W, Suarez-Pinzon WL, Sawicka J, Sawicki G, Schulz R. Imbalance between tissue inhibitor of metalloproteinase-4 and matrix metalloproteinases during acute myoctardial ischemia-reperfusion injury. *Circulation*. 2003;107:2487-2492

34. Fedak PW, Altamentova SM, Weisel RD, Nili N, Ohno N, Verma S, Lee TY, Kiani C, Mickle DA, Strauss BH, Li RK. Matrix remodeling in experimental and human heart failure: A possible regulatory role for TIMP-3. *Am J Physiol Heart Circ Physiol*. 2003;284:10

35. Fedak PW, Smookler DS, Kassiri Z, Ohno N, Leco KJ, Verma S, Mickle DA, Watson KL, Hojilla CV, Cruz W, Weisel RD, Li RK, Khokha R. TIMP-3 deficiency leads to dilated cardiomyopathy. *Circulation*. 2004;110:2401-2409

36. Sariahmetoglu M, Crawford BD, Leon H, Sawicka J, Li L, Ballermann BJ, Holmes C, Berthiaume LG, Holt A, Sawicki G, Schulz R. Regulation of matrix metalloproteinase-2 (MMP-2) activity by phosphorylation. *Faseb J*. 2007;21:2486-2495

37. Filipiak K, Kubiński K, Hellman U, Ramos A, Pascual-Teresa Bd. Human protein kinase ck2 phosphorylates matrix metalloproteinase 2 and inhibits its activity. *Chembiochem*. 2014;15:1873-1876

38. Koo BH, Kim YH, Han JH, Kim DS. Dimerization of matrix metalloproteinase-2 (MMP-2): Functional implication in MMP-2 activation. *J Biol Chem*. 2012;287:22643-22653

39. Rouet-Benzineb P, Buhler JM, Dreyfus P, Delcourt A, Dorent R, Perennec J, Crozatier B, Harf A, Lafuma C. Altered balance between matrix gelatinases (MMP-2 and MMP-9) and their tissue inhibitors in human dilated cardiomyopathy: Potential role of MMP-9 in myosin-heavy chain degradation. *Eur J Heart Fail*. 1999;1:337-352

40. Coker ML, Doscher MA, Thomas CV, Galis ZS, Spinale FG. Matrix metalloproteinase synthesis and expression in isolated LV myocyte preparations. *Am J Physiol*. 1999;277:H777-787

41. Hughes BG, Fan X, Cho WJ, Schulz R. MMP-2 is localized to the mitochondria-associated membrane of the heart. *Am J Physiol Heart Circ Physiol*. 2014;306:27

42. Kwan JA, Schulze CJ, Wang W, Leon H, Sariahmetoglu M, Sung M, Sawicka J, Sims DE, Sawicki G, Schulz R. Matrix metalloproteinase-2 (MMP-2) is present in the nucleus of cardiac myocytes and is capable of cleaving poly (ADP-ribose) polymerase (PARP) in vitro. *Faseb J*. 2004;18:690-692

43. Chow AK, Cena J, El-Yazbi AF, Crawford BD, Holt A, Cho WJ, Daniel EE, Schulz R. Caveolin-1 inhibits matrix metalloproteinase-2 activity in the heart. *J Mol Cell Cardiol*. 2007;42:896-901

44. Sawicki G, Leon H, Sawicka J, Sariahmetoglu M, Schulze CJ, Scott PG, Szczesna-Cordary D, Schulz R. Degradation of myosin light chain in isolated rat hearts subjected to ischemia-reperfusion injury: A new intracellular target for matrix metalloproteinase-2. *Circulation*. 2005;112:544-552

45. Buchholz B, Perez V, Siachoque N, Miksztowicz V, Berg G, Rodriguez M, Donato M, Gelpi RJ. Dystrophin proteolysis: A potential target for MMP-2 and its prevention by ischemic preconditioning. *Am J Physiol Heart Circ Physiol*. 2014;307:H88-96

46. Vance JE. MAM (mitochondria-associated membranes) in mammalian cells: Lipids and beyond. *Biochim Biophys Acta*. 2014;4:595-609

47. Lin H-B, Sharma K, Bialy D, Wawrzynska M, Purves R, Cayabyab FS, Wozniak M, Sawicki G. Inhibition of MMP-2 expression affects metabolic enzyme expression levels: Proteomic analysis of rat cardiomyocytes. *J Proteomics*. 2014;106:74-85

48. Vandenbroucke RE, Libert C. Is there new hope for therapeutic matrix metalloproteinase inhibition? *Nat Rev Drug Discov*. 2014;13:904-927

49. Fingleton B. MMPs as therapeutic targets – still a viable option? *Sem Cell Dev Biol*. 2008;19:61-68

50. Tuccinardi T, Martinelli A, Nuti E, Carelli P, Balzano F, Uccello-Barretta G, Murphy G, Rossello A. Amber force field implementation, molecular modelling study, synthesis and MMP-1/MMP-2 inhibition profile of (r)- and (s)-n-hydroxy-2-(N-isopropoxybiphenyl-4-ylsulfonamido)-3-methylbutanamides. *Bioorg Med Chem*. 2006;14:4260-4276

51. Rossello A, Nuti E, Orlandini E, Carelli P, Rapposelli S, Macchia M, Minutolo F, Carbonaro L, Albini A, Benelli R, Cercignani G, Murphy G, Balsamo A. New N-arylsulfonyl-N-alkoxyaminoacetohydroxamic acids as selective inhibitors of gelatinase A (MMP-2). *Bioorg Med Chem*. 2004;12:2441-2450

52. Golub LM, Lee HM, Ryan ME, Giannobile WV, Payne J, Sorsa T. Tetracyclines inhibit connective tissue breakdown by multiple non-antimicrobial mechanisms. *Adv Dent Res*. 1998;12:12-26

53. Smith GN, Jr., Mickler EA, Hasty KA, Brandt KD. Specificity of inhibition of matrix metalloproteinase activity by doxycycline: Relationship to structure of the enzyme. *Arthritis Rheum*. 1999;42:1140-1146

54. Golub LM, Ramamurthy NS, McNamara TF, Greenwald RA, Rifkin BR. Tetracyclines inhibit connective tissue breakdown: New therapeutic implications for an old family of drugs. *Crit Rev Oral Biol Med*. 1991;2:297-321

55. Caton J, Ryan ME. Clinical studies on the management of periodontal diseases utilizing subantimicrobial dose doxycycline (SDD). *Pharmacol Res*. 2011;63:114-120

56. Berman B, Perez OA, Zell D. Update on rosacea and anti-inflammatory-dose doxycycline. *Drugs Today*. 2007;43:27-34

57. Cerisano G, Buonamici P, Valenti R, Sciagra R, Raspanti S, Santini A, Carrabba N, Dovellini EV, Romito R, Pupi A, Colonna P, Antoniucci D. Early short-term doxycycline therapy in patients with acute myocardial infarction and left ventricular dysfunction to prevent the ominous progression to adverse remodelling: The TIPTOP trial. *Eur Heart J*. 2014;35:184-191

58. Hausenloy DJ, Yellon DM. Myocardial ischemia-reperfusion injury: A neglected therapeutic target. *J Clin Invest*. 2013;123:92-100

59. Timmis A. Acute coronary syndromes. *BMJ*. 2015;351

60. Eisen A, Giugliano RP, Braunwald E. Updates on acute coronary syndrome: A review. *JAMA Cardiol*. 2016;1:718-730

61. Gross GJ, Kersten JR, Warltier DC. Mechanisms of postischemic contractile dysfunction. *Ann Thorac Surg*. 1999;68:1898-1904

62. Ferdinandy P, Schulz R. Nitric oxide, superoxide, and peroxynitrite in myocardial ischaemia-reperfusion injury and preconditioning. *Br J Pharmacol*. 2003;138:532-543

63. Mohazzab HK, Kaminski PM, Wolin MS. Lactate and pO2 modulate superoxide anion production in bovine cardiac myocytes: Potential role of NADH oxidase. *Circulation*. 1997;96:614-620

64. Hille R, Nishino T. Flavoprotein structure and mechanism. 4. Xanthine oxidase and xanthine dehydrogenase. *Faseb J*. 1995;9:995-1003

65. Beckman JS, Beckman TW, Chen J, Marshall PA, Freeman BA. Apparent hydroxyl radical production by peroxynitrite: Implications for endothelial injury from nitric oxide and superoxide. *Proc Natl Acad Sci U S* . 1990;87:1620

66. Okamoto T, Akaike T, Nagano T, Miyajima S, Suga M, Ando M, Ichimori K, Maeda H. Activation of human neutrophil procollagenase by nitrogen dioxide and peroxynitrite: A novel mechanism for procollagenase activation involving nitric oxide. *Arch Biochem Biophys*. 1997;342:261-274

67. Szabo C, Zingarelli B, Salzman AL. Role of poly-ADP ribosyltransferase activation in the vascular contractile and energetic failure elicited by exogenous and endogenous nitric oxide and peroxynitrite. *Circ Res*. 1996;78:1051-1063

68. Yasmin W, Strynadka KD, Schulz R. Generation of peroxynitrite contributes to ischemia-reperfusion injury in isolated rat hearts. *Cardiovasc Res*. 1997;33:422-432

69. Beckman JS. Parsing the effects of nitric oxide, S-nitrosothiols, and peroxynitrite on inducible nitric oxide synthase–dependent cardiac myocyte apoptosis. *Circ Res*. 1999;85:870-871

70. Turer AT, Hill JA. Pathogenesis of myocardial ischemia-reperfusion injury and rationale for therapy. *Am J Cardiol*. 2010;106:360-368

71. Letavernier E, Zafrani L, Perez J, Letavernier B, Haymann J-P, Baud L. The role of calpains in myocardial remodelling and heart failure. *Cardiovasc res*. 2012;96:38-45

72. Halestrap AP, Pasdois P. The role of the mitochondrial permeability transition pore in heart disease. *BBA - Bioenergetics*. 2009;1787:1402-1415

73. Montfort I, Perez-Tamayo R. The distribution of collagenase in normal rat tissues. *J Histochem Cytochem*. 1975;23:910-920

74. Weber KT, Pick R, Janicki JS, Gadodia G, Lakier JB. Inadequate collagen tethers in dilated cardiopathy. *Am Heart J*. 1988;116:1641-1646

75. Olson MW, Bernardo MM, Pietila M, Gervasi DC, Toth M, Kotra LP, Massova I, Mobashery S, Fridman R. Characterization of the monomeric and dimeric forms of latent and active matrix metalloproteinase-9. Differential rates for activation by stromelysin 1. J Biol Chem. 2000;275:2661-2668

76. Moshal KS, Tipparaju SM, Vacek TP, Kumar M, Singh M, Frank IE, Patibandla PK, Tyagi N, Rai J, Metreveli N, Rodriguez WE, Tseng MT, Tyagi SC. Mitochondrial matrix metalloproteinase activation decreases myocyte contractility in hyperhomocysteinemia. *Am J Physiol Heart Circ Physiol*. 2008;295:H890-H897

77. Boixel C, Fontaine V, Rucker-Martin C, Milliez P, Louedec L, Michel JB, Jacob MP, Hatem SN. Fibrosis of the left atria during progression of heart failure is associated with increased matrix metalloproteinases in the rat. *J Am Coll Cardiol*. 2003;42:336-344

78. Lindsey ML, Escobar GP, Mukherjee R, Goshorn DK, Sheats NJ, Bruce JA, Mains IM, Hendrick JK, Hewett KW, Gourdie RG, Matrisian LM, Spinale FG. Matrix metalloproteinase-7 affects connexin-43 levels, electrical conduction, and survival after myocardial infarction. *Circulation*. 2006;113:2919-2928

79. Cheung P-Y, Sawicki G, Wozniak M, Wang W, Radomski MW, Schulz R. Matrix metalloproteinase-2 contributes to ischemia-reperfusion injury in the heart. *Circulation*. 2000;101:1833-1839

80. McDonough JL, Arrell DK, Van Eyk JE. Troponin I degradation and covalent complex formation accompanies myocardial ischemia/reperfusion injury. *Circ Res*. 1999;84:9-20

81. Gao WD, Atar D, Liu Y, Perez NG, Murphy AM, Marban E. Role of troponin i proteolysis in the pathogenesis of stunned myocardium. *Circ Res*. 1997;80:393

82. Panteghini M, Bunk DM, Christenson RH, Katrukha A, Porter RA, Schimmel H, Wang L, Tate JR. Standardization of troponin I measurements: An update. *Clin Chem Lab Med*. 2008;46:1501-1506

83. LeWinter MM, Granzier HL. Cardiac titin and heart disease. *J Cardiovasc Pharmacol*. 2014;63:207-212

84. Singh RB, Hryshko L, Freed D, Dhalla NS. Activation of proteolytic enzymes and depression of the sarcolemmal Na+/K+-ATPase in ischemia-reperfused heart may be mediated through oxidative stress. *Can J Physiol Pharmacol*. 2012;90:249-260

85. Baghirova S, Hughes BG, Poirier M, Kondo MY, Schulz R. Nuclear matrix metalloproteinase-2 in the cardiomyocyte and the ischemic-reperfused heart. *J Mol Cell Cardiol*. 2016;94:153-161

86. Bers DM. Cardiac excitation-contraction coupling. *Nature*. 2002;415:198-205

87. Bers DM. Calcium cycling and signaling in cardiac myocytes. *Annu Rev Physiol*. 2008;70:23-49

88. Beavers DL, Landstrom AP, Chiang DY, Wehrens XH. Emerging roles of junctophilin-2 in the heart and implications for cardiac diseases. *Cardiovasc Res*. 2014;103:198-205

89. Hwang PM, Sykes BD. Targeting the sarcomere to correct muscle function. *Nat Rev Drug Discov*. 2015;14:313

90. Wootton LL, Argent CCH, Wheatley M, Michelangeli F. The expression, activity and localisation of the secretory pathway ca2+-atpase (spca1) in different mammalian tissues. *BBA - Biomembranes*. 2004;1664:189-197

91. Hinken AC, Solaro RJ. A dominant role of cardiac molecular motors in the intrinsic regulation of ventricular ejection and relaxation. *Physiology*. 2007;22:73-80

92. Burkhoff D. Explaining load dependence of ventricular contractile properties with a model of excitation-contraction coupling. *J Mol Cell Cardiol*. 1994;26:959-978

93. Primeau JO, Armanious GP, Fisher ME, Young HS. The sarcoendoplasmic reticulum calcium ATPase. *Subcell Biochem*. 2018;87:229-258

94. Frank KF, Bölck B, Erdmann E, Schwinger RHG. Sarcoplasmic reticulum Ca2+-ATPase modulates cardiac contraction and relaxation. *Cardiovasc Res.* 2003;57:20-27

95. Vangheluwe P, Louch WE, Ver Heyen M, Sipido K, Raeymaekers L, Wuytack F. Ca2+ transport ATPase isoforms SERCA2a and SERCA2b are targeted to the same sites in the murine heart. *Cell Calcium*. 2003;34:457-464

96. Lipskaia L, Keuylian Z, Blirando K, Mougenot N, Jacquet A, Rouxel C, Sghairi H, Elaib Z, Blaise R, Adnot S, Hajjar RJ, Chemaly ER, Limon I, Bobe R. Expression of sarco (endo) plasmic reticulum calcium ATPase (SERCA) system in normal mouse cardiovascular tissues, heart failure and atherosclerosis. *Biochim Biophys Acta*. 2014;11:7

97. MacLennan DH, Kranias EG. Phospholamban: A crucial regulator of cardiac contractility. *Nat Rev Mol Cell Biol*. 2003;4:566

98. Mattiazzi A, Kranias EG. The role of CaMKII regulation of phospholamban activity in heart disease. *Front Pharmacol*. 2014;5

99. Magny EG, Pueyo JI, Pearl FM, Cespedes MA, Niven JE, Bishop SA, Couso JP. Conserved regulation of cardiac calcium uptake by peptides encoded in small open reading frames. Science. 2013;341:1116-1120

100. Nelson BR, Makarewich CA, Anderson DM, Winders BR, Troupes CD, Wu F, Reese AL, McAnally JR, Chen X, Kavalali ET, Cannon SC, Houser SR, Bassel-Duby R, Olson EN. A peptide encoded by a transcript annotated as long noncoding RNA enhances SERCA activity in muscle. Science. 2016;351:271-275

101. Vafiadaki E, Sanoudou D, Arvanitis DA, Catino DH, Kranias EG, Kontrogianni-Konstantopoulos A. Phospholamban interacts with HAX-1, a mitochondrial protein with anti-apoptotic function. *J Mol Biol*. 2007;367:65-79

102. Zhao W, Waggoner JR, Zhang Z-G, Lam CK, Han P, Qian J, Schroder PM, Mitton B, Kontrogianni-Konstantopoulos A, Robia SL, Kranias EG. The anti-apoptotic protein HAX-1 is a regulator of cardiac function. *Proc Natl Acad Sci U S A*. 2009;106:20776-20781

103. Bidwell PA, Liu G-S, Nagarajan N, Lam CK, Haghighi K, Gardner G, Cai W-F, Zhao W, Mugge L, Vafiadaki E, Sanoudou D, Rubinstein J, Lebeche D, Hajjar R, Sadoshima J, Kranias EG. HAX-1 regulates SERCA2a oxidation and degradation. *J Mol Cell Cardiol*. 2018;114:220-233

104. Adachi T, Weisbrod RM, Pimentel DR, Ying J, Sharov VS, Schoneich C, Cohen RA. S-glutathiolation by peroxynitrite activates SERCA during arterial relaxation by nitric oxide. *Nat Med*. 2004;10:1200-1207

105. Kho C, Lee A, Jeong D, Oh JG, Chaanine AH, Kizana E, Park WJ, Hajjar RJ. Sumo1-dependent modulation of SERCA2a in heart failure. *Nature*. 2011;477:601-605

106. Bidasee KR, Zhang Y, Shao CH, Wang M, Patel KP, Dincer UD, Besch HR, Jr. Diabetes increases formation of advanced glycation end products on sarco(endo)plasmic reticulum Ca2+-ATPase. *Diabetes*. 2004;53:463-473

107. Hu Y, Belke D, Suarez J, Swanson E, Clark R, Hoshijima M, Dillmann WH. Adenovirus-mediated overexpression of O-GlcNAcase improves contractile function in the diabetic heart. *Circ Res*. 2005;96:1006-1013

108. Stammers AN, Susser SE, Hamm NC, Hlynsky MW, Kimber DE, Kehler DS, Duhamel TA. The regulation of sarco(endo)plasmic reticulum calcium-atpases (SERCA). *Can J Physiol Pharmacol*. 2015;93:843-854

109. Ying J, Sharov V, Xu S, Jiang B, Gerrity R, Schöneich C, Cohen RA. Cysteine-674 oxidation and degradation of SERCA in diabetic pig aorta. *Free Radic Biol Med*. 2008;45:756-762

110. Toba K, Katagiri T, Takeyama Y. Studies of the cardiac sarcoplasmic reticulum in myocardial infarction. *Jpn Circ J*. 1978;42:447-453

111. Osada M, Netticadan T, Tamura K, Dhalla NS. Modification of ischemia-reperfusion-induced changes in cardiac sarcoplasmic reticulum by preconditioning. *Am J Physiol*. 1998;274:H2025-2034

112. Temsah RM, Netticadan T, Chapman D, Takeda S, Mochizuki S, Dhalla NS. Alterations in sarcoplasmic reticulum function and gene expression in ischemic-reperfused rat heart. *Am J Physiol*. 1999;277:H584-594

113. Gilchrist JS, Cook T, Abrenica B, Rashidkhani B, Pierce GN. Extensive autolytic fragmentation of membranous versus cytosolic calpain following myocardial ischemia-reperfusion. *Can J Physiol Pharmacol*. 2010;88:584-594

114. Singh RB, Chohan PK, Dhalla NS, Netticadan T. The sarcoplasmic reticulum proteins are targets for calpain action in the ischemic-reperfused heart. *J Mol Cell Cardiol*. 2004;37:101-110

115. Ali MA, Stepanko A, Fan X, Holt A, Schulz R. Calpain inhibitors exhibit matrix metalloproteinase-2 inhibitory activity. *Biochem Biophys Res Commun*. 2012;423:1-5

116. Talukder MAH, Kalyanasundaram A, Zuo L, Velayutham M, Nishijima Y, Periasamy M, Zweier JL. Is reduced SERCA2a expression detrimental or beneficial to postischemic cardiac function and injury? Evidence from heterozygous SERCA2a knockout mice. *Am J Phisiol Heart Circ Phisiol*. 2008;294:H1426-H1434

117. Talukder MAH, Yang F, Nishijima Y, Chen C-A, Kalyanasundaram A, Periasamy M, Zweier JL. Reduced SERCA2a converts sub-lethal myocardial injury to infarction and affects postischemic functional recovery. *J Mol Cell Cardiol*. 2009;46:285-287

118. Schultz Jel J, Glascock BJ, Witt SA, Nieman ML, Nattamai KJ, Liu LH, Lorenz JN, Shull GE, Kimball TR, Periasamy M. Accelerated onset of heart failure in mice during pressure overload with chronically decreased SERCA2 calcium pump activity. *Am J Physiol Heart Circ Physiol*. 2004;286:20

119. Shareef MA, Anwer LA, Poizat C. Cardiac SERCA2a/b: Therapeutic targets for heart failure. *Eur J Pharmacol*. 2014;724:1-8

120. Takeshima H, Komazaki S, Nishi M, Iino M, Kangawa K. Junctophilins: A novel family of junctional membrane complex proteins. *Molecular Cell*. 2000;6:11-22

121. Louch WE, Koivumaki JT, Tavi P. Calcium signalling in developing cardiomyocytes: Implications for model systems and disease. *J Physiol*. 2015;593:1047-1063

122. Reynolds JO, Chiang DY, Wang W, Beavers DL, Dixit SS, Skapura DG, Landstrom AP, Song LS, Ackerman MJ, Wehrens XH. Junctophilin-2 is necessary for t-tubule maturation during mouse heart development. *Cardiovasc Res*. 2013;100:44-53

123. Zhang H-B, Li R-C, Xu M, Xu S-M, Lai Y-S, Wu H-D, Xie X-J, Gao W, Ye H, Zhang Y-Y, Meng X, Wang S-Q. Ultrastructural uncoupling between t-tubules and sarcoplasmic reticulum in human heart failure. *Cardiovasc Res*. 2013;98:269-276

124. Crossman DJ, Ruygrok PR, Soeller C, Cannell MB. Changes in the organization of excitation-contraction coupling structures in failing human heart. *PLoS One*. 2011;6:e17901

125. van Oort RJ, Garbino A, Wang W, Dixit SS, Landstrom AP, Gaur N, De Almeida AC, Skapura DG, Rudy Y, Burns AR, Ackerman MJ, Wehrens XH. Disrupted junctional membrane complexes and hyperactive ryanodine receptors after acute junctophilin knockdown in mice. *Circulation*. 2011;123:979-988

126. Wu CY, Chen B, Jiang YP, Jia Z, Martin DW, Liu S, Entcheva E, Song LS, Lin RZ. Calpain-dependent cleavage of junctophilin-2 and t-tubule remodeling in a mouse model of reversible heart failure. *J Am Heart Assoc*. 2014;3:e000527

127. Guo A, Hall D, Zhang C, Peng T, Miller JD, Kutschke W, Grueter CE, Johnson FL, Lin RZ, Song LS. Molecular determinants of calpain-dependent cleavage of junctophilin-2 protein in cardiomyocytes. *J Biol Chem*. 2015;290:17946-17955

128. Murphy RM, Dutka TL, Horvath D, Bell JR, Delbridge LM, Lamb GD. Ca(2+)-dependent proteolysis of junctophilin-1 and junctophilin-2 in skeletal and cardiac muscle. *J Physiol*. 2013;591:719-729

129. Reddy LG, Jones LR, Pace RC, Stokes DL. Purified, reconstituted cardiac Ca2+-ATPase is regulated by phospholamban but not by direct phosphorylation with Ca2+/calmodulin-dependent protein kinase. *J Biol Chem*. 1996;271:14964-14970

130. Vasanji Z, Cantor EJ, Juric D, Moyen M, Netticadan T. Alterations in cardiac contractile performance and sarcoplasmic reticulum function in sucrose-fed rats is associated with insulin resistance. *Am J Physiol Cell Physiol*. 2006;291:C772-780

131. Smeazzetto S, Armanious GP, Moncelli MR, Bak JJ, Lemieux MJ, Young HS, Tadini-Buoninsegni F. Conformational memory in the association of the transmembrane protein phospholamban with the sarcoplasmic reticulum calcium pump SERCA. *J Biol Chem*. 2017;292:21330-21339

132. Itoh Y, Binner S, Nagase H. Steps involved in activation of the complex of pro-matrix metalloproteinase 2 (progelatinase A) and tissue inhibitor of metalloproteinases (TIMP)-2 by 4-aminophenylmercuric acetate. *Biochem J*. 1995;308:645-651

133. Biasini M, Bienert S, Waterhouse A, Arnold K, Studer G, Schmidt T, Kiefer F, Gallo Cassarino T, Bertoni M, Bordoli L, Schwede T. SWISS-MODEL: Modelling protein tertiary and quaternary structure using evolutionary information. *Nucleic Acids Res*. 2014;42:W252-258

134. Berman HM, Battistuz T, Bhat TN, Bluhm WF, Bourne PE, Burkhardt K, Feng Z, Gilliland GL, Iype L, Jain S, Fagan P, Marvin J, Padilla D, Ravichandran V, Schneider B, Thanki N, Weissig H, Westbrook JD, Zardecki C. The protein data bank. *Acta Crystallogr D Biol Crystallogr*. 2002;58:899-907

135. Rodrigues JP, Levitt M, Chopra G. KoBaMIN: A knowledge-based minimization web server for protein structure refinement. *Nucleic Acids Res*. 2012;40:W323-328

136. Luthy R, Bowie JU, Eisenberg D. Assessment of protein models with three-dimensional profiles. *Nature*. 1992;356:83-85

137. Kositprapa C, Zhang B, Berger S, Canty JM, Jr., Lee TC. Calpain-mediated proteolytic cleavage of troponin I induced by hypoxia or metabolic inhibition in cultured neonatal cardiomyocytes. *Mol Cell Biochem*. 2000;214:47-55

138. Kumar S, Ratnikov BI, Kazanov MD, Smith JW, Cieplak P. CleavPredict: A platform for reasoning about matrix metalloproteinases proteolytic events. *PLoS One*. 2015;10:e0127877

139. French JP, Quindry JC, Falk DJ, Staib JL, Lee Y, Wang KK, Powers SK. Ischemia-reperfusion-induced calpain activation and SERCA2a degradation are attenuated by exercise training and calpain inhibition. *Am J Physiol Heart Circ Physiol*. 2006;290:H128-136

140. Ver Heyen M, Heymans S, Antoons G, Reed T, Periasamy M, Awede B, Lebacq J, Vangheluwe P, Dewerchin M, Collen D, Sipido K, Carmeliet P, Wuytack F. Replacement of the muscle-specific sarcoplasmic reticulum Ca(2+)-ATPase isoform SERCA2a by the nonmuscle SERCA2b homologue causes mild concentric hypertrophy and impairs contraction-relaxation of the heart. *Circ Res*. 2001;89:838-846

141. Hearse DJ, Garlick PB, Humphrey SM. Ischemic contracture of the myocardium: Mechanisms and prevention. *Am J Cardiol*. 1977;39:986-993

142. Feng J, Schaus BJ, Fallavollita JA, Lee TC, Canty JM, Jr. Preload induces troponin I degradation independently of myocardial ischemia. *Circulation*. 2001;103:2035-2037

143. Temsah RM, Dyck C, Netticadan T, Chapman D, Elimban V, Dhalla NS. Effect of beta-adrenoceptor blockers on sarcoplasmic reticular function and gene expression in the ischemic-reperfused heart. *J Pharmacol Exp Ther*. 2000;293:15-23

144. Jorgensen AO, Arnold W, Pepper DR, Kahl SD, Mandel F, Campbell KP. A monoclonal antibody to the Ca2+ -ATPase of cardiac sarcoplasmic reticulum cross-reacts with slow type I but not with fast type II canine skeletal muscle fibers: An immunocytochemical and immunochemical study. *Cell Motility*. 1988;9:164-174

145. Blackwell DJ, Zak TJ, Robia SL. Cardiac calcium ATPase dimerization measured by cross-linking and fluorescence energy transfer. *Biophys J*. 2016;111:1192-1202

146. Gilchrist JS, Wang KK, Katz S, Belcastro AN. Calcium-activated neutral protease effects upon skeletal muscle sarcoplasmic reticulum protein structure and calcium release. *J Biol Chem*. 1992;267:20857-20865

147. Prudova A, auf dem Keller U, Butler GS, Overall CM. Multiplex N-terminome analysis of MMP-2 and MMP-9 substrate degradomes by iTRAQ-TAILS quantitative proteomics. *Mol Cell Proteomics*. 2010;9:894-911

148. Eckhard U, Huesgen PF, Schilling O, Bellac CL, Butler GS, Cox JH, Dufour A, Goebeler V, Kappelhoff R, Auf dem Keller U, Klein T, Lange PF, Marino G, Morrison CJ, Prudova A, Rodriguez D, Starr AE, Wang Y, Overall CM. Active site specificity profiling datasets of

matrix metalloproteinases (MMPs) 1, 2, 3, 7, 8, 9, 12, 13 and 14. *Data Brief*. 2016;7:299-310

149. Kranias EG, Hajjar RJ. Modulation of cardiac contractility by the phospholamban/SERCA2a regulatome. *Circ Res*. 2012;110:1646-1660

150. Wegener AD, Simmerman HK, Lindemann JP, Jones LR. Phospholamban phosphorylation in intact ventricles. Phosphorylation of serine 16 and threonine 17 in response to beta-adrenergic stimulation. *J Biol Chem*. 1989;264:11468-11474

151. Lytton J, Westlin M, Hanley MR. Thapsigargin inhibits the sarcoplasmic or endoplasmic reticulum Ca-ATPase family of calcium pumps. *J Biol Chem*. 1991;266:17067-17071

152. Lopaschuk GD, Tahiliani AG, Vadlamudi RV, Katz S, McNeill JH. Cardiac sarcoplasmic reticulum function in insulin- or carnitine-treated diabetic rats. *Am J Physiol*. 1983;245:H969-976

153 Solli AI, Fadnes B, Winberg J-O, Uhlin-Hansen L, Hadler-Olsen E. Tissue- and cell-specific co-localization of intracellular gelatinolytic activity and matrix metalloproteinase 2. *J Histochem Cytochem*. 2013;61:444-461

154. Gao CQ, Sawicki G, Suarez-Pinzon WL, Csont T, Wozniak M, Ferdinandy P, Schulz R. Matrix metalloproteinase-2 mediates cytokine-induced myocardial contractile dysfunction. *Cardiovasc Res*. 2003;57:426-433

155. Bravo-Sagua R, Rodriguez AE, Kuzmicic J, Gutierrez T, Lopez-Crisosto C, Quiroga C, Díaz-Elizondo J, Chiong M, Gillette TG, Rothermel BA, Lavandero S. Cell death and survival through the endoplasmic reticulum-mitochondrial axis. *Curr mol med*. 2013;13:317-329

156. Santos-Martinez MJ, Medina C, Jurasz P, Radomski MW. Role of metalloproteinases in platelet function. *Thromb Res*. 2008;121:535-542

157. Ardi VC, Kupriyanova TA, Deryugina EI, Quigley JP. Human neutrophils uniquely release TIMP-free MMP-9 to provide a potent catalytic stimulator of angiogenesis. *Proc Natl Acad Sci U S A*. 2007;104:20262-20267

158. Chan BYH, Roczkowsky A, Moser N, Poirier M, Hughes BG, Ilarraza R, Schulz R. Doxorubicin induces de novo expression of n-terminal truncated mmp-2 in cardiac myocytes. *Can J Physiol Pharmacol*. 2018

159. Lalu MM, Csonka C, Giricz Z, Csont T, Schulz R, Ferdinandy P. Preconditioning decreases ischemia/reperfusion-induced release and activation of matrix metalloproteinase-2. *Biochem Biophys Res Commun*. 2002;296:937-941

160. Wright PE, Dyson HJ. Intrinsically unstructured proteins: Re-assessing the protein structure-function paradigm. *J Mol Biol*. 1999;293:321-331

161. Ito K, Komazaki S, Sasamoto K, Yoshida M, Nishi M, Kitamura K, Takeshima H. Deficiency of triad junction and contraction in mutant skeletal muscle lacking junctophilin type 1. *J Cell Biol*. 2001;154:1059-1067

162. Phimister AJ, Lango J, Lee EH, Ernst-Russell MA, Takeshima H, Ma J, Allen PD, Pessah IN. Conformation-dependent stability of junctophilin 1 (JP1) and ryanodine receptor type 1 (RyR1) channel complex is mediated by their hyper-reactive thiols. *J Biol Chem*. 2007;282:8667-8677

163. Pasini E, Solfrini R, Bachetti T, Marino M, Bernocchi P, Visioli F, Ferrari R. The blood perfused isolated heart: Characterization of the model. *Basic Res Cardiol*. 1999;94:215-222

164. Bolli R. Myocardial 'stunning' in man. *Circulation*. 1992;86:1671-1691

165. Murphy E, Steenbergen C. Gender-based differences in mechanisms of protection in myocardial ischemia–reperfusion injury. *Cardiovasc Res*. 2007;75:478-486

166. Yusuf S, Hawken S, Ounpuu S, Dans T, Avezum A, Lanas F, McQueen M, Budaj A, Pais P, Varigos J, Lisheng L. Effect of potentially modifiable risk factors associated with myocardial infarction in 52 countries (the INTERHEART study): Case-control study. *Lancet*. 2004;364:937-952

167. Brower M, Grace M, Kotz CM, Koya V. Comparative analysis of growth characteristics of sprague dawley rats obtained from different sources. *Laboratory Animal Research*. 2015;31:166-173

168. Simms AD, Batin PD, Kurian J, Durham N, Gale CP. Acute coronary syndromes: An old age problem. *J Geriatr Cardiol*. 2012;9:192-196

169. Kupai K, Szucs G, Cseh S, Hajdu I, Csonka C, Csont T, Ferdinandy P. Matrix metalloproteinase activity assays: Importance of zymography. *J Pharmacol Toxicol Methods*. 2010;61:205-209

170. Wieckowski MR, Giorgi C, Lebiedzinska M, Duszynski J, Pinton P. Isolation of mitochondria-associated membranes and mitochondria from animal tissues and cells. *Nat Protoc*. 2009;4:1582-1590

171. Rizzi E, Castro MM, Ceron CS, Neto-Neves EM, Prado CM, Rossi MA, Tanus-Santos JE, Gerlach RF. Tempol inhibits TGF-beta and MMPs upregulation and prevents cardiac hypertensive changes. *Int J Cardiol*. 2013;165:165-173

Appendix

Western blotting

6x SDS PAGE loading buffer: 10 mL 0.5 M Tris in deionized water, pH 6.8, 10% (w/v) SDS, 30% (v/v) glycerol, 0.6 M DTT, and 0.012% (w/v) bromophenol blue.

Towbin buffer: 20% (v/v) methanol, 25 mM Tris, 192 mM glycine, and 0.005% (w/v) SDS.

TBS-T: 0.01 M Tris, pH 7.6, 0.1% (v/v) Tween, 0.1 M NaCl.

Gelatin zymography

Zymography loading buffer: 0.5 M Tris, pH 6.8, 30% (v/v) glycerol, 10% (w/v) SDS, and 0.012 % (w/v) bromophenol blue.

Zymography incubation buffer: 50 mM Tris, pH 7.6, 150 mM NaCl, 5 mM $CaCl_2$, and 0.05% (w/v) NaN_3.

Coomassie zymography staining solution: 0.05% (w/v) Coomassie Brilliant Blue G-250, 25% (v/v) methanol, 10% (v/v) acetic acid.

SDS-PAGE Gels

Tris-glycine SDS-PAGE 8% separating gel

This recipe makes two gels (1.5 mm thick).

Solution	Volume (mL)
40% (w/v) acrylamide / 3.3% (w/v) bis-acrylamide 29:1	3.000
0.5 M Tris / 0.4% (w/v) SDS, pH 6.8	3.750
H_2O	8.250
10% (w/v) ammonium persulfate	0.050
Tetramethylethylenediamine (TEMED)	0.010

Tris-tricine SDS-PAGE 16% separating gel

This recipe makes one gel (1.5 mm thick).

Solution	Volume (mL)
46.5% (w/v) acrylamide / 3% (w/v) bis-acrylamide	3.300
3 M Tris / 3% (w/v) SDS, pH 8.45	3.750
glycerol	1.000
H_2O	2.400
10% (w/v) ammonium persulfate	0.033
TEMED	0.004

Tris-tricine SDS-PAGE 10% spacing layer

This recipe makes a spacing layer for one gel (1.5 mm thick).

Solution	Volume (mL)
48% (w/v) acrylamide / 1.5% (w/v) bis-acrylamide	1.000
3 M Tris / 3% (w/v) SDS, pH 8.45	1.650
H_2O	2.350
10% (w/v) ammonium persulfate	0.025
TEMED	0.003

Tris-tricine SDS-PAGE 4% stacking layer

This recipe makes a stacking layer for one gel (1.5 mm thick).

Solution	Volume (mL)
48% (w/v) acrylamide / 1.5% (w/v) bis-acrylamide	0.330
3 M Tris / 3% (w/v) SDS, pH 8.45	1.000
H_2O	2.670
10% (w/v) ammonium persulfate	0.030
TEMED	0.003

Gelatin zymography 8% separating gel

This recipe makes separating layers for four gels (0.75 mm thick).

Solution	Volume (mL)
40% (w/v) acrylamide / 3.3% (w/v) bis-acrylamide 29:1	3.000
0.5 M Tris / 0.4% (w/v) SDS, pH 6.8	3.750
gelatin (20 mg/mL)	1.500
H_2O	6.750
10% (w/v) ammonium persulfate	0.050
TEMED	0.010